ANALYSIS OF OPTICAL PROPERTIES OF PARACRYSTALLINE ULTRASTRUCTURES IN HUMAN OOCYTES BY POLSCOPE MICROSCOPY CORRELATED TO EMBRYO QUALITY AND VIABILITY

YING SHEN

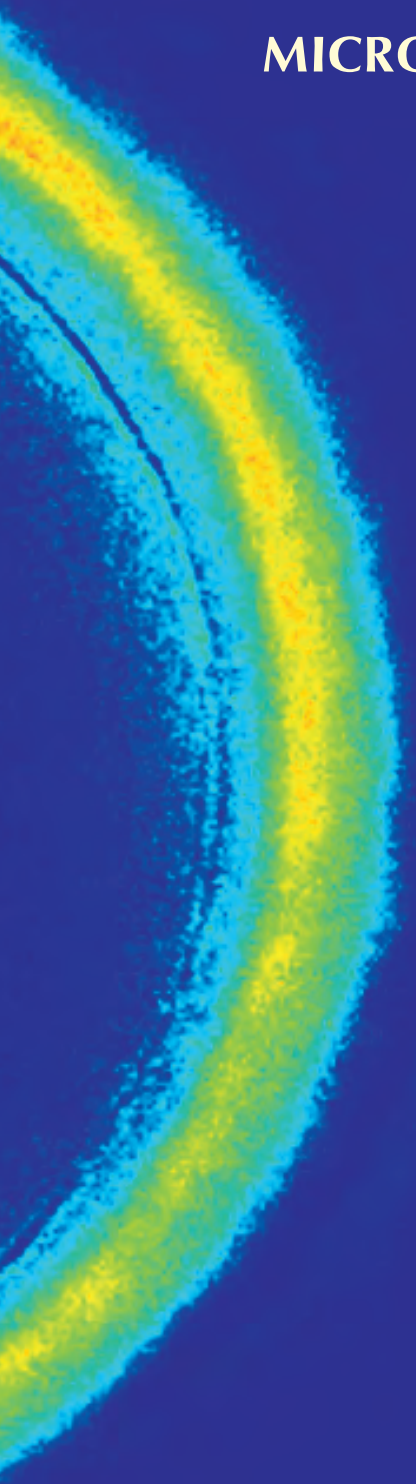

INAUGURALDISSERTATION
zur Erlangung des Grades eines
Doktors der Humanbiologie
des Fachbereichs Medizin der
Justus-Liebig-Universität Giessen

édition scientifique
VVB LAUFERSWEILER VERLAG

1. Auflage 2007

1st Edition 2007

VVB LAUFERSWEILER VERLAG
édition scientifique

STAUFENBERGRING 15, D-35396 GIESSEN
Tel: 0641-5599888 Fax: 0641-5599890
email: redaktion@doktorverlag.de

www.doktorverlag.de

Analysis of Optical Properties of Paracrystalline Ultrastructures in human oocytes by PolScope Microscopy Correlated to Embryo Quality and Viability

INAUGURALDISSERTATION
zur Erlangung des Grades eines
Doktors der Humanbiologie
des Fachbereichs Medizin der
Justus-Liebig-Universität Giessen

vorgelegt von

YING SHEN

aus Beijing, China

Gießen, 2006

Aus dem Medizinischen Zentrum für Frauenheilkunde und Geburtshilfe
des Fachbereichs Medizin der Justus-Liebig-Universität Gießen

Leiter: Prof. Dr. Dr. h.c. Hans-Rudolf Tinneberg

Gutachter: Prof. Dr. Dr. h.c. H.-R. Tinneberg

Gutachter: Prof. Dr. K. Steger

Tag der Disputation: 14. 05. 2007

1. Abstract

The spindle apparatus and the zona pellucida are two essential organelles in oocytes, which can be viewed by PolScope microscopy non-invasively, due to their composition of molecularly ordered, paracrystalline fibres. The spindle apparatus is responsible for the high fidelity of chromosome segregation during oogenesis. Disturbances in spindle assembly increase the risk of chromosome mal-segregation in oocytes. Accordingly, oocytes possessing a birefringent spindle in PolScope microscopy tend to have a better developmental potential compared to those without a spindle. The zona pellucida is an extracellular matrix surrounding mammalian oocytes and pre-implantation embryos with an essential role in oocyte development, fertilization and implantation. Failures in expression of zona proteins correlate to subfertility or infertility in animals. Low expression of the zona proteins by the growing human oocyte may indicate reduced developmental potential. Retardance of light and magnitude of birefringence is linearly correlated to number and alignment of microtubules. Therefore, high mean retardance magnitude may reflect oocytes with healthy, robust spindle and/or zona pellucida that have a high developmental potential. Low birefringence might be indicative of structures with few and unaligned fibres and oocytes with lower developmental capacity. To test this notion, the current study employed PolScope microscopy in the IVF centre of Giessen University to non-invasively and quantitatively assess spindle and zona morphology in living human oocytes before they were subjected to intracytoplasmic sperm injection (ICSI). Quality and viability of the embryos after insemination of oocytes with high or low birefringence was compared retrospectively.

In total, oocytes from 182 stimulated ICSI cycles were screened by PolScope after informed consent of patients. For the assessment of spindle morphology and texture, 676 oocytes (mean age of patients was 32.5 ± 4.4 years) were analysed that developed into pre-embryos and were assessed for PN scores to select embryos for transfer, blindly with respect to spindle birefringence. Mean magnitude of retardance of spindles and pole-to-pole length was retrospectively compared between all oocytes giving rise to high or low PN score embryos, and was also analysed with respect to maternal age. Mean retardance

was also compared between oocytes developing into non-transfer embryos and those selected for transfer after ICSI, respectively.
For the assessment of the zona morphology and texture, retardance magnitude and thickness of the inner, middle and outer layers of the ZP were quantitatively analysed by PolScope in 166 oocytes selected for transfer after ICSI (63 of the 103 cycles; mean age 32.8 ± 4.4 years) on the basis of pronuclear score at day 1. Blastomere number was determined at day 2. Data were compared between oocytes giving rise to conception cycles (CC; 65 oocytes/23 cycles) and non-conception cycles (NCC; 101 oocytes/40 cycles) and with respect to maternal age.

Results of the spindle analysis showed that magnitude of light retardance by the oocyte spindle was positively correlated to embryo quality after ICSI according to PN score in the IVF centre in Giessen. Good PN score pre-embryos were from oocytes with significantly higher birefringent spindles compared to lower PN score pre-embryos ($P < 0.001$). In addition, oocytes developing to pre-embryos with very poor quality had a significantly shorter spindle compared to those forming embryos with highest PN score ($P < 0.001$). Mean retardance was significantly higher in spindles of oocytes selected for transfer compared to non-transfer oocytes ($P < 0.001$). There was no clear relationship between maternal age and mean retardance in the cohort containing few patients ≥ 36 years.

Zona pellucida scoring revealed three distinctly different layers of the extracellular coat surrounding the human oocyte, whereas the zona appeared comparatively translucent, when viewed by a conventional light microscope equipped with Hoffmann interference optics. Embryos in the CC group tended to develop faster. The thickness of the inner zona layer was significantly different ($P < 0.001$), and the mean magnitude of light retardance was nearly 30% higher ($P < 0.001$) in the inner layer of the zona pellucida of oocytes contributing to a CC compared to a NCC. Nearly 90% percent of the oocytes containing a ZP with a mean retardance magnitude over 3.0 nm of the inner ZP layer contributed to a CC, significantly more compared with the NCC (χ^2-test, $P < 0.001$).

In conclusion, the study shows that oocytes with a high mean retardance of light by the spindle develop into pre-embryos with good PN score. This finding has been confirmed by a small cohort of 59 oocytes from an IVF centre in Milano, Italy. PN-scoring was originally developed to identify presumably high quality embryos and may be predictive for aneuploidy. Since PN-scoring cannot be used for selection in some counties due to ethical and legal considerations, analysis of mean spindle retardance by PolScope microscopy may be as useful as PN-scoring to identify oocytes with higher or lower developmental potential, and combining with PN-scoring may provide additional information on oocyte health and quality.

A high birefringent and thick ZP is related to the presence of a dense coat of highly ordered ZP filaments and thus appears to reflect health and developmental potential of an oocyte. The mean magnitude of light retardance by the ZP inner layer presents a new, unique, non-invasive marker for embryo viability after ICSI. Combining screening for birefringence of the spindle apparatus and the zona pellucida together with other methods like PN-scoring, analysis of oocytes by quantitative PolScope microscopy may contribute significantly to identify the highest quality oocytes in ICSI cycles, to reduce multiple embryo transfers, and to improve oocyte handling and treatment of patients.

2. Introduction

2.1 Oocyte Growth, Maturation, Fertilization, Implantation and Developmental Potential of Embryos after Fertilization

Truly in the sense of the Aristoteles words "*Ex Ovo Omnia*" oocytes are amongst the most remarkable animal cells. According to their totipotency, oocytes (or rather eggs) can differentiate into all germ cell layers and can develop into a new individual after fertilization. While parthenogenetic development may occur in several animal species, it is the maternal as well as the paternal genome that is required for normal development of the zygote in mammals (Illmensee *et al.,* 2006); imprinting processes and epigenetic marks contribute to define the developmental potential of germ cells as well as stem cells and differentiated somatic cells in mammals (De Rycke *et al.,* 2002). However, only in the last decades it has become clear that ooplasm contains unique still undefined factors, which are essential for normal embryonic development and may even reset the programme of differentiated somatic cell nuclei to provide conditions for development and differentiation from somatically derived chromatin for cloning (Rodriguez-Mari *et al.,* 2005). Thus, it is still one of the most important and intriguing questions in reproductive biology, but also of immense clinical relevance, in particular in assisted reproduction, to assess the basis of the origin, differentiation, quality and function of mammalian oocytes.

2.1.1 Oogenesis and Female Meiosis

Oogenesis is the development of a female gamete (oocyte), which begins already during prenatal life in primates. The details of oogenesis vary from species to species in mammals, but the general stage is similar. Primordial germ cells (PGCs) migrate to the forming gonad to become *oogonia*, which proliferate by mitosis for a period before differentiating into *primary oocytes.* As the PGCs move from the base of the allantois, they embark upon a complex migration, first into the endodermal epithelium of the hind gut, then into the mesentery, and finally into the genital ridges, which are bands of mesodermal tissue lying in the roof of the peritoneum. The mechanisms by which the PGCs are translocated from extragonadal sites to the genital ridges probably involve the active movement of PGCs, either along the tracts of extracellular matrix material or in response to chemotactic gradients by molecules released by the cells of the genital ridge

(Bendel-Stenzel *et al.,* 1998; Saito *et al.,* 2004). While oogonia divide mitotically, primary oocytes enter meiosis in female mammals in response to a stimulus provided by the somatic cells of the genital ridges (Yamaguchi *et al.,* 2005), while in males testicular cords develop and mitotic divisions eventually cease in the early embryonic gonad.

Meiosis is a unique process restricted to germ cells. Meiosis comprises usually a meiotic S-phase during which chromosomes replicate, followed by two successive nuclear divisions without intervening replication to produce one (in the female) or four (in the male) haploid gametes (Figure 2.1.1). After DNA replication and meiotic pairing and exchange bivalent chromosomes are formed which contain two recombined homologues each with two sister chromatids and homologues connected by chiasmata. Homologues usually separate at the first meiotic division reductively from each other (Figure 2.1.1). This is achieved by release of cohesion between chromatid arms resulting in chiasma resolution (Kudo *et al.,* 2006). During the second meiotic division the sister chromatids separate equationally, with detachment/ loss of centromere cohesion of sister chromatids, comparable to mitosis and without an intermittent DNA replication (Figure 2.1.1). Most processes in genetic recombination and exchange between originally paternally and maternally derived homologous chromosomes occur in prophase I. Following S-phase, the long prophase of meiosis I can be subdivided according to morphological criteria into five distinct stages, namely, leptotene, zygotene, pachytene, diplotene and diakinesis, associated with the assembly *(synapsis)* and disassembly *(desynapsis)* of the synaptonemal complex.

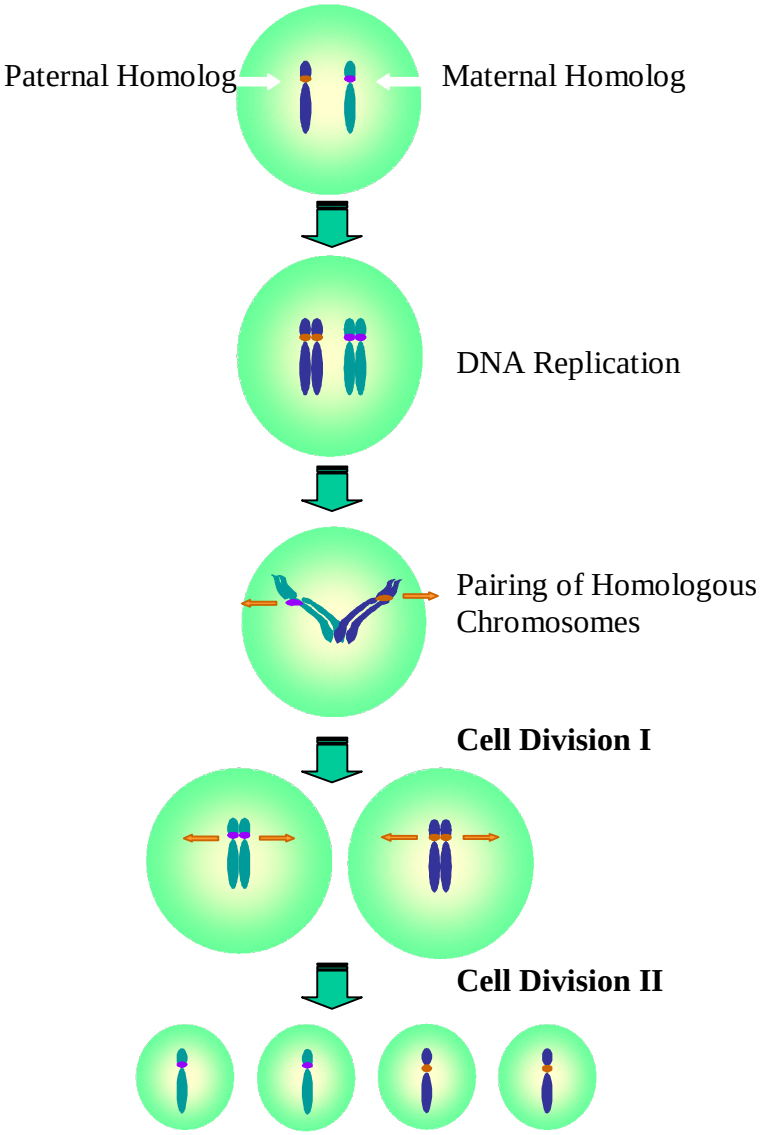

Figure 2.1.1 Reductional and equational separation of chromosomes at meiosis I and meiosis II

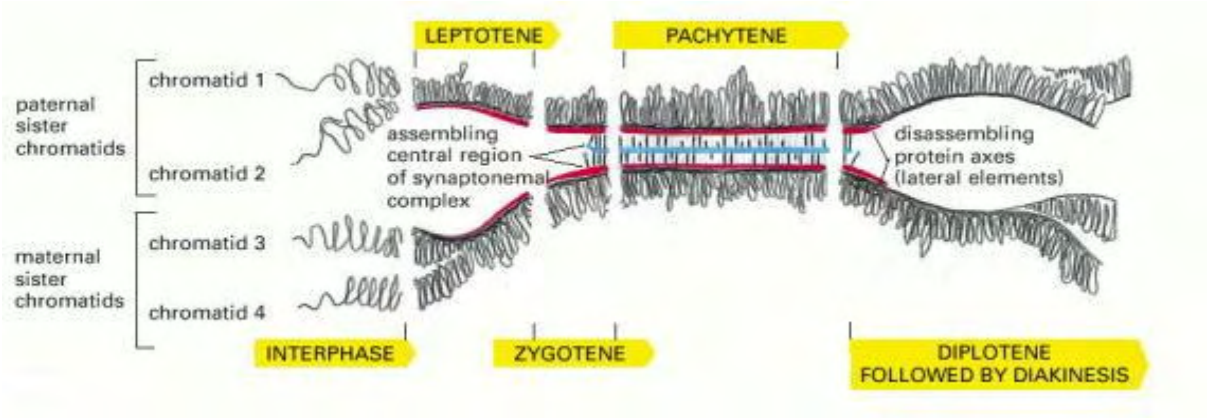

Figure 2.1.2 Formation of the synaptonemal complex and pairing of homologous chromosomes during prophase I of meiosis. A single bivalent is shown. At leptotene, the two sister chromatids condense, with chromatin extending from a common protein axis (red). The homologous sites get in contact such that in the pachytene stage two laterals and one central element composed of proteins of the synaptonemal complex (blue and red) mediates fulls synapsis. At diplotene stage homologous chromosomes disjoin and the synaptonemal complex disassembles, leaving chromosomes connected at sites of exchange where they remain physically attached at sites which later are recognized as chiasmata. Meiosis arrests after resolution of the synaptonemal complex after diplotene (termed dictyate stage) for up to decades in human oocytes (modified from Alberts *et al.,* 2002).

a. The leptotene stage is resumed by the end of the pre-meiotic DNA synthesis. During this stage chromosomes start to condense and each of them is attached to the nuclear envelope via an attachment plaque at its telomeres (Pawlowski and Cande, 2005). Along the chromosome arms the lateral elements of the synaptonemal complex begin to form (Figure 2.1.2).
b. In the zygotene stage, homologous chromosomes pair with each other over the entire chromosome length. The synaptonemal complexes fully develop with lateral elements at the chromosome axis and a central core that attaches the two homologues to each other. In addition, the chromosomes condense and shorten considerably during this stage (Figure 2.1.2).
c. At pachytene, synapsis is complete; the homologues further condense and now are fully paired. Genetic exchange occurs at sites defined by presence of recombination enzymes in recombination nodules on the synaptonemal complex

(Pawlowski and Cande, 2005; Cohen *et al.,* 2006) between two non-sister-chromatids in bivalents allowing meiotic exchange to take place. Later these sites are recognized as chiasmata (Figure 2.1.2).

d. Desynapsis occurs already in the stage of diplotene when homologous lose contact except for sites of cross-over. The sister chromatids remain attached to each other (Figure 2.1.3) by cohesion proteins. These binding points remain present for weeks, months or decades in the human: In oogenesis attachment needs to be maintained between the sister chromatids throughout the first meiosis arrest, termed dictyotene or dictyate stage until re-initiation of meiosis is triggered and homologues finally segregate after resumption of meiosis at anaphase I, shortly before the oocyte becomes ovulated. This means that the cohesion proteins remain stable or are sufficiently replaced to mediate chromosome contact by cohesion between sister chromatids and stabilize thus preservation of chiasmata.

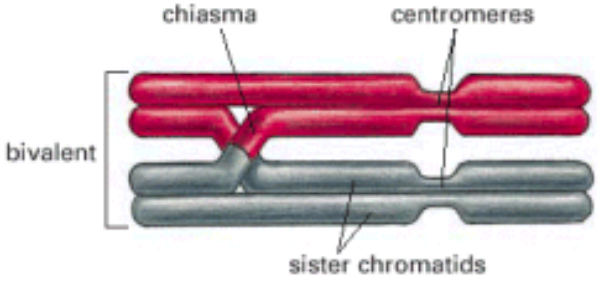

Figure 2.1.3 Paired homologous chromsomes during the transition to metaphase of meiotic division I (Alberts *et al.*, 2002).

e. In general, at meiosis arrest (throughout dictyate stage), the chromatin is decondensed in the nucleus of resting or growing oocytes except for heterochromatic regions. One or several nucleoli are formed which are needed for rRNA synthesis during oocyte growth, before resumption of maturation takes place. Lampbrush chromosomes for rapid rRNA synthesis may be formed in some vertebrates, like in amphibia, while oocytes in mammals like mouse and human possess characteristic non-surrounded nucleoli (NSN) and are highly transcriptionally active. Only shortly before resumption of maturation fully grown, maturation and developmentally competent dictyate stage oocytes with

intact nucleus (germinal vesicles, GV) possess a surrounded nucleolus (SN) and become transcriptionally repressed (De Felici *et al.,* 2005; Eichenlaub-Ritter, 1996).

In mammals, there are major differences in oogenesis and spermatogenesis. Male meiosis is continuously taking place without a meiotic arrest only after birth when puberty is reached. Spermatocytes undergo most of their differentiation after their nuclei have completed meiosis to become haploid. Unlike sperm, oocytes proliferate only in the fetus, enter meiosis before birth, and become arrested as primary oocytes in the first meiotic prophase, in which state they may remain for several decades within primordial follicles (Eichenlaub-Ritter, 1998). Individual oocytes mature from this strictly limited stock and are ovulated at intervals, generally one at a time, beginning at puberty. Although there is currently a debate on reformation of oocytes after birth, relevance of such *de novo* formation has been questioned (Eggan *et al.,* 2006).

2.1.2 Oocyte Arrest and Growth

After completion of pachytene stage and acquiring somatic cells enveloping the primary oocyte to form a primordial follicle with flattened granulosa cells surrounding the oocyte, mammalian oocytes remain arrested in the diplotene stage for a long period, which corresponds to the G2-phase of the cell cycle, with decondensed chromosomes. Only after birth the first wave of oocytes within primordial follicles may enter the growing stage (primary follicular stage), folliculogenesis takes place with excessive proliferation of granulosa cells (early preantral stage), and finally differentiation of the granulosa cells into mural and cumulus cells in response to oocyte-derived factors (Thomas and Vanderhyden, 2006) and antrum formation take place (see below). Only few or one of the follicles stimulated to resume growth becomes dominant and survives while others become atretic and die. Finally, depending on species, one (human) or several (e.g. rodents) fully-grown oocytes from large antral follicles may resume meiosis to metaphase II after the female has reached sexual maturity in response to the surge of lutenising hormone (LH) (Conti *et al.,* 2006). Continuously during the reproductive period cohorts of oocytes from primordial follicles enter the growing primary follicle pool and initiate growth and maturation, attaining the competence to be fertilized and support

embryogenesis (Gilbert *et al.,* 1983). Oocyte maturation encompasses a number of complex cellular processes (Gosden and Bownes, 1995; Briggs *et al.,* 1999; Moor *et al.,* 1998). Besides meiosis, cytoplasmic growth, organelles production and redistribution, stable transcription and translation occurs to support early embryonic cleavage, nuclear maturation (the acquisition of competence to resume meiosis at the time of antrum formation) and cytoplasmic maturation (with the acquisition of competence for sperm head penetration, decondensation of chromatin and support of embryogenesis from maternally provided gene products). Oocyte growth and maturation appear to be vulnerable to disruption by environmental insults, nutritional imbalances or hormonal disturbance that may ultimately lead to chromosomal anomalies or embryo loss (Moor *et al.,* 1998). Many studies have shown that the oocyte is incapable of resuming meiosis until it is fully grown (e.g. Eppig, 1993; Harada *et al.*, 1997; Papanikolaou *et al.,* 2005).
Within the primordial follicle, the human oocyte is initially very small, with a diameter of around 30µm. Following initiation of growth, the oocyte undergoes a 60-fold increase in volume, reaching its full diameter of 120µm at the time of antrum formation; well before the follicle reaches its full pre-ovulatory size (Gosden, 1999). Oocytes resume meiosis either after the LH (luteinizing hormone) surge, or following removal from the cumulus mass. *In vivo*, follicle size largely correlates with developmental potential (Eppig, 1993), showing that there is a progressive attainment of competence to resume meiosis, undergo fertilization, then complete meiosis and embark on embryogenesis (Mehlmann, 2005; Tsafriri *et al.,* 2005; Miyano *et al.,* 2003). Administration of hormones may accelerate the nuclear maturation of oocytes (Roberts *et al.,* 2005). Asynchrous nuclear and cytoplasmic maturation may affect chromosomal alignment on the spindle and predispose to chromosomal abnormalities (Roberts *et al.,* 2005), which correlate directly with reduced female fertility.

2.1.3 Folliculogenesis

Folliculogenesis is a lengthy process, encompassing initiation of growth of a cohort of primordial follicles from the resting pool, oocyte growth and granulosa cell proliferation. During foetal life, the developing ovaries become populated with primordial germ cells (oogonia), which continue to divide rapidly by mitosis until a few weeks before birth

(Gosden, 1999). The meiotically arrested oocytes become surrounded by somatic cells, forming primordial follicles which represent the first stage of folliculogenesis. Primordial follicles are recruited from a quiescent state into the growing pool by a still undefined signal (Nilsson *et al.,* 2002; Fortune *et al.,* 2000). Later, the maturing follicle becomes responsive to hormones, and produces steroids and growth factors, creating a specialized micro-environment for oocyte maturation. From early in gestation, many foetal oogonia enter meiosis and progress to the first prophase, where they arrest; these are now termed oocytes. Remarkably, they can remain arrested for up to 50 years until they start growing. At this stage, the oocyte is small and surrounded by a single layer of squamous "pregranulosa" cells on a basement membrane (Figure 2.1.4). The stimulation which initiates growth of the primordial follicle remains unknown (Carlsson *et al.,* 2006; Feyereisen *et al.,* 2006; Visser *et al.,* 2006). Most follicles in women of all ages are at the primordial stage, although the total number declines exponentially with age. From before birth, throughout later childhood, puberty, pregnancy and lactation, there is continual recruitment of small numbers of primordial follicles to start folliculogenensis. Initiation of growth is thought to be largely gonadotrophin independent (Picton *et al.,* 2003) and continues until the supply of primordial follicles is virtually exhausted, just after menopause. During the early stages of growth, with the formation of a primary follicle, the granulosa cells become cuboidal in shape and undergo cell division. Subsequently, the oocyte becomes surrounded by increasing layers of granulosa cells. When the follicle reaches the secondary stage, with two or more layers of granulosa cells, a layer of theca cells differentiates from the surrounding stroma around the follicle, and the oocyte starts to secrete the zona pellucida (Figure 2.1.4). During this time the human oocyte itself is growing, until it reaches its mature size of about 120µm in diameter. When there are several layers of granulosa cells, oocyte derived factors initiate differentiation into mural and cumulus granulosa cells (Picton *et al.,* 2003), and when the oocyte is fully grown, a fluid filled cavity (the antrum) appears within the follicle and starts expanding (Figure 2.1.4). A number of factors are thought to be important in early follicular development. For example, kit ligand (stem cell factor), expressed by granulosa cells in primordial follicles may be involved in the initiation of oocyte growth via the c-kit receptor present on the oocyte (Picton *et al.,* 1998). Conversely, the oocyte itself produces growth factors

that regulate granulosa cell proliferation, steroidogenesis and extracellular matrix deposition. Growth differentiation factor 9 (GDF-9) produced by the oocyte is essential for follicular development beyond the primary stage (Hussein *et al.,* 2006). Other growth factors that have been detected in early follicles include members of the insulin-like growth factor family (Walters *et al.,* 2006) and the transforming growth factor family (Jin *et al.,* 1997).

Follicular development from the stage of antrum formation to ovulation is subject to endocrine control, predominantly by FSH (follicle-stimulating hormone). In the later stages of follicle growth, the rate of cell division in the granulosa population slows down, and the cells differentiate and become steroidogenic, utilizing theca-derived androgen to produce increasing amounts of oestradiol. Complex para- and autocrine signalling events are required to regulate folliculogenesis and full acquisition of developmental competence by the oocyte (Eppig *et al.,* 2005; Sugiura *et al.,* 2005)

The primary oocyte of a large antral dominant follicle resumes meiotic maturation in response to the onset of the mid-cycle surge of LH (Conti *et al.,* 2006). A number of cytological events take place around the time the oocyte resumes meiosis, including organelle redistribution (e.g. mitochondrial clustering; migration of the cortical vesicles to the oolemma) and changes in the interactions between the oocyte and the cumulus (e.g. alterations in gap-junctional communication) (Albertini and Barrett, 2003). Increases in activity of phosphodiesterases and reduction in activity of protein kinase A are intrinsically involved in meiotic resumption, initiated by activation of maturation promoting factor (MPF or cyclin-dependent kinase 1) (Jensen *et al.,* 2002). The germinal vesicle breaks down, the spindle is formed, chromosomes align and then segregate to two spindle poles, and visibly, the first polar body is extruded. During this time, the previously tightly packed cumulus and corona cells become mucified and expands (Shimada *et al.,* 2006). The oocyte (now termed a secondary oocyte) is ovulated at metaphase II of meiosis, where it arrests again under the influence of CSF (cytostatic factor), and is only stimulated to complete meiosis by calcium- stimulated processes after fertilization (Hansen *et al.,* 2006; Shoji *et al.,* 2006).

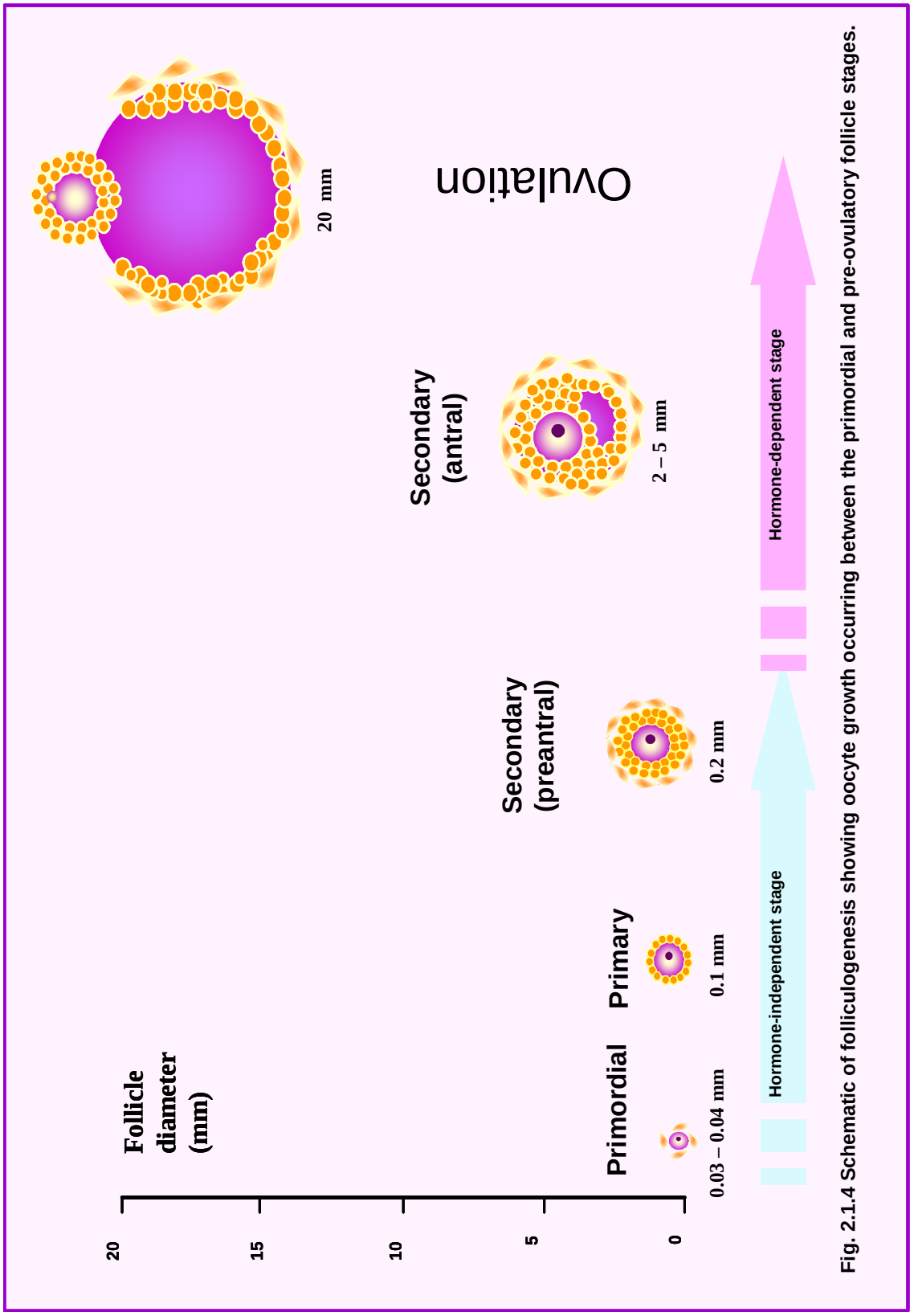

Fig. 2.1.4 Schematic of folliculogenesis showing oocyte growth occurring between the primordial and pre-ovulatory follicle stages.

2.1.4 Spindle Formation and Cell Divisions

The spindle apparatus is an essential cellular organelle, which is required for the segregation of homologous chromosomes during the first meiotic division (a reductional division) and sister chromatids during the second division (an equational division) at spermatogenesis and oogenesis. The spindle is a complex and highly dynamic assembly, suspended in a state of dynamic equilibrium and tensed for action that will begin in anaphase (Figure 2.1.5).

Spindle microtubule is a highly dynamic cylindrical structure formed of 13 linear protofilaments which are composed of many tubulin dimmers consisting of two monomers termed α- and β-tubulin (Figure 2.1.5 A). In the tubulin dimmer, α dimmer is always found with non-exchangeable GTP, whereas the nucleotide associated with the β dimmer can exchange freely (Alberts *et al.,* 2002). All of the spindle microtubules, except the kinetochore microtubules, are in a state of dynamic instability, with their free plus ends shifting stochastically between slow growth and rapid shrinkage (Figure 2.1.5 A). In addition, the kinetochore and overlapping microtubules exhibit a behaviour called *poleward flux*, with a net addition of tubulin subunits at their plus end, balancing a net loss at their minus ends, near the spindle poles (Figure 2.1.5 A, B). At the pole, depolymerization of microtubule minus ends (*poleward flux*) reels in attached chromosomes. At the inner region of the kinetochore, MCAK/XKCM1 induces microtubule depolymerization, while CENP-E localized to the outermost region of the kinetochore, the fibrous corona, and maintains attachment to the plus ends of shrinking microtubules. Cytoplasmic dynein, in association with dynactin, ZW10 and ROD, also localizes to the fibrous corona where its minus end-directed motility drives chromosomes poleward (Wordeman and Mitchison, 1995; Rieder and Salmon, 1998; Figure 2.1.5). A complex interaction between microtubules and motor proteins help oocytes to self-organize spindles (Maro *et al.,* 1985; Hyman *et al.,* 1991)

In meiosis the transition to M-phase and spindle assembly are induced by a high level of active MPF consisting of the cyclin-dependent kinase p34/cdc2 and M-phase cyclin B (Brunet and Maro, 2005). Spindle formation begins after the replication of MTOCs (microtubule-organizing centre), while chromosomes are condensing in the nucleus during prophase I. The MTOC organizes the assembly of microtubules in the cytoplasm.

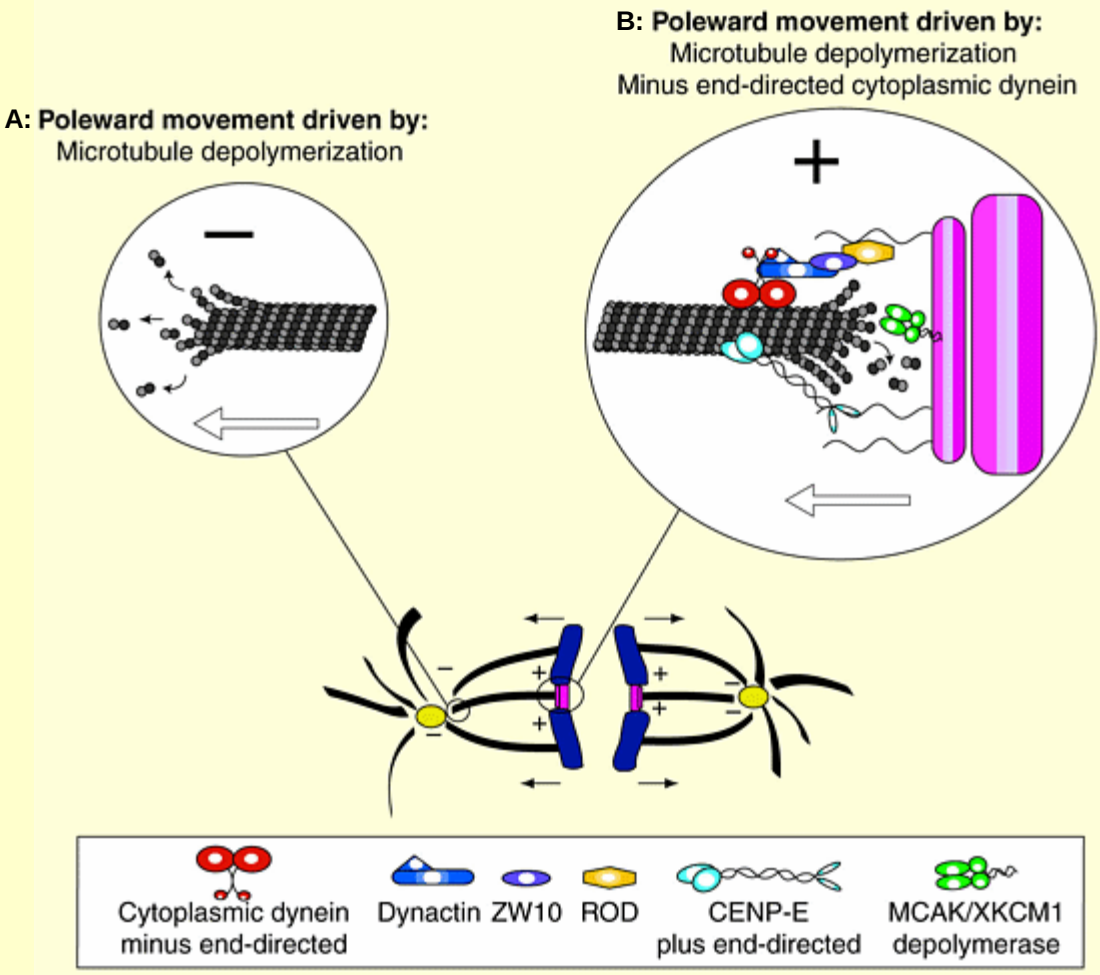

Figure 2.1.5 The highly dynamic structure of spindle apparatus (Banks and Heald, 2001). A: The microtubule is a cylindrical structure formed of 13 linear protofilaments composed of α- and β-tubulin dimmers. B: Depolymerisation of microtubule minus ends reels in attached chromosome.

In mitotic cells the centrosome consisting of a pair of centrioles and pericentriolar material is at the center of the MTOC (Bornens *et al.*, 1984; De Brabander, 1982). In mammalian oocytes is organized by multiple MTOCs, which do not contain centrioles in the presence of pericentriolar material (Szollosi *et al.*, 1972). In the first divisions after fertilization there is neo-formation of centrioles in mouse embryos while other mammals like humans have the centrioles of the sperm to organize the cytoplasmic microtubule network (Gueth-Hallonet *et al.*, 1993; Sathananthan *et al.*, 2006). This demonstrates that the pericentriolar material (PCM) is the substance which carries out the function of the

MTOC in the oocyte. There are many proteins in the PCM which are required for the assembly of microtubules (Maro *et al.,* 1985; Brunet and Maro, 2005). After breakdown of the nuclear membrane (germinal vesicle breakdown, GVBD), the microtubules of the spindle attach to the kinetochores on the chromosomes in order to arrange them on the metaphase plate. When the anaphase-promoting complex (APC, Figure 2.1.6), an ubiquitin ligase that targets the regulatory protein cyclin B for degradation resulting in chromatid separation is activated to induce degradation of the regulatory subunit of the MPF, cyclin B1, the oocyte enters anaphase (Homer 2006). Activation of APC also results in proteolysis of securin, a protein found in a complex with separase, a protease in M-phase. Release from securin activates separase to proteolytically cleave proteins from the cohesion complex holding the sister chromatids together (Eichenlaub-Ritter 1998; McKee 2004; Homer, 2006). Upon loss of cohesion at chromosome arms, chiasmata are resolved and sister chromatids are separated and drawn to both spindle poles by the spindle microtubules (Kudo *et al.,* 2006). After cytokinesis, on transition to the next interphase the chromosomes of mitotic cells are released and surrounded by the reformed nuclear membrane. At meiosis, second prometaphase and metaphase II are entered, and the loss of cohesion between centromeres of sister chromatids is again, triggered by activation of APC after fertilization.

All processes of spindle assembly are controlled by a regulatory system – the spindle assembly checkpoint system (SAC) (Tan *et al.,* 2005; Maiato *et al.,* 2004; Homer 2006; Figure 2.1.6). Many proteins have been identified as components of the spindle checkpoint. Mad (mitotic arrest-deficient) and bub (budding uninhibited by benomyl) proteins are known components of this system (Hoyt *et al.,* 1991; Li and Murray 1991 and Roberts *et al.,* 1994). During regulation of the cell cycle, the spindle checkpoint system is responsible for monitoring the attachment of microtubules to kinetochores on chromosomes and development of tension forces on bi-oriented chromosomes (Tan *et al.,* 2005). When the SAC is activated, it prevents activation of the anaphase-promoting factor (APC) and the transition from metaphase to anaphase (Figure 2.1.6). Exit from mitosis or meiosis may be delayed until disturbances are eliminated (Rudner and Murray, 1996; Homer 2006), or a long, persistent block may be induced. Long mitotic arrest may ultimately induce apoptosis and removal of aberrant somatic cells, e.g. in protection from

chromosomal aberrations and tumor progression (Weaver and Cleveland 2005; Kolman, 2005).

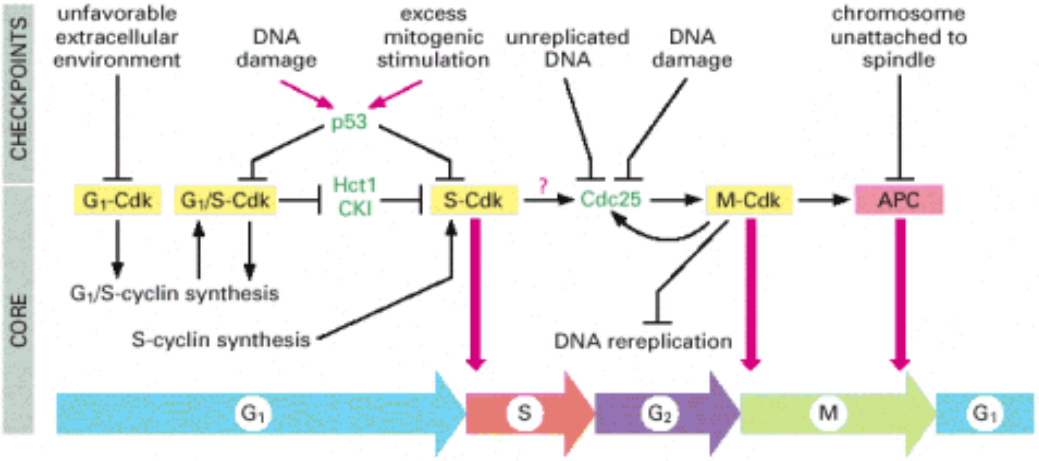

Figure 2.1.6 Stages at which checkpoint controls can arrest passage through the cell cycle. DNA damage due to irradiation or chemical modification prevents G_1 cells from entering the S phase and G_2 cells from entering mitosis. Unreplicated DNA prevents entry into mitosis. Defects in assembly of the mitotic spindle or the attachment of kinetochores to spindle microtubules prevent activation of the APC polyubiquitination system that leads to degradation of the anaphase inhibitor. Consequently, cells do not enter anaphase until all kinetochores are bound to spindle microtubules (adapted from Alberts *et al.*, 2002).

Compared to the mitotic spindle, the meiotic spindle in oocytes exhibits some characteristic features that are not common to other somatic cells. The meiotic spindle is a symmetrical, barrel-shaped structure containing anastral broad poles, located peripherally and radially oriented. In oocytes, pericentriolar material (PCM) carries out the function of MTOC (Szollosi *et al.*, 1972). In the cytoplasm of oocytes arrested in prophase I the critical concentration for tubulin assembly is so high that PCM cannot organize the polymerization of microtubules in the cytoplasm of oocytes before resumption of meiosis (Maro *et al.*, 1985). Oocyte growth is required to permit the oocyte to increase its size and synthesize the necessary RNA and proteins for cell cleavage after fertilization and early embryo development. The meiotic spindle checkpoint system appears different to the mitotic system in order to control the progression through two successive M-phases of meiosis I and II without an intermittent interphase. Oogenesis in humans and many other

mammals is discontinuous in that oocytes remain arrested at metaphase II after ovulation, in spite of the alignment of chromosomes at the spindle equator, a situation that leads to activation of APC in mitotic cells (Sun and Nagai, 2003). This is due to the activity of the cytostatic factor (CSF) involving synthesis and activity of the Mos kinase, MAP kinase activation and differential phosphorylation of several proteins in oocytes (Brunet and Maro, 2005).

According to the previous finding, it appeared initially that the spindle checkpoint is more relaxed in oogenesis relative to mitosis and male meiosis (LeMaire-Adkins *et al.,* 1997; Yin *et al.,* 1998b). Now it is known that especially the aged oocytes may contain fewer messages of components of the spindle checkpoint (Steuerwald *et al.,* 2005) Alterations in expression with age could thus have profound influences on oocyte quality and ability to segregate chromosomes correctly. It is unknown whether and to what extent sub-optimal conditions during oocyte growth and maturation may compromise checkpoint controls. Some components of the spindle checkpoint system, e.g. Mad2, behave differently in female meiosis as compared to male meiosis and mitosis. In female meiosis Mad2 protein is constitutively present at centromeres of metaphase II chromosomes in spite of aligned chromosomes, whereas it becomes dissociated from kinetochores at metaphase I and II upon congression of chromosomes in spermatogenesis and mitosis (Kallio *et al.,* 2000; Wassmann *et al.,* 2003). Emi 1 and Emi 2 are components of CSF inhibitors of the oocyte APC, which at the metaphase to anaphase transition at meiosis II (Schmidt *et al.,* 2006). Calcium transients and activation of Calcium calmodulin kinase II by fertilization then ultimately inactivates Emi2, causes release from inactivation of APC, and finally, APC activation, proteolysis of cyclin and cohesion protein and progression to anaphase II in mammalian oocytes (Schmidt *et al.,* 2006).

2.1.5 Aged Oocytes

Spindle aberrations are a hallmark of aged oocytes (Battaglia *et al.,* 1996; Volarcik *et al.,* 1998; Eichenlaub-Ritter *et al.,* 2004) and may also indicate that the expression patterns for cytoskeletal proteins and maternal factors are disturbed in the oocyte (Hamatani *et al.,* 2004). Certainly, exposures during maturation (Eichenlaub-Ritter *et al.,* 2002), freezing (Rienzi *et al.,* 2005; Bianchi *et al.,* 2005) and ageing processes (Eichenlaub-Ritter *et al.,*

2004) causing disturbances in the regulation of spindle formation are associated with a high risk of chromosome mal-segregation, and, in consequence, may lead to a reduced reproductive potential and survival of embryos and live births in humans (Plachot, 1992). Critical assessment of spindle integrity and function plays therefore an important role in determination of oocyte health and developmental competence in assisted reproduction (Keefe, 2003; Eichenlaub-Ritter *et al.,* 2002).

2.1.6 Zona Pellucida Formation

Growing and fully maturing oocytes are protected by a multi-laminar glycoprotein coat, termed the zona pellucida. The zona glycoproteins appear to be co-ordinately secreted by the oocyte during folliculogenesis, as shown in the mouse (Epifano *et al.,* 1995; Soyal *et al.,* 2000), while there is evidence from other species, including the human, that granulosa cells may also contribute to stage-dependent zona protein expression during folliculogenesis e.g. in humans (Sinowatz *et al.,* 2001; Bogner *et al.,* 2004; Gook *et al.,* 2004). Human oocytes express three highly conserved zona proteins, which change conformation after cortical granule extrusion at fertilization, as in the mouse (e.g. Moos *et al.,* 1995; Nikas *et al.,* 1994). Another human zona protein (ZPB) may contribute in unknown ways to species-specific sperm–oocyte interactions in human fertilization (Lefievre *et al.,* 2004). ZP1 proteins are required for the structural integrity of the zona pellucida (Greve and Wassarman, 1985; Wassarman *et al.,* 2004). At the ultrastructural level, the three-dimensional highly ordered filament structure of the zona pellucida has been confirmed by studies in mammalian oocytes, including human oocytes (Figure 2.1.7 A; Familiari *et al.,* 1992; Green, 1997; Wassarman *et al.,* 1999 and 2004; Oehninger, 2003). On the molecular level, the zona pellucida consists of a paracrystalline, three dimensional network structure composed of heterodimeric filaments of ZP2 and ZP3 proteins, cross-linked by ZP1 proteins, as originally proposed by Wassarman (Figure 2.1.7 B; Wassarman, 1988; Qi *et al.,* 2002; Wassarman *et al.,* 2004). Within the zona, the projections may form a hexagonal network together with zona fibrils, and thus may contribute to the three-dimensional organization of the extracellular space (Motta *et al.,* 1994; Albertini and Rider, 1994; Albertini and Barrett, 2003). Polarization microscopy

showed that the inner layer of fibres is radically organized while the outer layer envelopes the oocyte circularly (Figure 2.1.7 B, arrows).

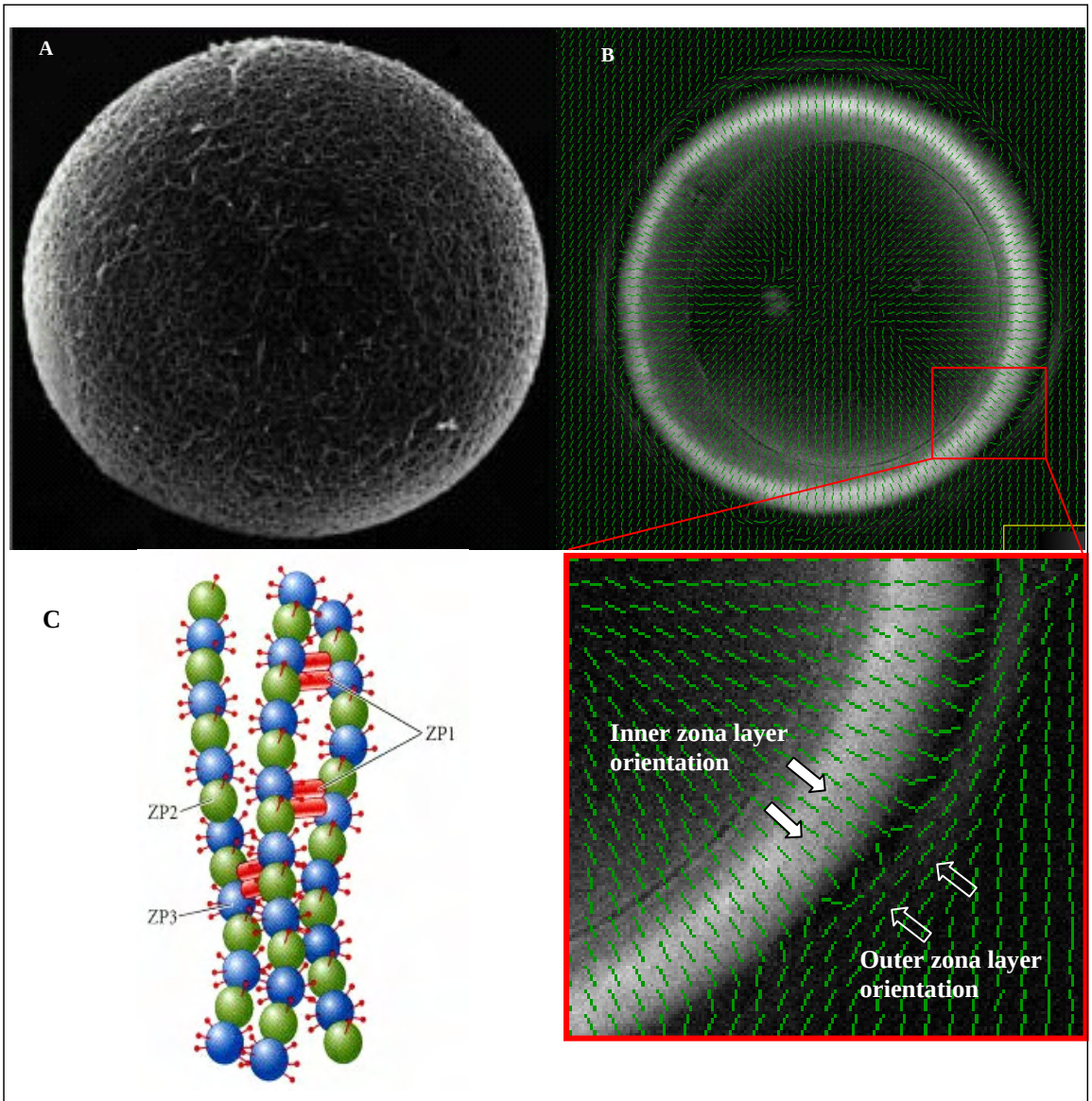

Figure 2.1.7 The three dimensional network of zona pellucida. A: The network structure of zona pellucida imaged by transmission electron-microscopy (Magerkurth *et al.*, 1999); B: The molecular orientation of zona pellucida shown with vectors (arrows) by PolScope microscopy; C: The network structure in molecular level (modified from Green, 1997).

ZP1 proteins are required for the structural integrity of the zona pellucida (Greve and Wassarman, 1985; Wassarman *et al.,* 2004). Although oocytes of mice lacking the *ZP1* gene are still secreting the ZP2 and ZP3 proteins, they possess a thinner and more loosely organized zona pellucida, relative to the wild type. The diameter of ovulated oocytes from the *ZP1* -/- homozygote is on average only half of that of oocytes from the wild type (Rankin *et al.,* 1999). This suggests that effective granulosa cell-oocyte signalling may depend on the presence of a functional, highly structured zona, and that disturbances cause sub-fertility. Apart from this, reduced expression of zona proteins during oocyte growth and folliculogenesis may indicate general problems in the highly orchestrated processes of maturation at the critical phase of oogenesis and folliculogenesis when oocytes acquire full nuclear and developmental competence.

The zona pellucida is also essential for oocyte fertilization and implantation development *in vivo* (e.g. Rankin *et al.,* 2001b). It serves taxon-specific sperm-binding (Tsubamoto *et al.,* 1999; Miller *et al.,* 2002; Wassarman, 2002), prevents polyspermy (Yanagimachi, 1994; Hoodbhoy and Dean, 2004), and protects embryos from mechanical stress prior to implantation (Herrler and Beier, 2000). Accordingly, defects in the zona pellucida are usually associated with fertilization problems or developmental abnormalities. For instance, mice lacking *ZP3* or *ZP2* genes are unable to form a zona pellucida and are sterile (Liu *et al.,* 1996; Rankin *et al.,* 2001a). Postovulated aging of oocytes associated structural changes and increased fertilization failures in mouse zona pellucida (Diaz and Esponda, 2004). Formation and retaining a functional structure of zona pellucida is therefore essential for the female fertility.

2.1.7 Organisation of Spindle Apparatus and Zona Pellucida May Reflect the True State of Oocyte Healthy and Their Developmental Competence

The spindle is formed during prophase I and serves to properly segregate chromosomes during meiosis. Experimental data obtained mainly from *in vivo* or *in vitro* maturing mouse oocytes suggest that formation of asymmetric, aberrant or mono- or multipolar spindles (e.g. de Pennart *et al.,* 1993; Eichenlaub-Ritter and Betzendahl, 1995; Zuelke *et al.,*1995; Tarin *et al.,* 1996; Yin *et al.,* 1998a,b; Can and Semitz, 2000; Cukurcam *et al.,*2004), disturbances in tubulin turnover or activity of motor proteins (Mailhes *et al.,*

2004), and ablation of surveillance mechanisms sensing chromosome attachment and spindle integrity (Eichenlaub-Ritter *et al.,* 2005; Homer *et al.,* 2005) frequently occur in association with oocyte aneuploidy, which may lead to an aneuploid oocyte and embryo with reduced developmental capacity, implantation failures or spontaneous abortion (Battaglia *et al.,* 1996; Shen *et al.,* 2005; Hodges *et al.,* 2002). In addition, spindle abnormalities and aberrant behaviour of chromosomes may be induced by failures in chromatin regulation, chromosome condensation or physical detachment of chromosomes at anaphase (e.g. Mailhes *et al.,* 1996; Tateno and Kamiguchi, 2001; De la Fuente *et al.,* 2004; Akiyama *et al.,* 2006).

Although the zona pellucida is formed already at early stages of oocyte growth it is involved in several important events during ovarian folliculogenesis and after fertilization. The zona pellucida is crossed by radially arranged transzonal cytoplasmic projections from the cumulus granulosa cells which project onto the oolemma or even invade the cytoplasm of the oocyte during oocyte growth and maturation. Cell-cell contacts on these cell processes provide the conditions for direct junctional coupling, cell-to-cell signalling, and exchange of molecules between the oocyte and the somatic compartment (Motta *et al.,* 1994; Albertini and Rider, 1994), which are important for oocyte growth and sustained meiotic arrest (Eppig 1991; Webb *et al.,* 2002). The zona pellucida is important for oocyte growth and folliculogenesis. Lacking in any ZP proteins may lead to dysfunction of the zona pellucida and disturbances in the granulosa cell-oocyte signalling events. Defects in the zona pellucida are usually associated with fertilization problems and developmental abnormalities (Liu *et al.,* 1996; Rankin *et al.,* 2001a). A treatment with anti-zona antibodies, which were detected in some infertile patients (Shivers and Dunbar, 1977), induced a significant reduction of mucification rate of follicles and maturation as well as fertilization rate of oocytes in mouse (Koyama *et al.,* 2005). Therefore, the organisation and texture of both spindle apparatus and zona pellucida may therefore help to identify the state of oocytes during growth and maturation as well as the autocrine signalling between the oocyte and the somatic compartment in the follicle, which is directly correlated with oocyte developmental competence after fertilization.

2.2 Methodologies to Evaluate the Sub-microscopic Structures (Spindle and Zona Pellucida) in Human Oocytes

2.2.1 Invasive Analysis Procedures for Illumination of Spindle Apparatus and Zona Pellucida

Biological materials are transparent or translucent. To view the ultrastructure of oocytes under a light microscope, exogenous dyes or fluorescent labels have been employed to enhance the contrast or colour of images/ cell organelles (fluorescent microscopy). Another way to study the fine structure of a biological sample is electron-microscopy using an electric beam which becomes altered by presence of heavy metals bound to cellular structures after fixation. However, both procedures are invasive. However, only a static view of the structure in fixed oocytes can be provided using those procedures.

2.2.1.1 Indirect Anti-tubulin Immunofluorescence and Laser Scanning Confocal Microscopy

Indirect anti-tubulin immunofluorescence is a method to assess spindles morphology and chromosomal behaviour (Eichenlaub-Ritter and Betzendahl, 1995). Conventionally, oocytes have to be extracted, fixed and placed on a poly-L-lysine coated slide for staining and later evaluation (Eichenlaub-Ritter and Betzendahl, 1995). A monoclonal anti-α-tubulin antibody binding to tubulin molecules specifically and a second polyclonal FITC conjugated antibody binding to the first monoclonal antibody can be employed for immune staining. The spindle can be analyzed by fluorescent microscopy and images saved for demonstration or evaluation by a digital camera. However, especially in oocytes treated by non-ionic detergent for better antibody penetration during or before fixation, the spindle may be flattened on the slide during the attachment process. Usually, with conventional fluorescence microscopy a two-dimensional image is obtained. In contrast, the oocyte spindle in the living state is three-dimensional and quantitative information on relative thickness or density of spindle fibres is hard to obtain (Shen *et al.,* 2005). The introduction of a clotting technique in which oocytes are first embedded in a matrix of a fibrinogen/thrombin clot prior to fixation and extraction to retain their 3-D dimensional shape and restrict extraction can overcome some of these problems but requires complex three-dimensional image reconstruction software (Hunt

et al., 1995). Under these conditions, however, spindles may be oriented by chance parallel or upside down or oblique with respect to the plane of view. Some programs have been developed to combine optical sections, and tilt them in the desired orientation for qualitative and quantitative assessments. However, this requires large data bases and optimizing to take optical sections of the spindle using laser beams by the confocal microscope.

Imaging by laser scanning confocal microscope has made it thereby possible to view the 3-D structure of spindle morphology and analyze chromosome congression accurately within the spindle body and the oocyte. The basic concept of confocal microscopy was originally developed by Marvin Minsky in the mid-1950s (Minsky, 1961; Minsky, 1988). Following Minsky's work, M. David Egger and Mojmir Petran fabricated a multiple-beam confocal microscope in the late 1960s that utilized a spinning disk for examining unstained brain sections and ganglion cells. During the late 1970s and the 1980s, advances in computer and laser technology, coupled to new algorithms for digital manipulation of images, led to a growing interest in confocal microscopy (Amos and White, 2003). Tony Wilson, Brad Amos and John White demonstrated the utility of confocal imaging in the examination of fluorescent biological specimens (Amos and White 2003, Hamilton and Wilson, 1982). Confocal microscopy offers several advantages over conventional wide field optical microscopy, including the ability to collect serial optical sections from thick specimens and reconstruct three-dimensional images that cannot be obtained through the microscope eyepieces by conventional microscopy.

2.2.1.2 Electron-Microscopy

Electron microscopes are scientific instruments that use a beam of highly energetic electrons to examine objects on a very fine scale. It was developed due to the limitations of conventional light microscopes, which are restricted in resolution by the physics of light and the aperture of the lenses to a maximal 500x or 1000x magnification. Electron microscopy can yield the information of the shape and size of particles/structures in the object, e.g. in biological samples usually those structures and cell organelles stained by osmium tetroxide, uranyl acetate and/or lead citrate. However, similar to

immunofluorescence microscopy, only fixed specimens can be observed by electron microscopy, and hundreds of sections sized only few micrometers in diameter have to be combined to yield a 3-D image of the fairly large human oocyte. Thus, only restricted numbers of cells have been studied in most cases; images are static, and, depending on contrast obtained by introduction of heavy metal staining after fixation by aldehydes, processes that may lead to morphological alterations.

2.2.2 Non-invasive Analysis of Ultra-Structures in Mammalian Oocytes

2.2.2.1 Development History of Polarized Light Microscopy

In order to avoid fixation of living cells for an analysis of morphology, e.g. in the study of spindle structure and formation, polarization microscopy has been employed in biology and medicine. Macromolecular structures, which are composed of ordered molecules, such as membranes, microtubules, microfilaments, have been observed with this method for about 50 years (Inoué, 1953). The images are obtained due to the optical properties of such components, namely birefringence. Birefringence is an intrinsic property of a sample, which contains structures with a crystalline/paracrystalline molecular order- irrespective of whether this is in a biological sample or ordered matter, for instance in crystals.

The conventional polarization microscope (Figure 2.2.1 b) is equipped with a polarizing filter to produce polarized light - usually linearly polarized light. An analyser lens is oriented such that only light vibrating in a plane perpendicular to that of the polarizer can pass. An additional optical system, termed compensator, is required to view biological materials, due to their weak birefringence, relative to the non-biological sample (Sato *et al.*, 1975; Oldenbourg, 1999). The compensator can be rotated and manually adjusted relative to the light path to allow light whose path has been changed by passing through the object to be viewed against a dark background to perform qualitative and quantitative polarization microscopy. When a birefringent specimen is placed between the polarizer and analyser, and the compensator optics is rotated such that the polarised light can pass through, it becomes visible (Figure 2.2.1 b). Due to the orientation dependence and the complicated manipulation of imaging, the application of conventional polarization microscopy in analysis of biological specimens has been limited for years.

Ten years ago, a new type of polarized light microscope, computer-assisted polarization microscopy (PolScope microscopy), was developed and has been used to detect birefringent structures in living cells (Oldenbourg *et al.,* 1993; Figure 2.2.1 a). This new system uses nearly circularly polarized light as an illumination source so that it is now possible to view birefringent structures irrespective of the orientation of the sample within the plane of view. In addition, the employment of a computer controlled liquid crystal compensator enhanced the sensitivity of the polarizing microscopy and ensured a quantification of the birefringence property of the sample without any mechanical readjustment to the optical components. A Colour-coded Doppler camera (CCD camera) and analysis software make it possible, to measure the specimen birefringence for all points of the image. For a couple of years, PolScope microscopy has been employed to analyze the spindle integrity and morphology in living oocytes of mouse, hamster and human (Liu *et al.,* 2000 a; Silva *et al.,* 1997; Wang *et al.,* 2001 a;b;c). Liu *et al.* (2000a) noted that the PolScope light intensity used to illuminate the sample (60µW) is similar to that of differential interference contrast (DIC), which was already employed in *in vitro* fertilization (IVF) in assisted reproduction for more than 20 years. Importantly, the initial analysis and more recent reports confirm that the developmental capacity of oocytes do not differ between the control and oocytes illuminated with the PolScope (Liu *et al.,* 2000a).

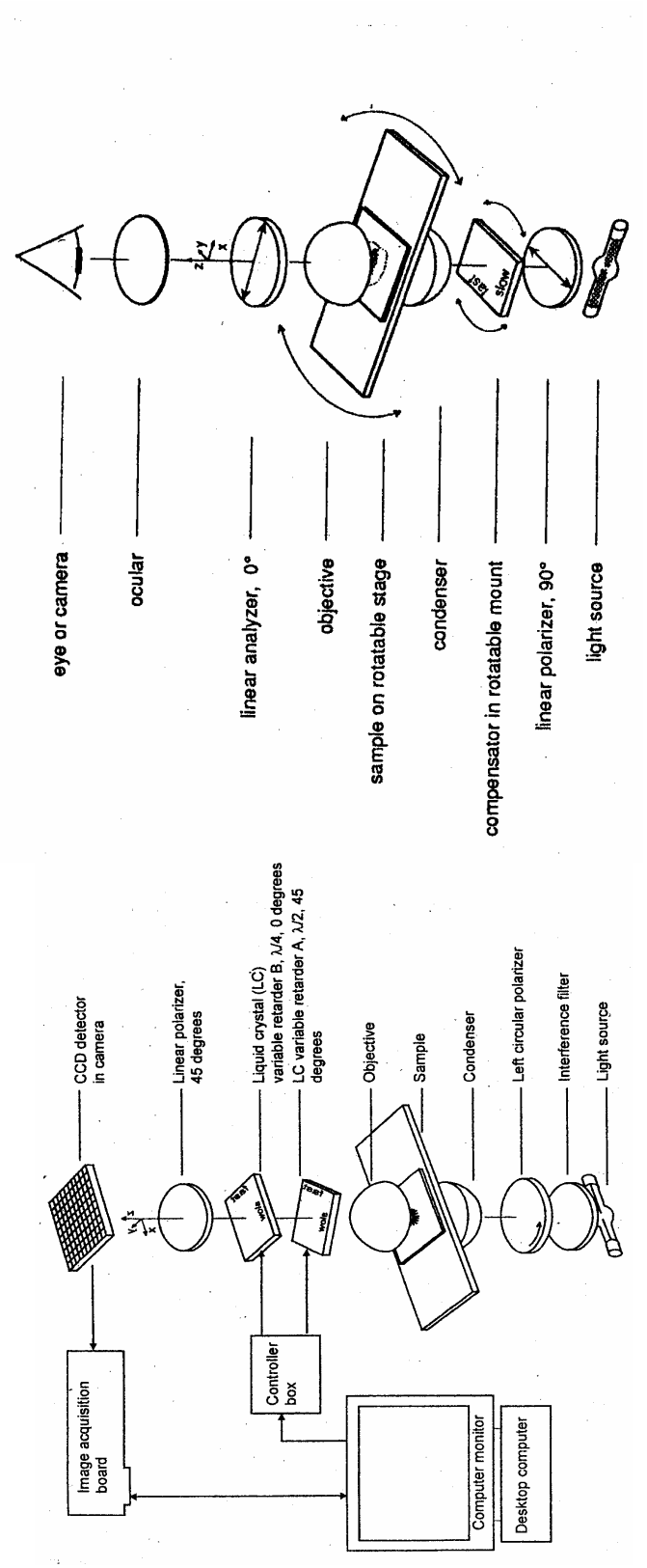

Figure 2.2.1 Conventional (b) and the newly developed (a) polarized light microscope

2.2.2.2 Quantitative Analysis of Birefringence Property Using Polarized Light Microscopy

When a light beam enters a birefringent body, it is split into two beams whose vibration planes are perpendicular to each other. One beam, which is called ordinary ray satisfies Snell's law of refraction [sin α (incidence angle) /sin β (refraction angle) = const.]. The other one does not satisfy Snell's law. It is called extraordinary ray. This is due to a difference in refractive index of the birefringent body for the two orthogonally polarized light beams (Oldenbourg, 1991; 1996). Polarization microscopy measures the relative change in phase between the two polarized beams, termed retardance, to quantify the birefringent property of the sample. Sato *et al.* (1975) was the first to quantify the birefringence of the spindle apparatus using polarization microscopy. It was demonstrated that highly aligned, paracrystalline ordered microtubules within the spindle were at the basis of the birefringent properties of this cell organelle. Furthermore, a positive correlation between spindle density and the retardance of light in the spindle has been determined using the conventional polarized light microscope. Thus, the relative magnitude of light retardation is an indicator for density, high order alignment, or thickness of a birefringent object. In 1993, Oldenbourg and his colleagues developed the computer supported enhanced polarization microscope (PolScope) to measure the distribution of birefringence in asters dispersed in lysates of *Spisula* oocytes (Oldenbourg *et al.*, 1993). In the following year, Tran *et al.* were the first to measure the birefringence of striated muscle using the newly developed PolScope (Tran *et al.*, 1994). They also quantified the retardance of polarized light by single and bundled *in vitro* polymerized microtubules (Tran *et al.*, 1995). A linear correlation between the peak retardance of light and the mean number of microtubules has been detected. It confirmed the previous finding that the birefringent property positively correlated with the density of a structure. Based on the positive correlation between fibre density and the retardance of light in the ultrastructure, quantitative analysis of the retardance has also been performed to assess oocyte health and developmental capacity. Oldenbourg *et al.* (1998) developed a novel quantification method to measure the birefringent property in two-dimensional levels. Recently, LaFountain and Oldenbourg (2004) succeeded to measure quantitatively by PolScope microscopy the retardance of light by kinetochore fibers of individual

chromosomes in meiotically dividing crane fly spermatocytes with respect to their behaviour on the spindle. They calculated microtubule density and traction forces on chromosomes that were segregating normally or had so called merotelic attachments (attachment of one centromere of a chromosome to both spindle poles).

2.2.2.3 Non-invasive Nature of PolScope Microscopy

The polarized light microscope has the potential to measure submicroscopic molecular order dynamically and non-destructively in living cells. The design of PolScope is based on the same principle of light, as used for differential interference contrast (DIC), which has been used for clinical purpose for over 20 years. PolScope utilizes nearly circular polarized light with a wavelength of 546 nm as light source, which contains no detrimental component in either infrared or ultraviolet fields. Moreover, the light intensity in the sample is approximately 60µW, which is also in the safe zone (Liu *et al.,* 2000a). Meiotic spindles in oocytes of many different mouse strains, such as CF1, C57B6, B6C3F1, as well as hamster have been viewed by PolScope microscopy (Liu *et al.,* 2000a). Studies with mouse oocytes viewed by PolScope suggested that PolScope microscopy is non-invasive since imaged oocytes had a similar developmental capacity in cleavage rate and pregnancy rate, in comparison with controls (Liu *et al.,* 2000a). A further study with 770 human oocytes from 87 ICSI cycles showed that the light illumination with PolScope did not appear to affect oocyte and embryo health in humans (Wang *et al.,* 2001c).

Observations in human oocytes that were subjected to ICSI for assisted conception supported the notion of the non-invasive nature of the technique and its safety with human oocytes. The rate of blastocyst formation of oocytes illuminated by PolScope (Wang *et al.,* 2001c) is equal to the rate of oocytes without illumination (Ebner *et al.,* 2005). PolScope allows assessing the dynamic changes in polymerization kinetics of organized sub-microscopic molecular structures of spindle (Liu *et al.,* 2000b). Thus, PolScope has the potential to observe the spindle in individual cells and provides a new tool to assess the spindle in human oocytes for clinical purposes and in experimental animals to test for dynamic interactions with spindle formation.

2.3 Human Infertility and Current Practices in Assisted Reproduction

2.3.1 Current Practices in Assisted Human Reproduction

Infertility affects more than 80 million people around the world. Although infertility may not be a public health priority in many countries, it is a central issue in the lives of the individuals who suffer from it.

Since the first birth of a child by *in vitro* fertilization, nearly 1 million babies have been born with the help of assisted reproductive technology (ART) (Soini *et al.,* 2006). The introduction of ART has resolved social and psychological pressures for infertile couples, particularly for the woman. In the past decades ART has been greatly improved. The introduction of intracytoplasmic sperm injection (ICSI) ensures a much better outcome for infertile couples with a male factor, a condition for which results of traditional treatment have not been satisfactory.

With all these advances, however, many challenges are still to be faced. The treatment of infertility by ART is expensive. The success rate of ART is currently around 25% live births per cycle (Fauser *et al.,* 2002). In other words, each couple should, in principle, repeat the ART program four times, to get a live birth. The relative high cost of ART procedures leaves many infertile people without the option of treatment. There is room for improving the success rates of assisted reproduction, in order to reduce the economic cost and psychological pressures on the patients. How to make ART more widely available and affordable for all who need is the current challenge that cuts across all others.

To improve the outcome of ART, more than one embryo is transferred back to the uterus in most countries. However, increase in the number of embryos for transfer induces an increased risk of multiple pregnancies (Soini *et al.,* 2006). An achievement of IVF treatment requires that methods should be improved such that a relatively large number of high quality oocytes can develop to live births for each patient.

However, it is well known that the risk of aneuploidy increases with advanced maternal age in oocytes, embryos and live birth such decreasing dramatically the implantation rates after *in vitro* fertilization (Gianaroli *et al.,* 2003). Certainly, selection of chromosomally normal embryos could help to improve the low success rate in ART, especially in women of advanced age (Battaglia *et al.,* 1996). Transferring euploid embryos has decreased the clinical abortion rate and increased the implantation rate in assisted reproductive

technologies (ART) (Munne, 2005; Soini *et al.,* 2006; Verlinsky *et al.,* 2004). Unfortunately, embryos with aneuploidy cannot be identified accurately using only the presently available morphological criteria (Gianaroli *et al.,* 2003; Magli *et al.,* 2001).

The attitudes towards embryo selection vary substantially in different countries. In most IVF programmes, embryos are transferred to the uterus at the cleavage stage at day 2 or 3 post-insemination (Dawson *et al.,* 1995). The implantation rate is around 12.5-15% in the last 15 years (Edwards and Craft, 1990). According to German Embryo Protection Law, embryo selection after IVF and ICSI have to occur at 18 hours post-insemination (Zollner *et al.*, 2002) using a pronuclear scoring system, based on the morphological character of the pronuclear configurations (PN) (Scott, 2003) or other morphological characteristics like presence of a halo etc.. Only those embryos, which are selected to be transferred, can be legally cultured after the PN stage. Culture of more than three embryos to cleavage stage or blastocyst stage is therefore prohibited. In Germany, the implantation rate with a selection of pre-embryos at PN stage is around 15% (DIR Jahrbuch 2004). In Italy, selection can be only on oocytes, not embryos, the timing of embryo selection, such that decisions are placed even before insemination, due to the ethical and legal constrains (Simini *et al.,* 1999). A prolonged culture to blastocyst stage, which by itself may result in development of the healthiest embryos, has been shown for some laboratories to improve the implantation rate after blastocyst transfer up to approximate 25 – 30% (Feinberg *et al.,* 2006). However, such methods are prohibited in those countries with religious or ethical concerns regarding the destruction of non-selected but basically viable embryos. Clearly, the presently used morphological criteria for pre-embryo selection (pronuclear scoring system) appear less efficient compared to the selection systems based on evaluations and criteria inherent to the embryo at the blastocyte stage. Improving the assessment criteria for oocyte quality, in order to select oocytes and embryos with the highest developmental potential as early as possible for transfer, is therefore becoming an essential issue, which may help to improve implantation rates, especially in counties like Germany or Italy.

2.3.2 *In vitro* Maturation of Human Oocytes is Becoming a Novel Method for Some Infertile Patients

Assisted reproduction technology (ART) has been successfully used to overcome male and partially female infertility, since the birth of the first child by *in vitro* fertilization (IVF) 20 years ago (Cohen *et al.,* 2005). However, IVF is time-consuming and expensive, and generates much stress, side effects and risk for complications. In general, IVF utilizes the principle of gonadotrophin administration for oocyte maturation prior to oocyte retrieval from mature follicles. There are several conditions, which restrict success of IVF. For instance, patients with ovarian hyperstimulation syndrome (OHSS) may suffer from severe side effects of the stimulation protocol. In addition, most oocytes remain at the germinal vesicle stage up to retrieval in some patient groups. For instance, patients with polycystic ovarian syndrome (PCOS), tend to have lower sensitivity to gonadotrophin stimulation. Therefore, *in vitro* maturation (IVM) of immature oocytes followed by fertilization *in vitro* and embryo transfer offers an alternative to conventional IVF treatment with increasing requirement for gonadotrophin non-sensitive patients. Treatment of IVM has many advantages, such as reduced cost, fewer potential side effects and, in particular, the risk of developing ovarian hyperstimulation syndrome (OHSS), due to the minimised drug administration (Chian, 2004; Mikkelsen, 2005). IVM technology also benefits young patients, especially those who have to undergo a potentially sterilizing chemo- or radiotherapy treatment prior to engaging in reproduction activities. In such cases, the ovary tissue of patients can be cryopreserved in liquid nitrogen at –196°C. Oocytes can be matured and fertilized *in vitro* before embryo transfer after the chemotherapy is over, patients are adult and want to conceive children of their own genetic background. Moreover, IVM technology also provides donor oocytes for patients who experience premature ovarian failure or those with gonadal dysgenesis.

Hormone stimulation promotes the maturation of most meiotic competent oocytes *in vivo*, but there are some oocytes (5-15%) remaining at germinal vesicle stage at the time of puncture. Fortunately, the majority of naked immature oocytes from ICSI patients mature spontaneously *in vitro* after 24-36 hours of culture (Combelles *et al.,* 2002). IVM can therefore provide more competent oocytes for fertilization *in vitro* and increase the chance of pregnancy in ICSI patients.

2.3.3 Assessing Oocyte Quality as a Way to Improve ART Outcomes

Oocytes are the only mammalian cells capable of forming a new individual after fertilization, whereas sperm provides mainly its chromatin/DNA and the sperm aster to the new offspring. Oocytes can therefore be regarded as the main source of cytoplasmic components beside of contributing their genome for the genesis of an embryo. Unfortunately, up to now oocytes with poor quality can still not be identified non-invasively by the present assessment criteria (Gianaroli *et al.,* 2003), whereas well-defined morphological criteria for sperm and embryo have been established (Henkel and Schill, 2003; Scott, 2003; Edwards and Hansis, 2005). Many morphological features associated with poor developmental competence have been demonstrated (Bolton *et al.,* 1989). However, the currently used imaging techniques in assisted reproduction provide only few essential information for diagnosis of oocyte dysfunction. The application of preimplantation genetic diagnosis (PGD) against aneuploidy and other chromosome abnormalities helps to select embryos with normal karyotype for transfer and reduce the rate of spontaneous abortion after implantation (Twisk *et al.,* 2006). However, invasive methods such as chromosomal analysis in polar bodies and blastomere are complicated, expensive and produce more pressure on patients. Up to now, only a few predictive non-invasive markers for oocyte quality have been identified on the basis of morphological criteria, which can be assessed in assisted reproduction by using conventional microscopy prior to insemination (Ebner *et al.,* 2003; Rienzi *et al.,* 2005).

Thus, the identification of non-invasive markers to achieve a high success rate of infertility treatment has raised increasing interest. The search should be intensified in order to achieve pregnancies since there appear currently only few options to improve treatment regimens and it would be in the interest of the clinician as well as to the benefit of the patients to simple, cheap and safe methods to identify oocyte of the highest quality.

In this respect, orientation independent polarizing microscopy (PolScope) was a breakthrough. Two essential structures in oocytes are composed of a molecularly ordered structure that has been accessible to polarization microscopy, the spindle apparatus and the zona pellucida. According to the finding in earlier studies (Sato *et al.,* 1975; Tran *et al.,* 1994; 1995; Oldenbourg *et al.,* 1998), the birefringent property may describe the organisation, i.e. density and texture, of a macromolecular structure properly. The newly

developed method has been successfully employed in a preliminary study to investigate the alteration of spindle morphology in the presence of tubulin-depolymerising and stabilising agents (Nocodazole and Taxol) in *in vitro* maturing mouse oocytes. During 60 minutes exposure to 1μM Taxol the time and dose-dependent elongation of spindle was observed in living oocytes (Eichenlaub-Ritter *et al.,* 2002). The dose response in shortening of interpolar distance of meiotic spindle induced by Nocodazole was also determined in living mouse oocytes and confirmed by conventional immunofluorescence in fixed oocytes (Shen *et al.,* 2005). The study using animal material showed that PolScope is an especially sensitive method to reveal influences of chemicals on spindle integrity in oocytes and established a novel system to assess spindle mass and integrity *in vivo*, based on the birefringent property of spindle. The newly developed non-invasive methodology has been therefore employed to retrospectively assess the quality of human oocytes by analysing for the first time the optical properties of spindle and zona pellucida by analysing mean retardance magnitude of light using polarization microscopy.

3. Aim of the Study and Experimental Design

3.1 Requirement of Identifying the Oocyte Quality to Improve the Success Rate of ART

The number of infertile couples is increasing not least because of advanced maternal age. Also, the quality of gametes has deteriorated owing to lifestyle habits and environmental factors. Since the first birth of a baby by IVF in 1978, we have seen an explosive development in human assisted reproduction. ART is becoming the major procedure to overcome human infertility. However, large reviews of studies on the safety of ART suggest a slight elevated risk of birth defects in children born following ART (Hampton, 2004; Ludwig and Diedrich, 2002). Besides multiple gestations there is also a growing concern for structural anomalies and long term health effects. Embryo culture appears to be a powerful diagnostic tool, yielding useful information regarding the viability of the human embryo (Balaban and Urman, 2003). However, embryo culture and embryo selection at cleavage or blastocyst stage are prohibited in some countries due to religious or ethical considerations regarding the destruction of non-selected but viable embryos (Zollner *et al.*, 2002; Simini, 1999). Thus, predictive and accurate selection of healthy oocytes and pre-embryos with high viability is essential in countries with restrictive legislation and religious or ethical considerations regarding the embryo protection, to improve the success rate of ART.

3.2 Aims of the Study

The study was mainly designed to establish an efficient, non-invasive strategy for selection of high quality human oocytes prior to ICSI by analysis of mean magnitude of retardance of light by the oocyte spindle and zona pellucida using polarization microscopy. This method may provide more information of the oocytes' developmental capacity after insemination, than the currently used non-invasive morphological criteria, and may therefore also be useful in quality control (e.g. optimising handling/culture of oocytes), treatment of patients (e.g. with respect to hormonal regimen etc.), counselling (e.g. identification of patients with low/high quality of oocytes), and optimising success rate (e.g. by selection of the best high quality oocytes/embryos for transfer). Furthermore, the study was aimed at exploring the potential of non-invasive analysis to reduce numbers

of transfer embryos and optimise timing for ICSI (e.g. ICSI in metaphase II but not telophase I oocytes).

The diploma study published recently (Shen *et al.*, 2005), was already focussed on exploring the potential of PolScope microscopy to assess spindle structure in mammalian oocytes, using the mouse as a suitable animal model (Eichenlaub-Ritter and Boll, 1989). In this, high numbers of maturation competent oocytes can be obtained from ovaries of prepubertal or young, adult females, they can be matured to metaphase II and methodology for conventional immunofluorescence, for confocal microscopy and chromosomal analysis after spreading and C-banding were available (Tarkovski, 1966). PolScope microscopy was initially established in this model, to ensure its non-invasive nature and potential to reveal spindle aberrations before progressing to human oocytes. In fact, it was possible to successfully employ PolScope microscopy in this mouse model to study the dose-dependent shortening of the spindle pole-to-pole distance in mouse oocytes matured in the presence of tubulin-depolymerising cytostatic drug nocodazole and show dynamic elongation of the metaphase II spindle in mouse oocytes exposed to the microtubule stabilising drug taxol (Eichenlaub-Ritter *et al.*, 2002). Initial analysis of human oocytes to optimise handling in protection of living human oocytes, spare immature oocytes from ICSI cycles were *in vitro* matured to metaphase II and viewed by PolScope (Wang *et al.*, 2001c).

The optimised methodologies, which can be employed within the present study performed with cumulus-cell denuded human oocytes from ICSI cycles with consent of patients and the ethical committee, addressed the following questions:

1. Qualitative assessment:
    a. Is PolScope microscopy a safe methodology for clinical use? Does the imaging of human oocytes using PolScope microscopy induce a reduction of implantation rate and pregnancy rate?
    b. Can the findings of previous studies be confirmed that the presence of a birefrigent spindle and the location of a birefringent spindle relative to the first polar body correlate positively with fertilization rate, the quality of pre-embryos and pregnancy rate?

c. Can immature human oocytes from a hormone-stimulated cycle develop normally to metaphase I and express a birefrigent spindle at meiosis I and II when placed into appropriate media and cultured *in vitro*? Is the proportion of *in vitro* maturing oocytes expressing a birefringent spindle as high as the one in *in vivo* maturing oocytes?

2. Quantitative Analysis:
   a. Is there a correlation between organisation of spindle fibres assessed by retardance magnitude and the interpolar distance of the spindle and the developmental potential of oocytes after fertilization determined by PN score?
   b. How do high-order network structure of the human zona pellucida and zona thickness correlate to quality of human oocytes and embryos obtained after ICSI and transfer?
   c. How predictive is quantitative assessment of the human zona pellucida by PolScope for quality of oocytes in assisted reproduction?

3.3 Experimental Design

Oocytes from ICSI cycles with consent of patients were included in the study. After puncture, mature oocytes were imaged by PolScope within two hours after retrieval. Data were saved for further qualitative and quantitative analysis of spindle apparatus and zona pellucida. Eighteen hours post-insemination, fertilization rate and the quality of pre-embryos (according to pronuclear score) were assessed in all inseminated oocytes. 2-3 pre-embryos with presumably highest developmental potential were selected for embryo transfer (ET) at day 2 or day 3. 2-3 weeks after ET, the hCG level in blood was determined to assess the biochemical pregnancy.

Immature oocytes (at germinal vesicle stage at retrieval) from stimulated cycles were cultured *in vitro* continually for up to 48 hours. Oocytes were imaged by PolScope for the expression of a metaphase I and II birefringent spindle during the *in vitro* maturation. Oocytes were fixed for immunofluorescence after analysis by PolScope.

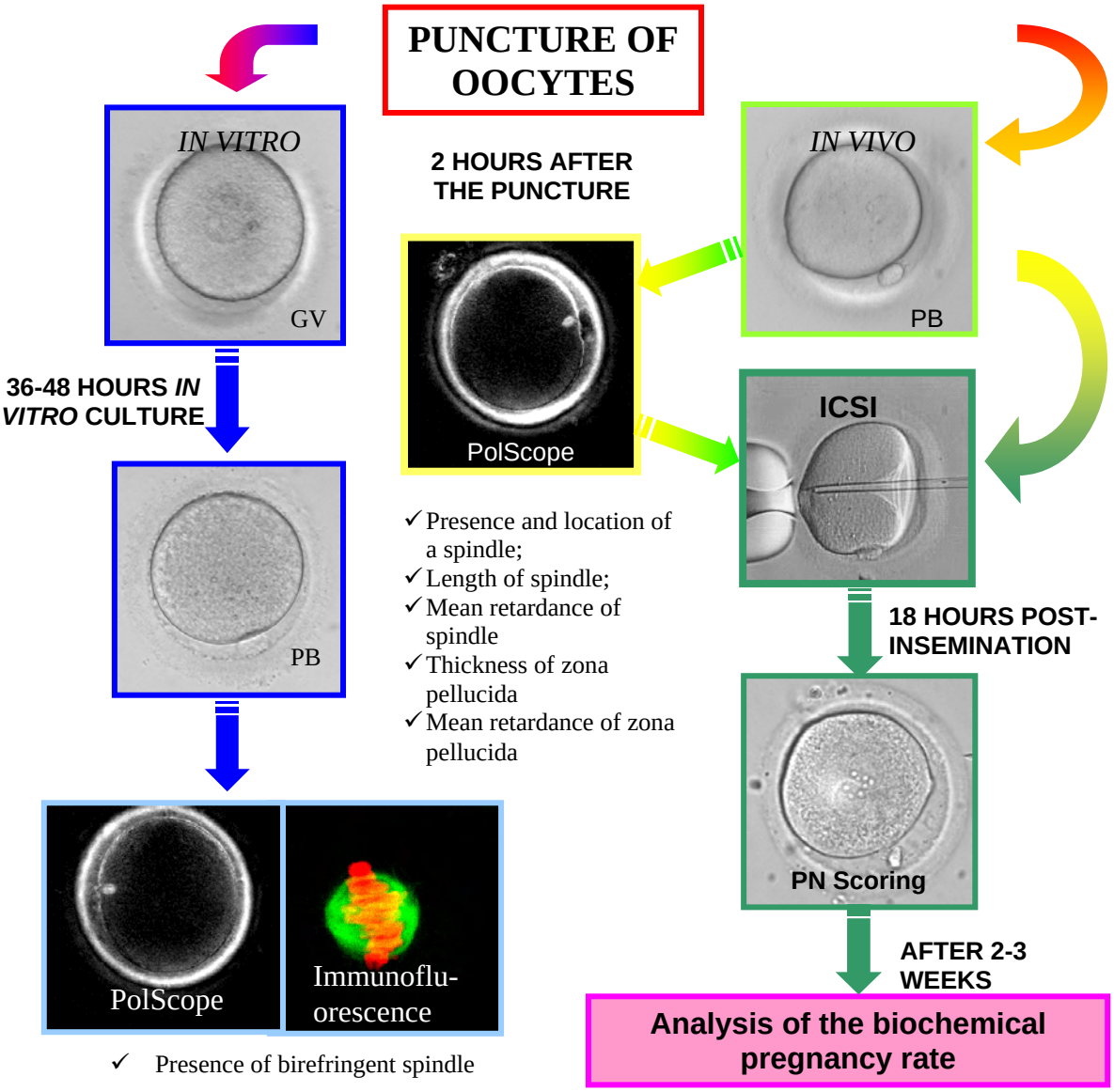
PUNCTURE OF OOCYTES
IN VITRO
GV
36-48 HOURS IN VITRO CULTURE
PB
PolScope
Immunoflu-orescence
✓ Presence of birefringent spindle
2 HOURS AFTER THE PUNCTURE
PolScope
✓ Presence and location of a spindle;
✓ Length of spindle;
✓ Mean retardance of spindle
✓ Thickness of zona pellucida
✓ Mean retardance of zona pellucida
IN VIVO
PB
ICSI
18 HOURS POST-INSEMINATION
PN Scoring
AFTER 2-3 WEEKS
Analysis of the biochemical pregnancy rate

4. Materials and Methods

4.1 Source of Human Oocytes

In total, oocytes from 182 ICSI patients (mean age, 32.5 ± 4.5 years) were imaged by PolScope microscope during a period of 2 years after informed consent of the patients. Male sub-fertility was the indication in all cases. In the initial part of the study, fate of 620 oocytes from 77 ICSI cycles (mean maternal age, 33.2 ± 4.7) viewed by PolScope were compared to 950 oocytes from 130 ICSI cycles (mean maternal age, 32.3 ± 4.8) randomly allocated to "control" (no PolScope analysis). In the quantitative assessment for spindle retardance 676 oocytes from 103 cycles were included. For analysis of spindle expression 56 oocytes matured *in vitro* with a mean age of 31.9 ± 4.4 years and 1369 oocytes matured *in vivo* with a mean age of 32.5 ± 4.5 years were used. The quantitative analysis of zona pellucida included 166 transferred oocytes of 63 ICSI cycles. The study protocol and design was approved by the ethic committee of the University Hospital of Giessen.

4.2 Retrieval and Culture of Oocytes

Throughout the study, human oocytes were obtained from ICSI patients undergoing controlled ovarian stimulation induced by GnRH agonist (HMG, Menogon®, Ferring Germany) in either a long- (130 patients; with a mean maternal age of 30.2 ± 2.8 years) or a short-treatment protocol (52 patients, with a mean maternal age of 37.2 ± 1.7 years). Ovulation was trigged by administration of 10.000 human chorionic gonadotrophin (hCG, Organon Germany) 36 hours prior to puncture, when the dominant follicles were > 20 mm in diameter and E2-level in blood was approximately 1,000 pg/ml.

Retrieval of oocytes was performed by ultrasound-guided transvaginal aspiration. Cumulus-oocyte-complexes (COCs) were retrieved and collected in HEPES-buffered human tubule fluid medium (HTF medium, Irvine Scientific, USA) supplemented with 10% human serum albumin (Behring, Marburg Germany). After briefly exposure to 80 IU/ml hyaluronidase (Sigma, Germany), cumulus cells were removed by repeated gentle aspiration with hand-drawn glass pipette. Denuded oocytes were washed two times in fresh HTF + 10% HSA. Nuclear maturity of oocytes was identified under a stereomicroscope (Olympus SZH-ILLK, Japan). Mature oocytes (PB) were fertilized *in vitro* with sperm microinjection in 2 hours after oocytes retrieval. Oocytes arrested at

germinal vesicle (GV) stage, which were excluded from an ICSI program, were collected and cultured *in vitro* (s. Chapter 4.3).

4.3 Analysis of Maturation Kinetics of Immature GV-stage Human Oocytes *in vitro*

After retrieval, oocytes with an intact germinal vesicle (GV) were cultured *in vitro* in universal IVF medium (Cat. 10310060, MediCult) equilibrated at 37°C in an atmosphere of 5% CO_2 plus 95% air up to 48 hours. Oocytes were scored for the proportion of polar body formation at 12, 24, 30, 36 and 48 hour of the culture under a stereo microscope and the expression of a birefringent metaphase I and metaphase II spindle using PolScope microscopy. Oocytes possessing a birefringent spindle or without spindle were fixed for indirect anti-tubulin immunofluorescence.

4.4 Invasive Analysis of Spindle Apparatus in Fixed Oocytes by Indirect Anti-tubulin Immunofluorescence

For analysis of spindle morphology of *in vitro* maturing human oocytes, indirect anti-tubulin immunofluorescence was employed in this study. Oocytes were either fixed and then viewed directly or were fixed by the clotting-technique procedure according to procedures developed by Hunt *et al.* (1995) and Eichenlaub-Ritter and Betzendahl (1995).

4.4.1 Solutions and Chemicals

4.4.1.1 Ring-solution and Fibrinogen Preparation for Use in Fibrin clots

For immunofluorenscence analysis oocytes had to embedded in a thrombin/fibrinogen clot. Fibrinogen (Calbiochem, 341-573) was aliquoted and stored at -20°C. Shortly before use, 0.005g fibrinogen was dissolved in 500µl ringer-solution and pre-warmed to 37°C. The components and concentration of the ringer-solution is shown in the Table 4.1.

4.4.1.2 PBS Solution

PBS tablets were purchased from Oxoid, England. 1 PBS tablet was dissolved in 100ml ddH_2O. PBS solution was autoclaved and stored at room temperature for use. PBS plus 2% Triton X-100 (Sigma, T-9284) was made up and stored at 4°C. During fixation of oocytes the solution was pre-warmed and kept at 37°C.

Table 4.1 Components of solutions.

Solutions	Chemicals
Ringers (50ml)	NaCl 0.45g
	KCl 0.021g
	$CaCl_2$ 0.0125g
	ddH_2O Up to 50 ml, sterile filtered and stored at 4°C
10% NGS (500 ml)	50ml normal goat serum (Gibco BRL)
	500µl Triton X-100 (Sigma, T-9284)
	0.1g Na-Azid (Sigma, A-2002)
	450 ml PBS solution
	Saved at 4°C for 1 month use
5% NGS (20ml)	1 ml normal goat serum
	19 ml PBS solution
0.1% NGS (500ml)	500µl normal goat serum
	500ml PBS solution
	Stored at 4°C
Thrombin solution	250 units thrombin
	1.5 ml PBS
	1 ml ddH_2O
5x SB-stock (50ml)	7.55g Pipes (Sigma, P-6757) It should be dissolved at first in 50ml dd H_2O. PH should be adjusted to 7.5 prior to adding following chemicals.
	0.25g $MgCl_2 \cdot 6H_2O$
	0.235g EGTA (Sigma, E-4378)
Simple-Fix (10ml)	2ml 5xSB-stock
	100 µl Triton X-100 (Sigma, T-8787)
	540µl Formaldehyde (Sigma, F-1268). Formaldehyde should be added shortly before use.
	0.5 mM Taxol (Sigma, T-7402) stock was made up in DMSO at first and stored at -20°C. 20µl stock solution was added into Simple-Fix to make a final concentration of Taxol in Fix = 1µM.
	ddH_2O 7.34ml
PBS/Triton	PBS + 2% Triton X-100

4.4.1.3 Thrombin-Solution

Thrombin from bovine plasma was purchased from Sigma (T-6634). 250 units thrombin was dissolved in 1ml ddH_2O (Baxter Belgian, 001428) and 1.5ml PBS. The solution was aliquoted and kept frozen at -20°C until use.

4.4.1.4 NGS Wash Solution

NGS wash solutions (0.1% and 10%) were made up for washing fixed specimen and storing slides. In addition, 5% NGS solution was used for dilution of antibodies.

4.4.1.5 5x SB-stock

5xSB-stock solution was composed of PIPES, $MgCl_2$ and EGTA. PIPES has to be solved at a pH of 6.1-7.5. Therefore, the pH of PIPES solution should be adjusted to 7.5, before the addition of the other chemicals.

4.4.1.6 Simple-fix

To make up the fixative solution, 2 ml 5x SB-stock was diluted in 7.34ml ddH_2O. 100µl Triton X-100 and 20µl 0.5mM Taxol were added to the solution afterwards. Shortly before use, 540µl Formaldehyde was freshly added to the solution.

4.4.1.7 Other Chemicals

The chemicals in Table 4.2 were also used for the indirect anti-tubulin immunofluorescence.

Table 4.2 other chemicals and solutions used for indirect anti-tubulin immunofluorescence.

Poly-L-Lysine (Sigma, P-1524)	1mg/ml solution for coating slides
1,4-Diazobicycles-octane (DABCO, Sigma)	2mg DABCO was in 1 ml PBS with 20% glycerol and stored at 4°C.
Methanol	100% Methanol was stored at -20°C for use.
Propidium Iodide (Sigma, Deisenhof)	1µg/ml in 5% NGS
Monoclonal anti-α-tubulin antibody from mouse (Sigma, T-9026)	Stored at -70°C, diluted 1:400 in 5% NGS wash solution before use
Polyclonal anti-mouse antibody from rabbit FITC conjugated (Sigma, F-7506)	Stored at -20°C shortly before use diluted 1:50 in 5%NGS wash solution before use
Vulcanising solution (Tip Top Stahlgruber, Munich, Germany)	

4.4.2 Procedure

4.4.2.1 Preparation of Slides

Slides were immersed into 100% methanol for 1 minute for cleaning of slides. Two rings of 1 cm diameter were then marked with a vulcanising solution (Tip Top Stahlgruber, Munich). Slides were dried in air for more than one night. Shortly before transferring oocytes to the slides, the marked area (ring 2) on the slides was washed with drops of the following solution (Figure 4.4.1):

- 1 mg/ml poly-L-lysine
- 2 x washing with ddH_2O

The coating with poly-L-lysine was necessary to attach the Fibrin clot stably onto the slide.

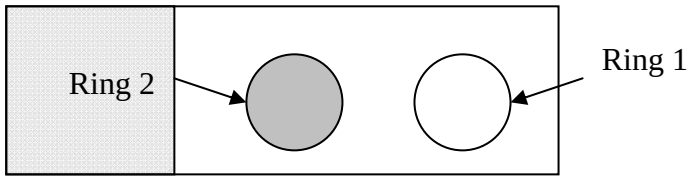

Figure 4.4.1 Preparation of slides for immunofluorescence: 3µl and 1µl Fibrinogen solutions were placed in ring 1 and ring 2, respectively, and covered with mineral oil. Oocytes was drawn from medium and washed in ring 1 shortly. Then it was transferred to ring 2. 1 µl Trombin solution was added immediately into ring 2 to embed oocytes into the Fibrin clot.

4.4.2.2 Preparation of Clot

3 µl fibrinogen was placed in ring 1 (wash drop), 1 µl fibrinogen in ring 2 (clot drop). Both droplets were covered with mineral oil and pre-warmed to 37°C. Thrombin solution was kept on ice for use.

4.4.2.3 Placement of Oocytes in a Fibrin Clot

Oocytes were individually fixed onto slides within the clot, so that each slide contained one oocyte. For this, the oocyte was transferred into the wash drop on the slide at first. A minimal amount of medium, transferred with the oocyte was transferred into the wash

drop. After washing, the oocyte was immediately transferred to the clot drop in ring 2. 1µl Thrombin solution was added to the clot drop quickly to induce clotting.

4.4.2.4 Fixation of Oocytes

After placing on the warm object stage heated at 37°C for 30 seconds, the slide was then washed with pre-warmed PBS containing 2% Triton-X-100 non-ionic detergent. The oocytes trapped within the fibrin clots were fixed subsequently in pre-warmed simple-fix solution containing 2% formaldehyde, 1% Triton X-100, 0.1 M PIPES, 5 mM $MgCl_2$, 1µM Taxol and 2.5 mM EGTA (all chemicals were purchased from Sigma, Deisenhofen, Germany) in a plastic slide holder for 15 minutes and washed in 0.1% NGS for 15 minutes. After washing, oocytes were moved to 10% NGS for at least 1 hour. The fixed oocytes were stored in 10% NGS for labelling by antibody.

4.4.2.5 Indirect Anti-Tubulin Immunofluorescence

Monoclonal anti-α-tubulin antibody was diluted with 5% NGS (1:400). 15µl of antibody solution was transferred to the slide, and the oocyte was incubated in a humid atmosphere with the first antibody at 37°C for 1 hour. Alternatively oocytes covered by antibody solution were stored at 4°C over night. Slides were subsequently washed in pre-warmed 10% NGS at 37°C for 1 hour. The second antibody (polyclonal anti-mouse fluorescence isothiocyanate (FITC) conjugated antibody) was diluted with 5% NGS (1:50). Incubation of the second antibody was also for 1 hour at 37oC. Slides were finally washed in 10% NGS at 37°C for 1 hour before chromosome staining with 1 µg/ml Propidium Iodide was carried out for 10 minutes in the dark.

Before sealing the slide the silicon ring was removed and 20µl anti-fading solution (DABCO) was added. After covering with a cover slip the slide was sealed with vulcanising solution and stored at 4°C in the dark until viewing by confocal microscope.

4.4.3 Analysis of Spindle Morphology and Chromosomal Behaviour

Spindles were illuminated with a TCS SP2 laser scanning confocal microscope (Leica, Germany). Images were saved as *.tif files with the appropriate software. Optical images of the spindle were combined to provide an image of the whole spindle apparatus and the relative positioning and congression (alignment) of chromosomes on the spindle.

4.5 Non-invasive Analysis of Birefringent Structures in Living Oocytes by PolScope Microscopy

The SpindleView™ imaging (SPV) system is a fully-integrated set of microscope accessories that combines a unique liquid crystal-based orientation-independent polarizing light (PolScope) technology to assess the morphology and integrity of birefringent structures in living oocytes non-invasively. The PolScope™ technology is based on techniques originally developed by Dr. Rudolf Oldenbourg at the Marine Biological Laboratory at Woods Hole, Massachusetts (Oldenbourg, 1995 and 1996).

4.5.1 Installation of the Hardware

SpindleView™ imaging system consisted of a Pentium III 800Hz computer, a spindle view controller box, a LC-compensator, CCD camera and the SpindleView™ analysis software. For the current study the SpindleView™ imaging system was installed on a Nikon Eclipse TE-2000 inverted microscope, equipped with Hoffman interference optics, 10 x, 20 x and 40 x strain-free objective lenses (Figure 4.5.1).

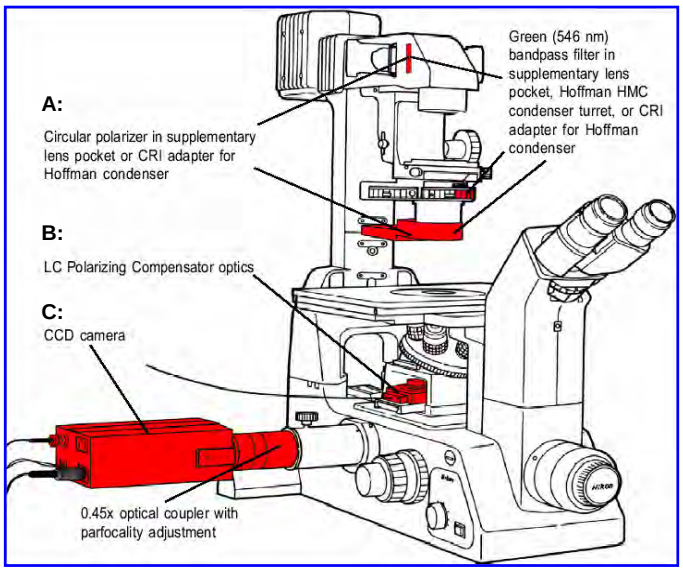

Figure 4.5.1 The set-up overview of SpindleView™ imaging system (s. Chapter 4.5). A: Nearly polarized light producer composed of a polarized filter in 546 nm and a Hoffman HMC condenser. B: LC polarizing compensator optics was connected through the control box to a Pentium III computer. C: Images were recorded by a CCD camera and saved as *.bmp files in the computer.

4.5.2 The SpindleView Software and Oocyte Imaging

The imaging software, SpindleView imaging system, was pre-installed in the computer. The user interface of the SPV system is shown in Figure 4.5.2. To achieve oocyte's imaging more easily and quickly, the major steps, which were required for imaging of oocytes, are listed in the user interface (Item A on the Figure 4.5.2); all the action buttons are shown on the left in tool bar (Item E). In the camera view window, the live video image of the oocyte is identical to the one observed by the eyepiece (Item B); the processed image is shown in the active image window (Item C); the identification data of samples of patients are stored under the image window (Item D).

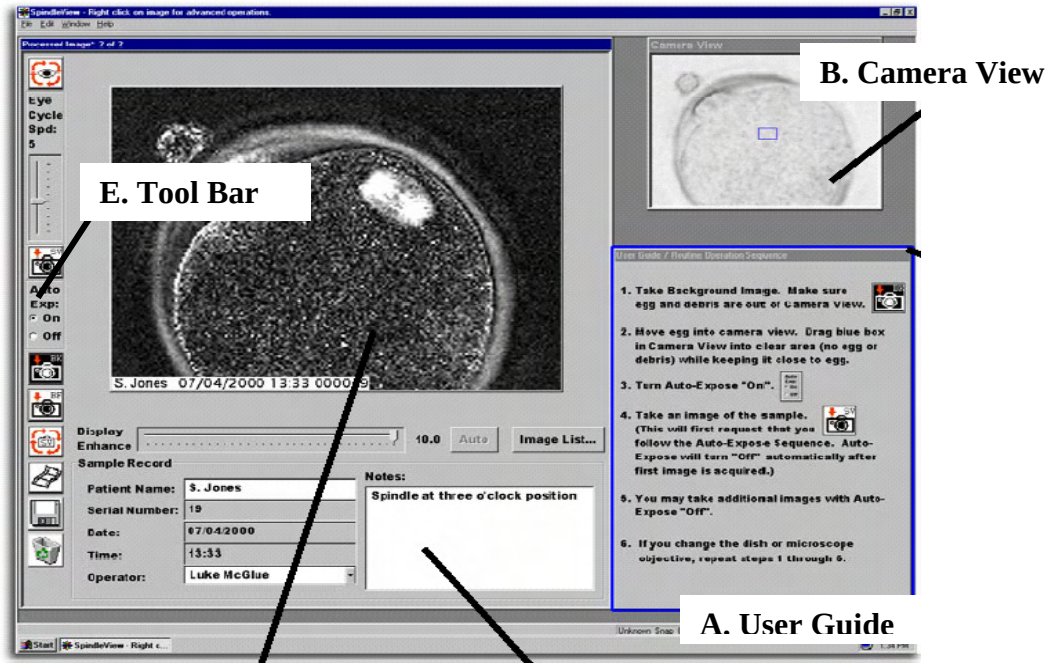

Figure 4.5.2 The full-screen view of the SpindleView software. A. Interactive User Guide; B. Live Video Window; C. Active Image Window; D. Sample Record Window; E. Tool Bar

4.5.3 Imaging of Birefringent Structures in Living Human Oocytes

2 h after retrieval, oocytes were transferred individually to a pre-warmed 5-µl droplet of injection medium (HEPES buffered human tubule fluid medium) overlaid with

equilibrated mineral oil (Sigma, Germany) in a WillCo Wells BV dish (Ref. No.: GWSt-5040, Amsterdam, Netherlands). To avoid any prolonged handling and viewing of the oocytes before ICSI, the images of oocytes obtained by standard illumination through the oocyte equator and automatic microscope setting (see below) were saved for quantitative analysis without using them for selection of embryos. The object stage of the microscope was heated by a temperature control system at 37°C (Minitub HT300, Tiefenbach, Germany) during the observation. Alignment of the microscope and calibration of the software were performed before oocyte imaging. For a calibration failure the following steps have to be check out, if

1. the liquid crystal (LC) polarizing compensator optic module was installed on the microscope and connected to the cable to the connector on the back of spindle view controller box.
2. the spindle view controller box was connected to the computer. Then connect power transformer to the back of the controller box.
3. a 546 nm (wavelength) green interference filter was placed in the supplementary lens pocket.
4. the video cables was connected to the computer.
5. the condenser turret turned to “A” position.
6. the controller box was turned on before start the spindle view software.

Quantitative analysis of the retardance magnitude of the birefringent structures in oocytes, namely zona pellucida and spindle apparatus, was performed along a line scan across the entire structure. All the measurements were performed by the same person and blindly with respect to clinical factors, such as the age of patients, numbers of additional oocytes and pregnancy rate.

4.5.3.1 Quantitative Assessment of the Birefringent Property of the Zona Pellucida

The organisation of ZP fibres and the thickness of zona pellucida were quantitatively analysed in 63 ICSI cycles in 2003 (Table 4.3). The quantitative analysis of the thickness and retardance of zona pellucida was performed along three line scans across the entire zona pellucida, which was perpendicular to the cell membrane on a cord from the oocyte

centre towards the oolemma and zona (Figure 4.5.3). Since thickness and texture of the human zona pellucida may be heterogeneous for individual oocytes and within each zona layer, one line scan was usually performed in an area away from the first polar body providing a profile of thickness and magnitude of retardance of the tri-layered structure at 0.5 µm steps (Figure 4.5.3, area A). A second line scan was located approximately 180º away from the first one, extending the line from the first measurement through the oocyte centre outwards (area B). The third area of a line perpendicular to the first two scans was performed (at an angle of about 90°, area C). So, three measurements were performed in different areas of the zona of each oocyte. The average retardance magnitude was calculated for each oocyte from three cross-section scans of each individual oocyte.

Table 4.3 Summary of data on patient included in quantitative PolScope analysis of zona pellucida

	CC	NCC
Patients:		
Number of Patients	23	40
Maternal Age[1]	32.7 ± 3.8	32.9 ± 4.7
Number of Attempts[1]	2.0 ± 1.4	2.5 ± 1.2
Peak Oestradiol Levels (ng/ml)[1]	1670.7 ± 783.5	1566.3 ± 651.5
Number of Follicles[1]	12.2 ± 3.6	12.4 ± 5.2
Number of Mature Oocytes[1]	7.9 ± 3.2	7.9 ± 3.7
Fertilization Rate (%)[2]	82.8	84.5
Transferred Oocytes:		
Number of Transferred Oocytes	65	101
Percentage of Transferred Oocytes with Birefringent Spindles (%)[2]	93.2	95.0
Percentage of Oocytes with Displaced Spindle (%)[2]	12.3	9.9
Average Number of Transferred Embryos/ Patient[1]	2.8 ± 0.4	2.6 ± 0.6
Percentage of Embryos Transferred at day 2 (%)[2]	100	95
Percentage of Embryos Transferred on day 3 (%)[2]	0	5

[1] T-test, P > 0.1, no significant difference between the CC and NCC group.
[2] Chi^2-test, P > 0.1, no significant difference between the CC and NCC group.

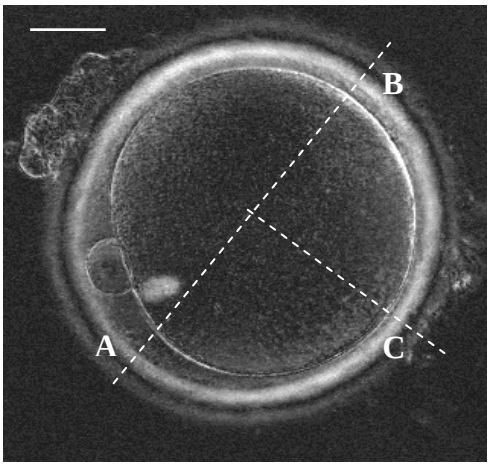

Figure 4.5.3 Quantitative measurement of retardance magnitude and thickness through three line scans across entire zona pellucida (dotted line). The measurements were performed in three different areas. The first and second measurements were located ~ 180º from each other (area A and B) and the third measurement (area C) was perpendicular to the two first measurements. Bar = 30 µm

Maximal differences (in percent of the highest value) in zona retardance of the inner layer between the three measurements in each oocyte were compared statistically.

For quantitative comparisons between retardance of zona layers in germinal vesicle oocytes, metaphase II oocytes and pre-implantation embryos, Pelletier *et al.* (2004) defined the retardance magnitude of individual layers of the zona by taking one value at the midpoint of eight cords through the layer and then calculating the average of the eight points. However, the zona pellucida is an extremely heterogeneous, net-like structure in oocytes (Magerkurth *et al.*, 1999). The value of single measure point cannot describe the three dimensional organisation of ZP protein fibres within the zona pellucida. The mean values of the retardance magnitude were therefore calculated using all measurement points spaced 0.5 µm apart along the whole cross section curve for each layer (Figure 5.4.2), except for the two outermost points (indicated by the area between the arrows in Figure 5.4.2). Since the retardance may steeply increase or rise more gradually going from the inside towards the outside of the zona, and retardance in the perivitelline space may not be close to zero, the outer measurement points of the layers defining boundaries for determination of thickness of each zona layer were usually designated at the site of an increase over two measurement points (indicated by vertical stippled lines in Figure 5.4.2). The middle layer was defined by the dark area between the boundaries of the outer and inner layer (between the dotted vertical lines in the middle of Figure 5.4.2). The

average retardance was calculated initially from the three line scans for each individual oocyte.

For comparison between the conception cycles (CC) and non-conception cycles (NCC), average retardance and thickness was normalized from two to three oocytes used in transfer for each patient to avoid bias between two and three embryo transfers. It has been avoided to measure an area with an abnormal zona phenotype, e.g. in cases where a zona layer was split into two sub-layers (Figure 5.4.1 F, arrows). In these cases, the three measurements were performed in areas close to the normal cross-section regions but adjacent to the split zona area, such that the zona was still in close proximity to the oolemma. Only 3 such oocytes were examined. In each case only one single oocyte with a split zona was used in transfers including one to two additional embryos.

A few oocytes, which were used for transfer, could not be evaluated for zona morphology because granulosa cells were still attached after isolation, and the boundaries of the zona layers could not be unambiguously identified. However, all of the 65 oocytes comprising embryos transferred after ICSI in the CC group and 101 oocytes of the 104 embryos later used for transfer in the NCC group were included in the calculations.

4.5.3.2 Quantitative Assessment of the Birefringent Property of the Spindle Apparatus

Oocytes obtained during a period of two years from 182 stimulation cycles for ICSI with a mean maternal age of 32.5 ± 4.5 years were initially examined non-invasively by PolScope after informed consent. The quantitative study is reporting exclusively the data from 103 cycles of these 182 cycles, with a total of 1140 oocytes, in which quantitative rather than only qualitative PolScope microscopy was performed (Table 4.4). Fertilization with respect to positioning of the spindle in individual oocytes could be also analysed in 731 of 739 oocytes with a spindle from a total of 1140 polar body oocytes from patients with a mean maternal age of 32.5 ± 4.4 years (Table 4.4). Furthermore, 792 embryos from oocytes with (n = 676) and without (n = 116) spindle were analysed for pronuclear-score 18 h after ICSI (Table 4.4). 676 oocytes developing into pre-embryos, in which pronuclear (PN) scores were determined individually, were included in the quantitative assessments of mean length and retardance of the spindle, and PN sores were compared to 116 oocytes without birefringent spindle obtained from the same patients (Table 4.4).

From the 676 embryos obtained after ICSI and pronuclear scoring 268 embryos were selected for transfer, 254 of which contained a birefringent spindle before fertilization (Table 4.4). Mean retardance of spindles of transfer oocytes in conception cycles (100 oocytes) was compared to that in non-conception cycles (154 oocytes) (Table 4.4). Also, maternal age and mean retardance was compared between all oocytes/embryos in conception (n = 246) and non-conception cycles (n = 430), including transfer and non-transfer oocytes (Table 5.2).

According to the expression of a birefringent spindle oocytes were divided into two groups. One comprised oocytes expressing a birefringent spindle (Figure 5.2.2 D), while no spindle was detectable in the other group of oocytes (Figure 5.2.2 E). Fertilization of oocytes with and without a spindle was scored retrospectively. The development of oocytes with and without spindle to pre-embryos was determined quantitatively with respect to PN score of the pre-embryos.

In oocytes with spindle, irrespective of spindle localization, spindle length and retardance of light was quantitatively assessed by PolScope software along a line scan parallel to the spindle long axis from one to the other spindle pole in the centre of the spindle body (Figure 5.3.1a). Similar to ZP, the mean retardance magnitude of the spindle in each oocyte was also calculated by averaging retardance of points spaced 0.5 µm apart along the whole cross section curve. The two outermost points were not included in assessment (as indicated by the arrows in Figure 5.3.1e).

The localisation of the metaphase II spindle relative to the first polar body was analysed in oocytes containing a birefringent spindle, as well. Spindle deviation angle was described by the line connecting the oocyte centre with the middle of the meiotic spindle and a line connecting the oocyte centre with the centre of the first polar body (Figure 5.2.5). Fertilization rate was assessed and compared between those oocytes containing a spindle close to the first polar body (≤40° distance, Figure 5.2.5) and those with the spindle located further away from first polar body (deviation angle of >40°, Figure 5.2.5). The proportion of oocytes developing to a pre-embryo with 2 PN, with abnormal fertilization pattern (1PN and ≥3 PN) and the number of unfertilised oocytes was determined for the group of oocytes with and without spindle, and for oocytes with the spindle in proximity (≤ 40°) or away from the first polar body (> 40°).

Table 4.4 Summary of data on patients included in qualitative PolScope analysis of spindles in oocytes, numbers of oocytes with and without spindle, numbers of oocytes assessed for pronuclear scores and variables between patients whose oocytes contributed to a CC or NCC.

Qualitative Analysis	Total	CC	NCC
Patients:			
Number of Patients	103	42	61
Maternal Age[1]	32.5 ± 4.4	32.5 ± 3.9	32.4 ± 4.3
Number of Attempts[1]		2.1 ± 1.6	2.7 ± 1.4
Peak Oestradiol Levels (ng/ml)[1]		1643.7 ± 735.5	1553.6 ± 645.5
Number of Follicles[1]		11.8 ± 3.7	12.2 ± 5.0
Number of Polar Body Oocytes[1]		8.5 ± 3.6	8.8 ± 4.1
Fertilization Rate (%)[2]		81.2	82.3
Oocytes:			
Total Number of Oocytes		1140	
Number of Mature Oocytes		897	
Mature Oocytes with Spindle (%)		739 (82.4)	
Oocytes Assessed for Displacement of Spindle before ICSI (Without / With Displacement)		731 (620/111)	
Oocytes Assessed for PN scoring after ICSI (With / Without Spindle)		792 (676/116)	
Oocytes Assessed for Mean Retardance and PN score after ICSI (Non-transferred / Transferred)		676 (422/254)	
Oocytes Transferred after ICSI:	Total	CC	NCC
Number of Transferred Oocytes after ICSI	268	105	163
Transfer of Oocytes with Birefringent Spindles (%)[2]	254	100 (95.2)	154 (94.5)
Oocytes with Displaced Spindle (%)[2]		6/100 (6)	22/154 (14.3)
Oocytes Stimulated by Short Protocol (%)[2]		21/105 (20)	35/163 (21.5)
Average Number of Transferred Embryos/ Patient[1]		2.5 ± 0.6	2.7 ± 0.8
Transfers at day 2 (%)[2]		41/42 (97.6)	57/61 (93.4)
Mean Retardance of Light by Spindle in Transfer Oocytes (nm) [1]		1.65 ± 0.43	1.67 ± 0.44
Mean Length of Spindle in Transfer Oocytes (µm)[1]		12.9 ± 2.0	12.8 ± 1.8

[1] t-test, $P > 0.1$, no significant difference between the CC and NCC group.
[2] Chi^2-test, $P > 0.1$, no significant difference between the CC and NCC group.

4.6 Assessment of PN score for Embryo Selection, Development of Embryos at Day 2 and Pregnancy

The selection of eggs used for embryo transfer was performed at the pronuclear stage, 18 hours post-insemination. The criteria of PN score were according to standard criteria used in the IVF centre at Giessen University. The criterion of PN score was developed in IVF centre Giessen, based on Scott and Smith (1998). If the pronuclei were separated, non-equal in size or difficult to identify, they were given a score of E. If the pronuclei were clear and closed aligned, they were given a score from A to D, based on the position of nucleolar precursor bodies (NPB) as following: a) NPBs aligned at the pronuclear junction and the number of NPB was between 3 and 10, score A; b) if the NPBs were polarised at the pronuclear junction but aligned not very well, score B; c) NPBs scattered in cytoplasm and their number was over 7, score C; d) asymmetric alignment of NPBs or the number of NPBs was over 10 or below 5, score D.

Selection was based on the position of both pronuclei and the alignment of NPB in the pronuclei (modified scoring criteria from Scott and Smith, 1998) (see Figure 4.6.1) as well as the overall morphology of the pro-embryo.

In embryo selection for transfer the following factors were especially considered:

1. PN score of the embryo should be as high as possible, usually A-D according to our criteria, but in a few cases, where no other embryos were available, embryos with PN score E were also used for transfer.
2. The cytoplasm should be homogenous and the oocyte without deformations.
3. The localization of the nucleoli should be similar in both pronuclei (Nagy *et al.*, 2003). A peripheral accumulation of nucleoli in only one PN would be considered as an indicator of poor quality of the embryo (see Figure 4.6.1).
4. The presence of a halo was considered as an indicator of high quality of the embryo (Stalf *et al.*, 2002), and was therefore used as additional indicator in embryo selection, especially when selection occurred between embryos of otherwise similar morphology.

In embryos with a score of A and B (group 1), there was close nuclear apposition and NPB were symmetrically distributed either in close apposition to the nuclear periphery where pronuclei face each other (score A) or were similar in number and still in close

proximity to each other in the half of the nucleoplasm where pronuclei were apposed to each other (score B). Embryos with a score of C were assigned to group 2 for assessment of average retardance. Embryos with a score of D with uneven numbers, and/or asymmetric distribution of nucleoli within the nucleoplasm of the paternal and maternal pronuclear were assigned to group 3. Finally, embryos with a score of E with nuclei and/or NPB not clearly distinct or unevenly sized nuclei or such away from each other together with embryos possessing 1 or ≥3 pronuclei were assigned to group 4. The mean retardance magnitudes for spindles in oocytes giving rise to an embryo in each of the four groups was compared. Furthermore, average retardance of spindles of oocytes selected for transfer after ICSI was also compared with mean retardance of spindles in oocytes not used for transfer.

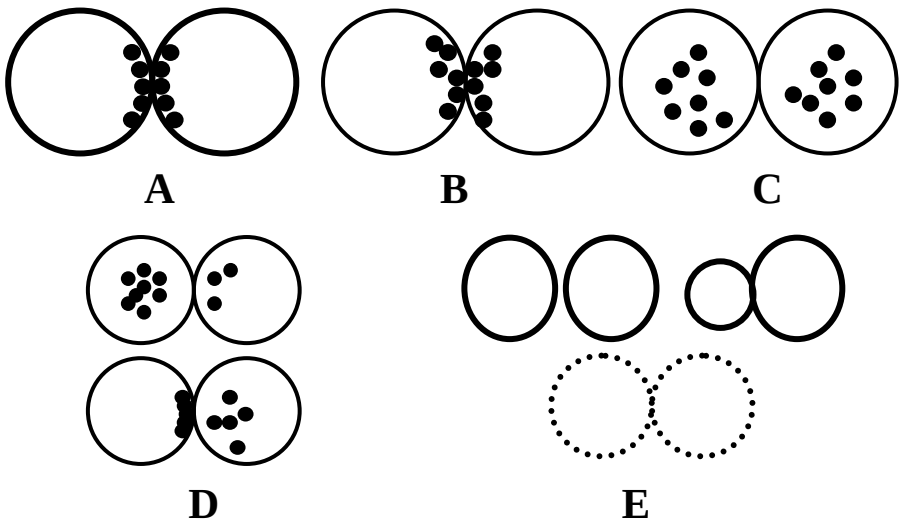

Figure 4.6.1 Pronuclear-scoring system modified from Scott and Smith 1998 (s. Chapter 3.6). (A–D) Score A–D: pronuclei closely apposed, further designation according to the position of nucleoli as follows: (A) Score A: three to 10 NPB aligned at the pronuclear junction. (B) Score B: NPB polarized but not highly apposed at pronuclear junction. (C) Score C: More than seven NPB scattered in nucleoplasm. (D) Score D: asymmetric distribution of NPB and/or numbers of NPB >10 or <5. (E) Score E: NPB spatially separated, unequal in size and/or not clearly distinguishable.

Two to three embryos with the presumably best quality were selected for embryo transfer, blindly with respect to spindle data. Embryos were usually transferred to the uterus on day 2. In a few cases (5 cycles), embryos were transferred only on day 3 after oocyte retrieval, due to practical considerations. A pregnancy was considered, when the patient had positive results in the pregnancy test three times, two weeks after embryo transfer.

4.7 Statistical Analysis

Two-tailed Student T-Test was used for the quantitative analysis of the retardance magnitude of zona and spindle, and thickness of zona layers. Linear regression test was used to calculate the relationship of retardance and thickness of the inner zona layer. Two-way-ANOVA test was used for assessing the correlation between zona thickness and retardance and reproductive age within the CC and NCC groups. *Chi*^{2}-test was performed to compare the fertilization rate of oocytes with and without a birefringent spindle, and the proportion of 2PN formation in the oocytes containing a spindle nearby the polar body and far away from the polar body, and to compare the number of oocytes with a high retardance magnitude (> 3 nm), intermediate magnitude of retardance (3-2 nm), and low magnitude of retardance (< 2 nm) of the inner layer of the zona between the CC and NCC group. U-Test was used for the analysis of the heterogeneous properties of the zona pellucida. Logistic regression analysis was performed to assess the sensitivity of the retardance data in comparison to PN score and embryo development at day 2. Significance was considered as $P < 0.05$ for each statistical analysis. All the analyses were performed with SPSS 12.0 and SAS software.

5. Results

5.1 Assessment of Spindle Formation in Immuature Oocytes from ICSI Cycles

56 immature human oocytes from 33 ICSI cycles with a mean patient age of 31.9 ± 4.4 years were included in the analysis. After retrieval, GV-stage oocytes were cultured for 12h to 48 h in 5 µl microdroplets of universal IVF medium (MediCult, 10310060) and analysed at 12 h, 24 h, 30 h, 36 h and 48 h by PolScope. Some oocytes were subsequently fixed for immunofluorescence analysis. Characteristically, GV-stage oocytes did not contain a birefringent spindle or a first polar body. Tubulin immunofluorescence revealed a dispersed network of cytoplasmic microtubular fibres, no spindle apparatus, and chromatin retained within a nucleus (Figure 5.1.1 a, a'). By 12 hours of culture *in vitro* 64.3% of the immature oocytes had resumed meiosis and undergone GVBD. Most oocytes did not contain a visible spindle apparatus and were cultured further. However, in a few oocytes, a birefringent metaphase I spindle was first identified at this time (Figure 5.1.2). At 24 h of culture, only 6% of all immature oocytes remained arrested at the GV stage. The majority, 62.5% of the human oocytes (35 from 56 oocytes), underwent GVBD and 16.1% of the GVBD oocytes expressed a birefringent metaphase I spindle by 24 h of culture. Fixation revealed well-aligned bivalents on the metaphase I spindle, composed of a dense network of microtubule fibres and a typical barrel-shaped spindle that had migrated to the cell periphery (Figure 5.1.1 b, b'). Although spindle microtubules appeared parallel aligned and ordered in the fixed meiosis I oocytes, frequently, oocytes were still in late prometaphase I stage with chromosomes in the process of congression and not all aligned at the equator (Figure 5.1.1 b'). Approximately 17.9% of the oocytes had reached telophase I and 14.3% of them had emitted a first polar body at 24 h of maturation *in vitro* (Figure 5.1.2). Oocytes fixed at telophase I had typically a central, interpolar microtubular bundle (Figure 5.1.1 c'), which was sometimes already quite devoid of microtubules while other oocytes contained a more dense assembly of microtubular fibres in the interpolar space (not shown). At 30 h of culture the majority of the *in vitro* maturing oocytes had emitted a first polar body although most did not possess a birefringent metaphase II spindle at this time (Figure 5.1.2). A birefringent spindle was detected in only 16.1% of the PB oocytes at 30 h of culture. After 36 h of culture, the percentage of oocytes with PB had increased to 66.1%. However, only about one third of these *in vitro* maturing oocytes

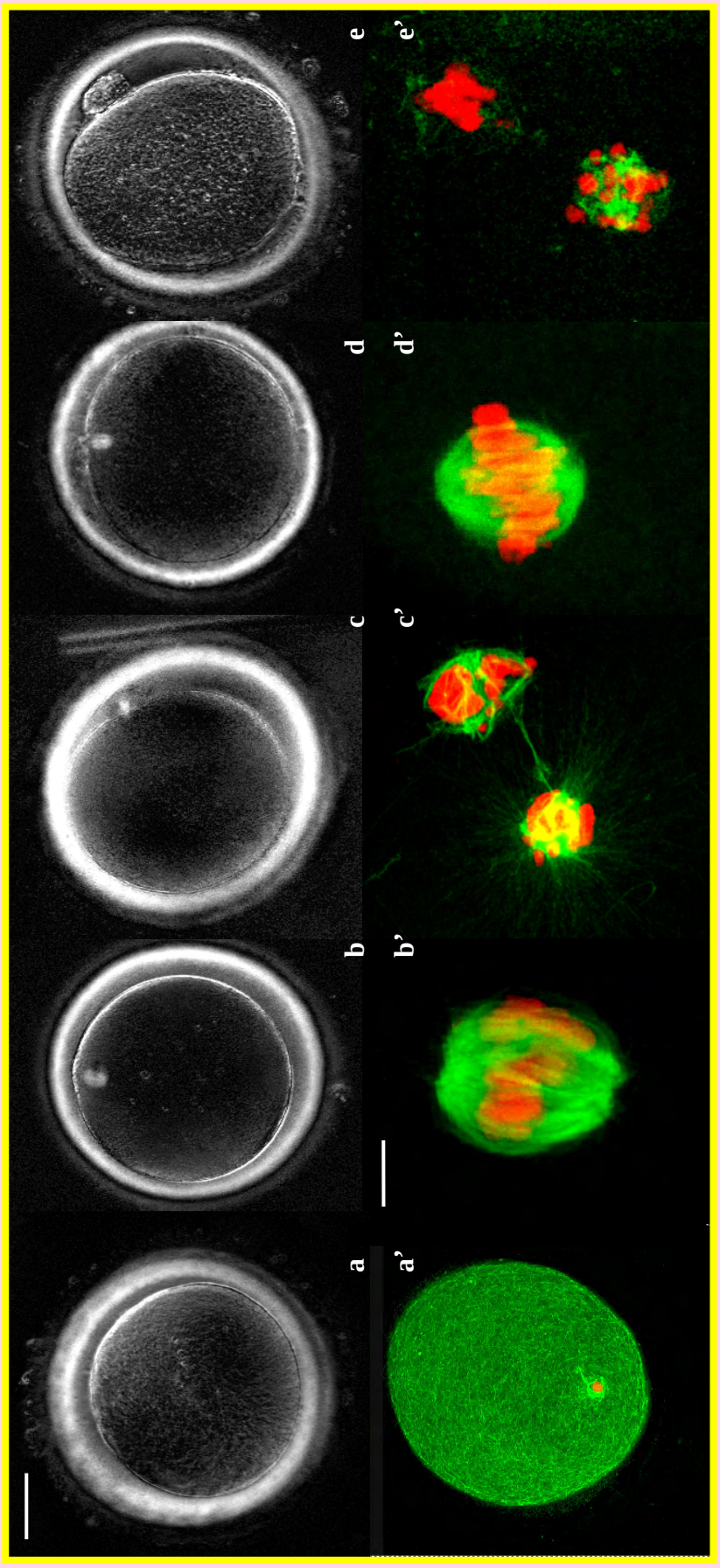

Figure 5.1.1 Comparison of spindle images obtained by PolScope in the living oocytes (a-e) with images of fixed oocytes stained for tubulin immunofluoresecene (green) and chromosomes (orange) (a' to e'). Stages of oocyte maturation *in vitro*maturing oocytes: GV oocytes (a, a'), metaphase I (b, b'), telophase I (c, c'), metaphase II with birefringent spindle (d, d'), and aged metaphase II without birefringent spindle (e, e'). For further explanation of culture time and development, see text. Bar in a for a-e and a': 30 µm. Bar in b' for b'- e': 6 µm.

(11 PB of 56 cultured oocytes, 19.6 %) possessed a birefringent spindle (Figure 5.1.2). This was significantly different from oocytes matured *in vivo* (83.9% of total 1369 oocytes; $P < 0.001$).

Tubulin immunofluorescence revealed a compact barrel-shaped spindle with well-aligned chromosomes in *in vitro* maturing metaphase II oocytes (Figure 5.1.1 d, d'). Oocytes without a visible birefringent spindle often contained also a spindle apparatus, but the latter was frequently asymmetric, and contained only few, unordered spindle fibres, and scattered chromosomes (Figure 5.1.1 e, e'). Interestingly, the percentage of oocytes expressing a birefringent spindle (MII in Figure 5.1.2) decreased dramatically upon prolonged culture of oocytes from 36 h to 48 h (Figure 5.1.2), while that without spindles (PB in Figure 5.1.2) increased, indicating that spindles were highly susceptible to degenerate upon a meiotic arrest of only 12 h to 18 h. Overall the analysis of *in vitro* maturing oocytes by PolScope accurately depicted the formation of a metaphase I and metaphase II spindles, as well as the kinetics of spindle formation with respect to polar body emission and percentage of mature oocyte capable to develop to and arrest at meiosis II non-invasively under defined culture conditions and stimulation protocols.

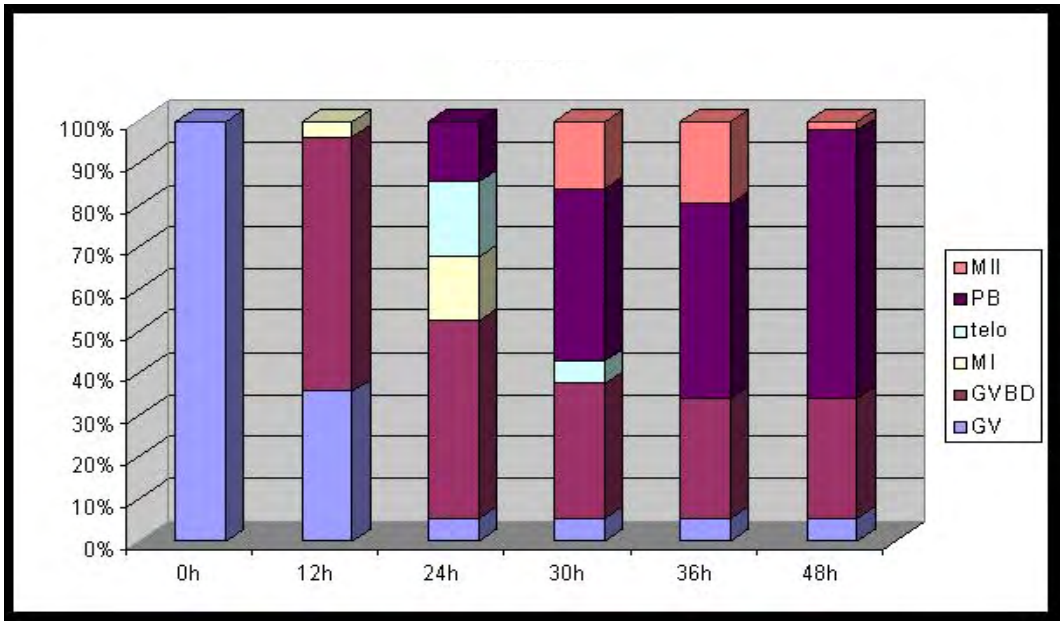

Figure 5.1.2 Kinetics of spindle formation in *in vitro* maturing naked oocytes retrieved from follicles in ICSI cycles at GV stage. GV: Oocytes with a germinal vesicle; GVBD: Oocytes without a detectable birefringent spindle at germinal vesicle breakdown stage; MI: Oocytes with a detectable metaphase I spindle; Telo: oocytes at telophase I stage; PB: Oocytes with first polar body but without a detectable metaphase II spindle; MII: Oocytes with first polar body and a birefringent metaphase II spindle.

5.2 Qualitative Analysis of Expression of a Birefringent Spindle Apparatus in Human *in vivo* Maturing Oocytes Using PolScope Microscopy

5.2.1 Non-invasive Nature of PolScope Microscopy

PolScope has been employed to non-invasively analyse the oocyte's health and their developmental potential after insemination since several years (Wang *et al.*, 2001a;b;c; Rienzi *et al.*, 2003; 2005). In the current study biochemical pregnancy rate of patients (PolScope group; n = 77) whose oocytes were viewed by PolScope has been compared to that of patients randomly allocated to "control" group (no PolScope group; n = 130), in the initial part of the current study to ensure that PolScope viewing has no detrimental effect on oocyte quality and developmental potential.

The biochemical pregnancy rate in the PolScope group was 31.2 %. It was comparable to the pregnancy rate of group of patients who had not been subjected to PolScope analysis prior to ICSI (32.3 %). Thus, there was no statistical significance in pregnancy rate between the control and PolSope group groups (P > 0.1; Figure 5.2.1).

In view of the apparent non-invasive nature of PolScope microscopy, the study could be continued in a retrospective way to compare initially the presence or absence of a spindle in oocytes with outcomes after ICSI.

Figure 5.2.1 Comparison of biochemical pregnancy rate in Polscope and non Polscope group

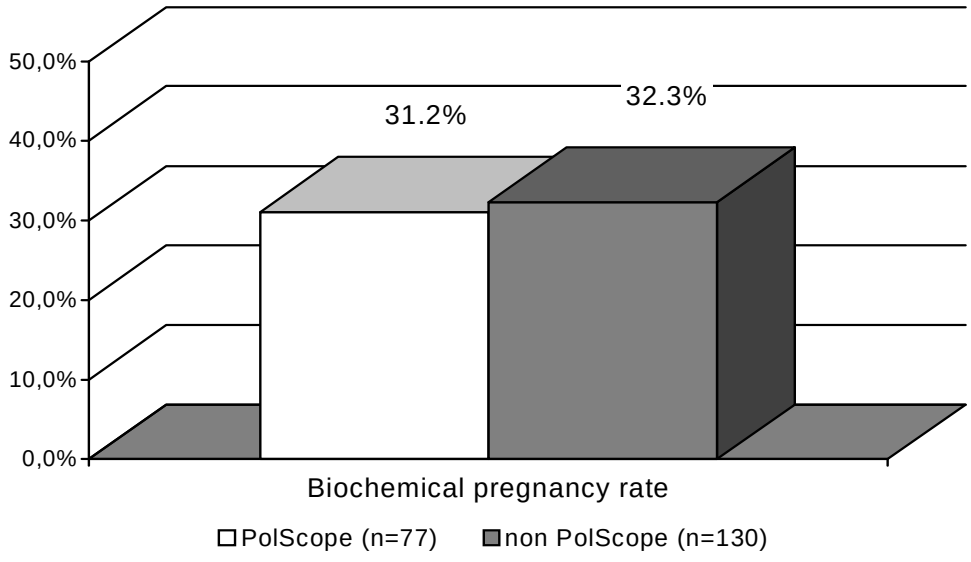

5.2.2 Presence of a Birefringent Spindle in Human Living Oocytes Matured *in vivo*

Oocytes from 182 stimulated ICSI cycles were included in the 2-year study. In total, 1821 oocytes were retrieved by ultrasound-guided transvaginal aspiration. On average 10.0 ± 6.1 oocytes were retrieved per cycle. After denudation of oocytes, 324 oocytes arrested at GV (Figure 5.2.2 A) and GVBD (Figure 5.2.2 B) stage were excluded from the study (Table 5.1). 1497 oocytes with a first polar body (PB) were subjected to the PolScope analysis. During the observation, telophase I spindles were detected in 128 PB oocytes by PolScope (Figure 5.2.2 C). These 128 oocytes in telophase I stage were excluded from the quantitative assessment and comparisons with outcomes in the study. Finally, the presence of a birefringent spindle was analysed in 1369 PB oocytes (Figure 5.2.2 D; Table 5.1). 83.9% of the 1369 oocytes expressed a birefringent metaphase II spindle (Figure 5.2.2 D), whereas the spindle apparatus was not detected by PolScope in 16.1% of the retrieved oocytes (n = 220, Figure 5.2.2 E).

In the examined 182 stimulated cycles, 430 oocytes from a cohort from 73 patients did not contain a birefringent spindle. All 13 oocytes from 2 cycles contained no birefringent spindle at all (Table 5.1). No significant differences in mean patient age and average number of oocytes per cycle were detected in cohorts contributing to cycles with one or all oocytes without spindles versus those that contained only oocytes with spindles.

Table 5.1 Summary of data on expression of a birefringent spindle of total 182 cycles

	Number of cycles	Mean patient age per cycle (years)*	Number of MII oocytes	Number of oocytes per cycle*
Cycles in which all oocytes had a birefringent spindle	73	32.8 ± 5.0	430	5.9 ± 2.9
Cycles in which all oocytes failed to express a birefringent spindle	2	32.5 ± 3.5	13	6.5 ± 3.5
Cycles with one or few oocytes without a birefringent spindle	107	32.3 ± 4.1	926	8.7 ± 4.9
Total	182	32.5 ± 4.4	1369	7.5 ± 4.5

* One-way ANOVA: no significant differences, P>0.1.

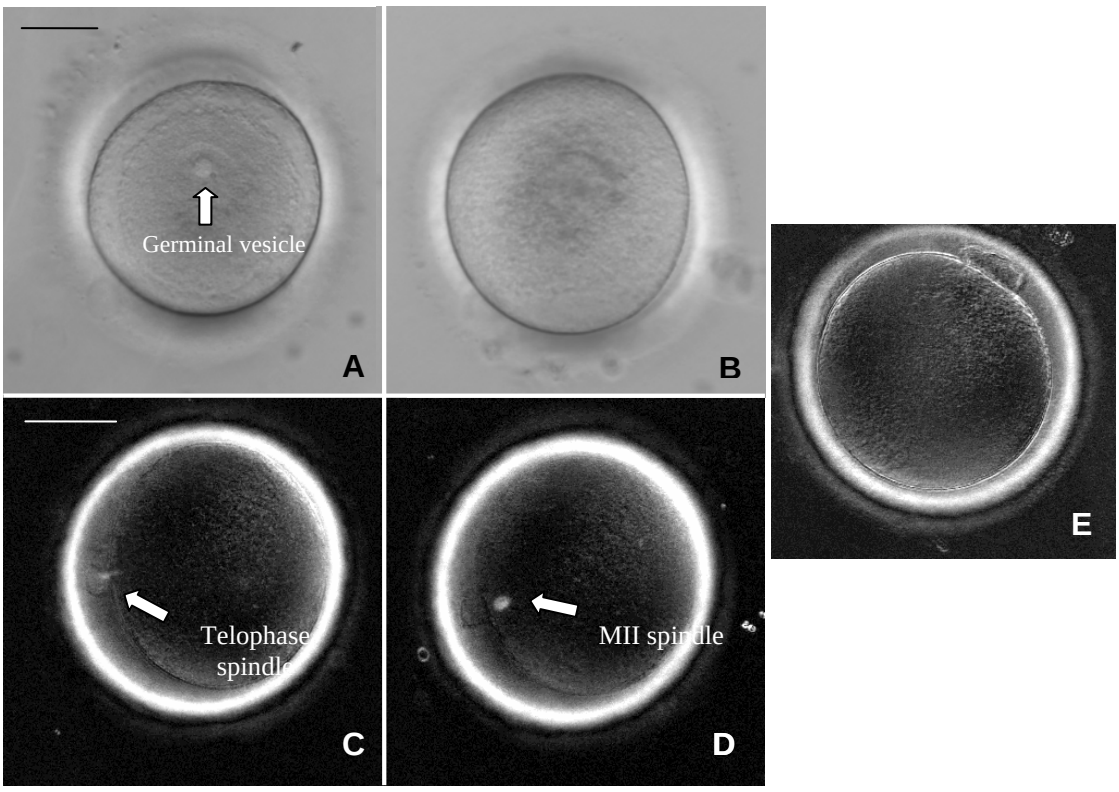

Figure 5.2.2 Oocytes retrieved from stimulated cycles. A: Oocytes arrested at the germinal vesicle (GV) stage; B: Meiotically delayed or blocked oocytes with germinal vesicle breakdown; C: Oocytes with a telophase I spindle in the process of first polar body formation; D: Oocyte with a birefringent metaphase II spindle; E: Typical oocytes without a birefringent spindle but a visible first polar body. Bar in A for A and B = 40um. Bar in C for C-E = 40um.

5.2.3 Fertilization Rate of Oocytes with and without Birefringent Spindles

Fertilization occurred in 88.4% of the oocytes possessing a spindle and in only 66.4% of the oocytes possessing no birefringent spindle. χ^2-test revealed a significantly difference between the two groups ($P < 0.001$; Figure 5.2.3). Accordingly, absence of a birefringent spindle appeared to correlate to a high risk of fertilization failure.

5.2.4 Fate of Oocytes with and without a Birefringent Spindle

At 18 hours post-insemination the fertilization and quality of pre-embryos was assessed using a modified pronuclear (PN) scoring system initially proposed by Scott and Smith (1998) (Stalf *et al.*, 2002). Due to practical reasons, data of the assessment were only collected in 103 ICSI cycles in the course of the current study (Figure 5.2.4). The development to a good, mediocre or suboptimal PN score embryo of the 792 fertilized oocytes from 103 cycles is shown in Figure 5.2.4 (676 oocytes with birefringent spindle and 116 oocytes without birefringent spindle). The proportion of pre-embryos with PN score A, B and C, which are presumably of highest quality from the cohort was significantly higher for oocytes possessing a birefringent spindle, compared to oocytes without a birerefringent spindle (* 34.2% vs. 19.9%; $P < 0.001$; Figure 5.2.4). Conversely, the percentage of oocytes forming a pre-embryo with a score D or E, or with abnormal fertilization tended to be higher in the oocytes without a birefringent spindle, although differences did not reach statistical significance. The data suggest that the presence of a birefringent spindle is usually associated with formation of an embryo of best PN score and developmental potential.

Figure 5.2.3 Fertilization rate of oocytes with and without a birefringent spindle

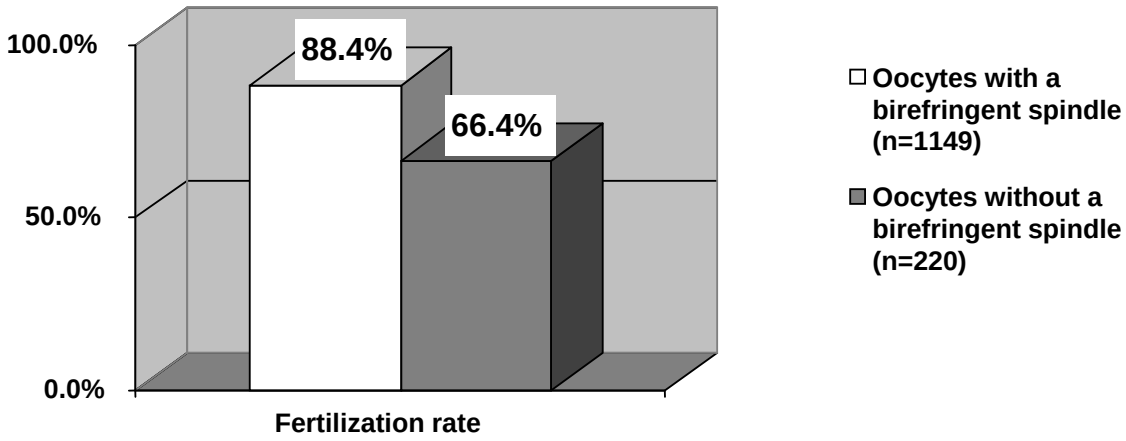

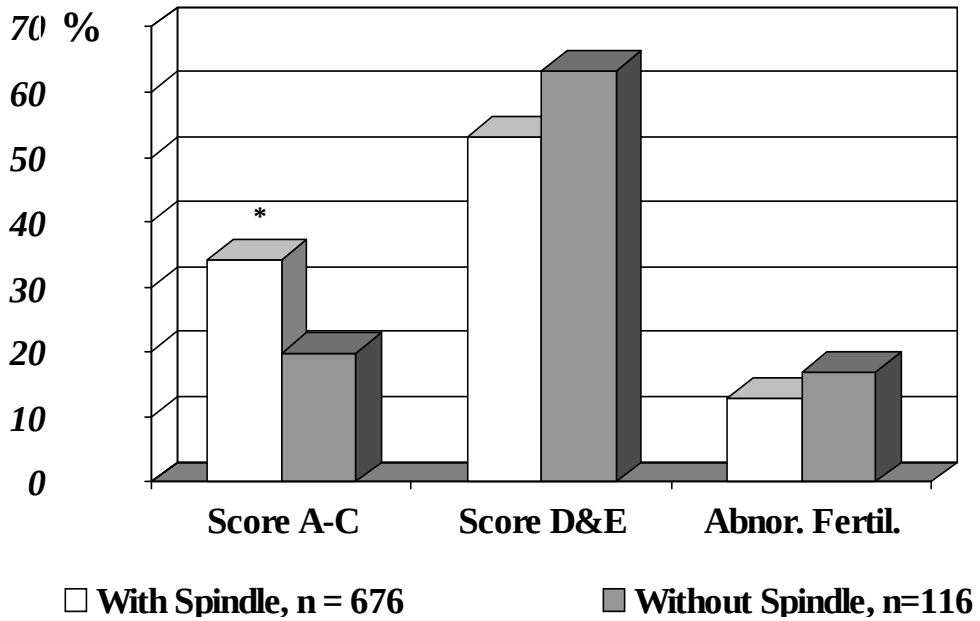

Figure 5.2.4 Development of oocytes with and without birefringent spindle: Grouping of pre-embryos according to pronuclear score A-C, D&E or abnormal fertilization. The proportion of presumably high quality embryos with good PN score (A-C) was statistically significantly lower for oocytes possessing no birefringent spindle (grey bars) compared to oocytes with a spindle (open bars) (* 19.9% vs. 34.2%; P < 0.001)

5.2.5 Fate of Oocytes with and without a Displaced Spindle

731 oocytes from the 103 cycles were included in the analysis of the localisation of the metaphase II spindle relative to the PB in the oocyte. The majority of the 731 oocytes contained a spindle close to the first polar body with a deviation angle below 40° (Figure 5.2.5). A spindle displacement over 40° relative to the first polar body was found in only 15.2% of the oocytes. The oocytes without pronounced spindle displacement had a relatively higher fertilization rate with formation of a 2PN pre-embryo compared to the oocytes with displacement of the spindle from the first polar body ($P < 0.01$) (Figure 5.2.5). In contrast, the rate of oocytes showing abnormal fertilization patterns (one pronucleus or more than three pronuclei) was similar in both groups (Figure 5.2.5).

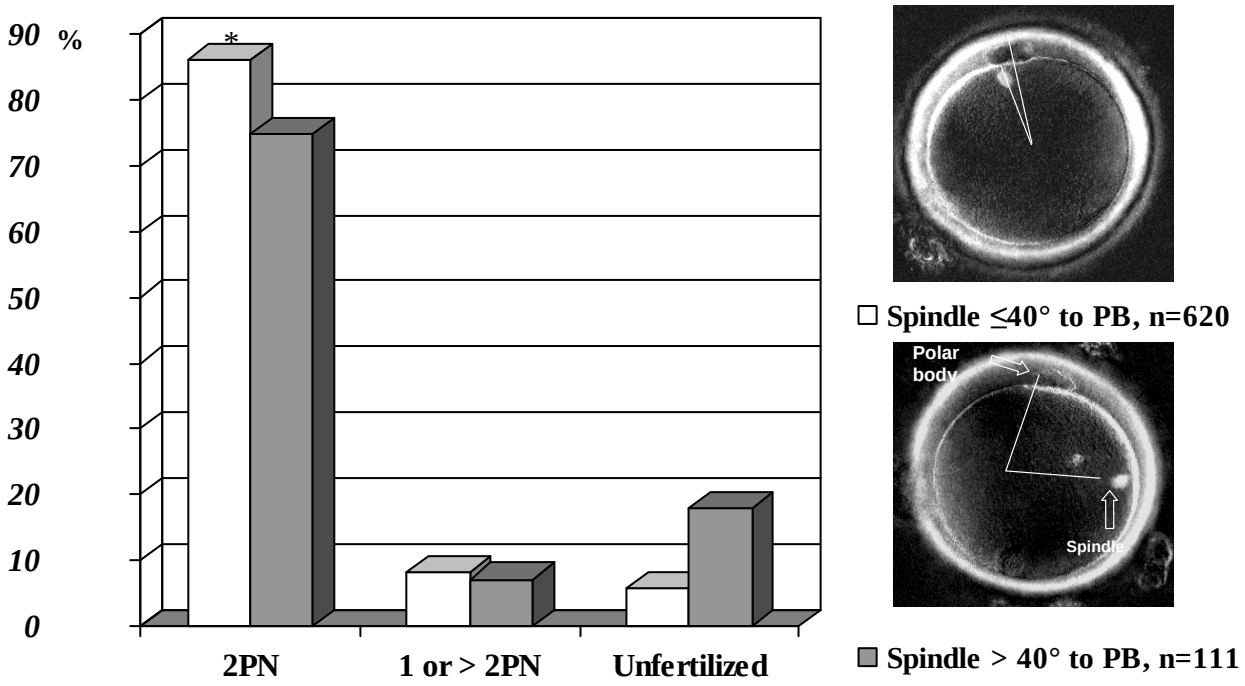

Figure 5.2.5 Comparison of the fertilisation rate and development to 2 PN pre-embryos or pre-embryos with 1 or >2 PN of cohorts of oocytes with a spindle close to the first polar body (≤ 40°) and such with the spindle located at an angle of > 40° away from the spindle in 731 oocytes from 103 stimulation cycles (*χ^2-test, P < 0.01).

5.3 Quantitative Assessment of Spindles in Oocytes with Respect to Developmental Potential/PN score

5.3.1 Oocytes Included to the Quantitative Assessment

The quantitative study is reporting exclusively the data from 103 cycles of these 182 cycles (Table 4.4). In total, 1140 oocytes were retrieved from 103 stimulated cycles. 792 embryos from the total of 1140 oocytes with (n = 676) and without (n = 116) spindle were analysed for pronuclear-score 18 h post-insemination (Table 4.4). 676 oocytes expressing a birefringent metaphase II spindle and developing into pre-embryos, in which pronuclear (PN) scores were determined individually, were included in the quantitative assessments of mean length and retardance of the spindle. PN sores of the 676 oocytes with spindle have been compared to 116 oocytes without birefringent spindle obtained from the same patients (Chapter 5.2.4). According to PN scoring assessment, 268 of the 676 pre-embryos were selected for embryo transfer, in which 105 embryos from 42 cycles contributed to a

conception and the other 163 embryos from 61 cycles failed to contribute to a conception (A conception was determined, when the patient had positive results in the pregnancy test three times in two weeks after embryo transfer.). In 268 embryos, 254 of them (94.8%) contained a visible metaphase II spindle prior to fertilization (Table 4.4).

5.3.2 Retardance Magnitude and Pole-to-pole Distance of the Meiotic Spindle of Human Oocytes

The presence of a birefringent metaphase II spindle was not only qualitatively but also quantitatively analysed as described in material and methods. Similar to previous studies (Wang *et al.*, 2001c; Moon *et al.*, 2003), the majority (over 80%) of *in vivo* maturing human oocytes contained a birefringent spindle. The presence of a birefringent spindle correlated with a high fertilization rate (Figure 5.2.3) and high pre-embryo quality (Fig 5.2.4).

To obtain more information on correlations between spindle morphology and average retardance and developmental potential, 676 embryos were grouped into 4 subgroups, according to their PN score.

Subgroup 1contained oocytes forming embryos with a PN score of A or B;

Subgroup 2 contained oocytes forming embryos with a PN score of C;

Subgroup 3 contained oocytes forming embryos with a score of D;

Subgroup 4 contained oocytes forming embryos with a score of E or with an abnormal fertilization (one PN or more than three PNs).

Characteristic images and the patterns of line scans of spindles in human oocytes developing into embryos of higher or sub-optimal PN score are shown in Figure 5.3.1. Light retardance was measured at 0.5 μm intervals across the entire spindle in a cross-section along a line scan of the long axis of the meiotic spindle in human oocytes. In Figure 5.3.1 e, the striped line was from an oocyte developing into a pre-embryo with PN score A (Figure 5.3.1 b), characteristic for oocytes in subgroup 1. The solid line was from an oocyte forming a pre-embryo with a PN score D after fertilization, characteristic for subgroup 3 (Figure 5.3.1 c). The dotted line marked by triangles corresponds to the retardance curve of an oocyte developing into a pre-embryo with lowest quality (abnormal fertilization) (Figure 5.3.1 d).

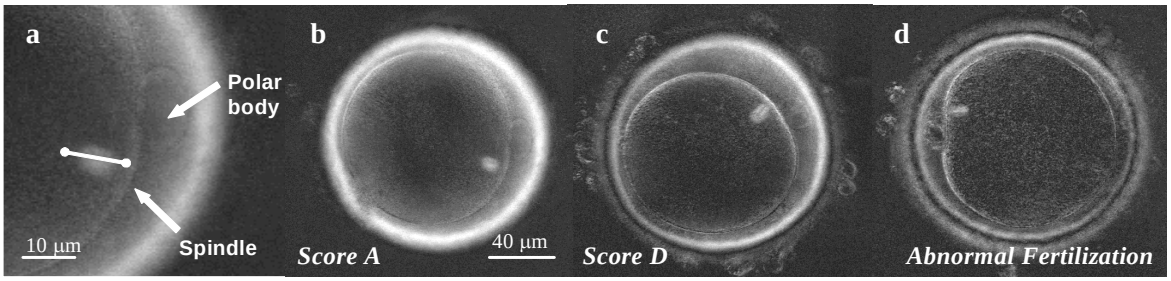

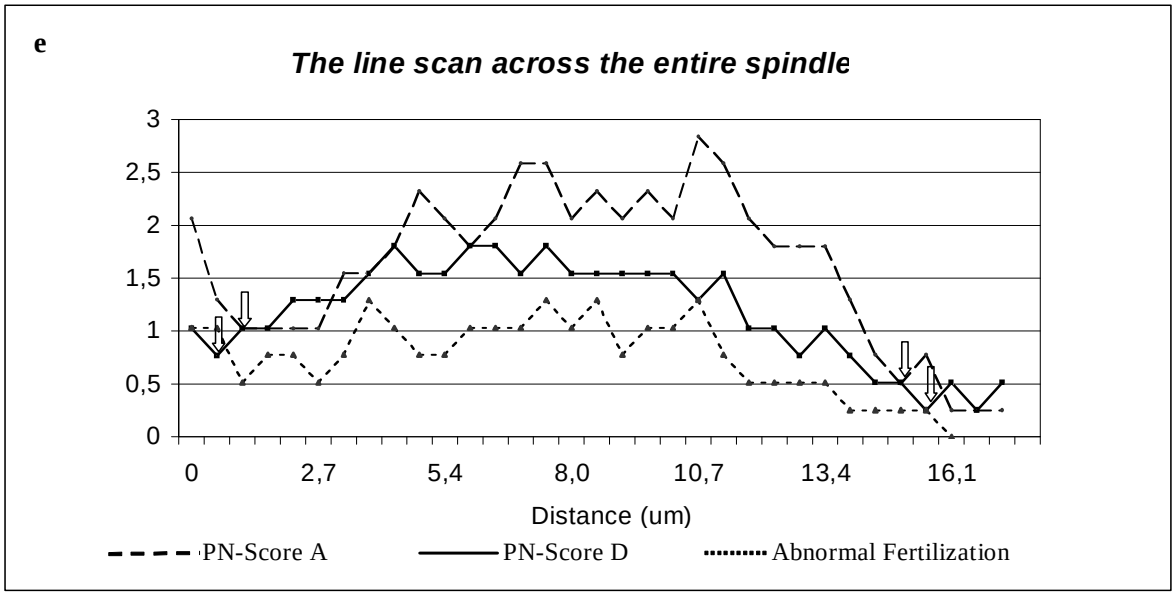

Figure 5.3.1 Line scan of the meiotic metaphase II spindle for analysis of retardance (a) and images of oocytes forming a pre-embryo with pronuclear score A (b) and D (c), or abnormal fertilization (d). Characteristic examples of retardance curve of a line scan (e) through the spindle apparatus of an oocyte forming a pre-embryo with score A (striped line), with a score D (solid line) or with abnormal fertilisation (dotted line). Vertical dotted lines depict outer boundaries of the spindle measured on the line scan of the oocyte developing into a pre-embryo with pronuclear score D. Open arrows show the outer boundary and the two measurement points excluded from the calculation of the average magnitude of retardance of light by the spindle. Bar in a: 10 µm. Bar in b for b-d: 40 µm.

Table 5.2: Quantitative assessment of mean retardance of light and spindle length in all oocytes selected or non-selected for transfer developing into pre-embryos with different PN score after ICSI: PN score of pre-embryos of all oocytes from patients of different age according to criteria by Scott and Smith (1998).

PN score of Pre-embryo	Numbers of Pre-embryos Derived by Oocytes with Spindle	Mean Maternal Age / Oocyte	Mean Retardance (nm)	Mean Length of Spindle (μm)
Group 1: Score A,B	180	31.9 ± 4.2	1.72 ± 0.43	12.7 ± 1.8
Group 2: Score C	51	32.0 ± 3.8	1.53 ± 0.40[a]	12.5 ± 1.6
Group 3: Score D	324	32.2 ± 4.0	1.52 ± 0.44[b]	12.6 ± 1.7
Group 4: Score E and Abnormals	121	31.2 ± 4.3	1.39 ± 0.46[b]	11.7 ± 1.7 [c,d]
Total	676	32.2 ± 4.2	1.55 ± 0.45	12.5 ± 1.8
Total in Non-Conception Cycles	430	32.1 ± 3.7	1.56 ± 0.46	12.4 ± 1.8
Total in Conception Cycles	246	32.3 ± 4.5	1.53 ± 0.44	12.6 ± 1.8

Two tailed Students T-Test: Significant difference to group 1: [a]$P < 0.05$; [b]$P < 0.001$; [c]$P=0.001$. Significant difference to group 3: [d] $P=0.005$.

The mean retardance magnitudes of meiotic spindles was quantitatively analysed for each sub-group. Oocytes of group 1 forming embryos with a PN score of A or B contained spindles with the highest birefringence with a mean value of 1.72 nm. The mean retardance magnitudes were 1.53 nm and 1.52 nm for subgroups 2 and 3, respectively. These values were not statistically different from each other, but significantly lower compared to subgroup 1 ($P < 0.001$, Tab 5.2). The oocytes developing into embryos with poor quality (subgroup 4) had a spindle with an even lower retardance magnitude of only 1.39 nm (Table 5.2), significantly lower compared to subgroup 1 and 3. The retardance magnitude of subgroup 4 was nearly 20% lower compared to group 1.

The pole-to-pole distance of the metaphase II spindle in living human oocytes was also analysed by PolScope microscopy in the four sub-groups. Mean spindle length was similar in sub-group 1, 2 and 3. However, a significantly shorter spindle was characteristic for oocytes developing into embryos with poor quality (subgroup 4) compared to the other three groups (Table 5.2, $P < 0.001$). However, there was no significant difference in mean length of spindles in cohorts of oocytes giving rise to a conception cycle (CC; 12.6 ± 1.8 µm; Table 5.2) versus those of a non-conception cycle (NCC; 12.4 ± 1.8 µm; Table 5.2).

5.3.3 Maternal Age and Spindle Organisation

Mean maternal age of patients having oocytes with a highly birefringent spindle (mean retardance over 1.55 nm) was compared to that giving rise to oocytes with a spindle with low birefringence (mean retardance below 1.55 nm). Mean age of patients with highly birefringent spindle was 32.3 ± 4.1 (324 oocytes) while that with low birefringence was 31.5 ± 4.1, respectively, (352 oocytes) not significantly different from each other for this group of patients, in which 4 to 20 oocytes were available for analysis. Mean retardance of spindles in all oocytes of patients older than 36 years (1.53 ± 0.44 nm) did also not differ much from that in intermediate age (31-35 years; 1.54 ± 0.42 nm) or younger patients (≤ 30 years; 1.58 ± 0.49 nm). However, there was a tendency for a slight decrease in mean retardance of the spindle in older compared to younger oocytes selected for transfer (Table 5.3), but this did not reach statistical significance.

5.3.4 Biochemical Pregnancy in Oocytes with Lower or Higher Mean Retardance of the Spindle

The mean retardance of spindles in oocytes, which were selected at pronuclear stage for transfer after ICSI (254 oocytes) was significantly higher, compared to oocytes giving rise to pre-embryos, which were not selected for transfer according to their comparatively poorer PN score (422 oocytes) (1.66 ± 0.43 nm vs.1.49 ± 0.43 nm, $P < 0.001$; Table 5.3). Of the total of 268 transfer oocytes, 254 possessed a spindle (Table 4.4). There was no

tients that were selected

Non-Transferred

Age (years)	Total			Transferred		Non- transferred	
	Cycles	Oocytes	Mean retardance (nm)	Oocytes	Mean retardance (nm)	Oocytes	Mean retardance (nm)
≤ 30	40	271	1.58 ± 0.49	100	1.70 ± 0.47	171	1.51 ± 0.49
31-35	37	273	1.54 ± 0.42	94	1.69 ± 0.41	179	1.46 ± 0.41
≥ 36	26	132	1.53 ± 0.44	60	1.58 ± 0.42	72	1.50 ± 0.46
Total	103	676	1.55 ± 0.45	254	1.66 ± 0.43	422	1.49 ± 0.44[a]

[a] Oneway ANOVA: Significant different to transferred.

significant difference in mean retardance of spindles between transfer oocytes giving rise to conception cycles versus those contributing to a non-conception cycle (1.65 ± 0.43 nm vs.1.67 ± 0.44 nm; Table 4.4). There was also no significant difference in mean retardance magnitude of spindles in non-transferred oocytes between CC versus NCC cycles (1.46 ± 0.43 nm vs.1.50 ± 0.46 nm) or in the total cohort of oocytes obtained by individual patients, including transfer and non-transfer oocytes between CC and NCC oocytes (1.53 ± 0.44 nm vs. 1.56 ± 0.46 nm; Table 5.2). There was also no other parameter like number of follicles or number of polar body oocytes, or fertilization rate, which could be identified to be distinct between the CC and NCC group (Table 4.4). In conclusion, from the cohort of patients most of which were belonging to the age range up to 35 years there was no conclusive evidence that mean retardance of the spindle was dramatically reduced in oocytes. However, there was a slight decrease in mean retardance by the spindles of oocytes chosen for transfer (presumably the best ones from the cycles) between the groups under and over 36 years.

5.3.5 Mean Retardance in Relation to Transfers with Good or Mediocre/Low PN scores and Preganancy Rate

Usually, more than one embryo of same or different PN score (2-3 embryos) were actually transferred in each cycle. If only one high quality oocyte/embryo is needed and responsible for the pregnancy, averaging may not be useful to reveal correlations between retardance, PN scores and conception. Therefore oocytes were grouped according to transfers, in which either 2 to 3 good PN score embryos (PN score A-C, corresponding to group 1 and 2 in Table 5.2) were present or only one good pre-embryo together with embryos of PN score D-E (group 3 and 4 in Table 5.2), or transfers in which only two to three embryos of lowest PN scores (D and E) were present.

About 43-47% of those cycles with at least one good PN score embryo of PN score A-C led to a conception (Table 5.4). In contrast, only 31.4% of cycles involving low PN score embryos resulted in a conception. The percentage of pre-embryos contributing to conceptions with transfer of only 2-3 low PN score embryos was significantly lower compared to those with at least one embryo with PN score A-C (Table 5.4). Of note, mean retardance of the spindle of transfer oocytes was lowest in the group with no good PN score embryo at transfer (1.55 ± 0.36 nm), significantly lower compared to the groups

Table 5.4 Conception (biochemical pregnancy) in patients with transfer of two or more pre-embryos with good PN score (A-C), with only one good PN score embryo and one or two lower score embryos (D-E), or transfer with two to three embryos with no good PN score (A-C) in correlation to average mean retardance and mean spindle length of oocytes used for transfer after ICSI in the cycle.

Good PN score Embryos in Transfers	Numbers of Patients	Mean Maternal Age (y)	Average number of Transferred Embryos	Conception (% in Group)	Total Number of Transferred Pre-embryos (without spindle)	Pre-embryos in Conception (% of Group)	Mean Retardance of the Spindle (nm)	Mean Spindle Length (µm)
≥ 2 with PN score A-C	32	31.6 ± 4.6	2.6 ± 0.5	14 (43.8)	82 (3)	33 (42.2)	1.78 ± 0.47[b]	12.9 ± 1.8
One with PN score A-C	36	32.6 ± 4.3	2.6 ± 0.6	17 (47.2)	92 (4)	38 (41.3)	1.63 ± 0.45[b]	13.0 ± 2.0
None with PN score A-C	35	33.0 ± 3.6	2.7 ± 0.7	11 (31.4)	94 (7)	29 (30.9)[a]	1.55 ± 0.36[b]	12.5 ± 2.0
Transferred Embryos	103	32.4 ± 4.2	2.6 ± 0.7	42 (40.8)	268 (14)	100 (37.3)	1.66 ± 0.43	12.8 ± 1.9

[a] χ^2-test: asymtotic significance; $P < 0.05$.
[b] One-way ANOVA: Significant difference between all groups; $P < 0.05$.

with one good embryo (1.63 ± 0.45 nm) and with 2 or 3 good pre-embryos with score A-C in transfers (1.78 ± 0.47 nm; Table 5.4). Mean spindle length was similar in all three groups. Thus, oocytes with low birefringent spindles appeared to develop frequently into low PN score pre-embryos after ICSI and subsequently contributed significantly less frequent to a conception compared to those with highly birefringent spindles.

5.4 Quantitative Analysis of the Zona Pellucida of Human Oocytes Using PolSocpe Microscopy and Developmental Potential

In order to find another potentially critical parameter related to high developmental potential and cytoplasmic maturity of oocytes, the zona pellucida was retrospectively analysed in images of oocytes taken before ICSI and later chosen for transfer according to criteria defined by pre-embryo morphology/ PN score on day 2.

5.4.1 Characteristic Morphology of the Human Zona Pellucida in Oocytes of the CC and NCC Group

The human zona pellucida appears transparent and fairly uniform in structure when viewed with a conventional light microscope equipped with phase contrast or differential interference (DIC) optics (Figure 5.4.1 A). In contrast, enhanced polarized light microscopy reveals three distinctly different layers of the extracellular coat surrounding the human oocyte (Figure 5.4.1 B). An inner layer appears as the lightest refractile, bright and thickest layer of the human zona pellucida in all oocytes observed by PolScope imaging in this study. The inner (IL) and the outermost layer (OL) facing the medium or cumulus are separated by a thin middle layer (ML), which does not change the light path much and therefore appears dark and non-refractile (Figure 5.4.1 B). However, as noticed already by Pelletier *et al.* (2004), the morphology of the zona pellucida may be rather heterogeneous around individual oocytes (Figure 5.4.1 D-F), and within cohorts of oocytes from individual patients. The texture of the zona pellucida was quite homogenous in individual oocytes from other cohorts (Figure 5.4.1 C).

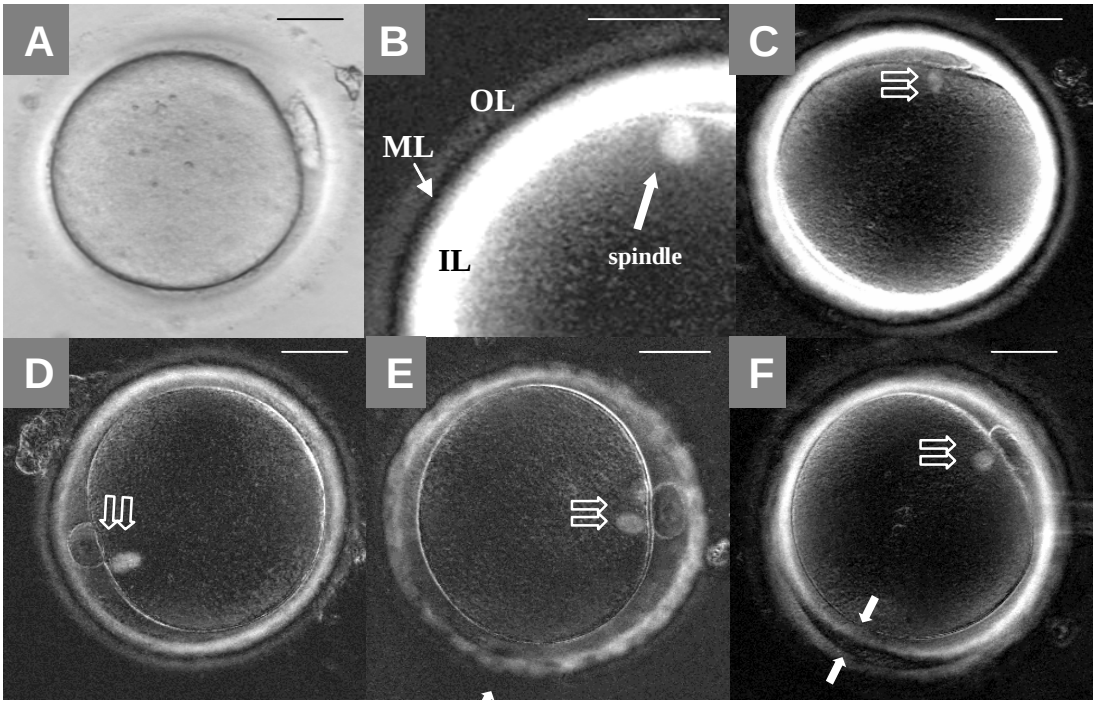

Figure 5.4.1 Images of human oocytes selected for embryo transfer. A: The zona pellucida of human oocytes imaged by light microscope appears transparent and uniform; B: The three-laminar architecture of zona pellucida imaged by PolScope-microscopy; C: Oocytes of CC group contained a bright and thick zona pellucida. D-F: Oocytes from non-pregnant patients showed different abnormal phenotypes of zona pellucida: thin (D), irregular (E) or sub-split into two layers (F). Bar=25µm

The variability in zona morphology within cohorts of oocytes from individual patients and between oocytes from different patients appeared mainly related to differences in the relative homogeneity and birefringence and brightness of the inner layer of the zona pellucida (Figure 5.4.1 C-F). In a few oocytes the zona pellucida appeared especially irregular or thin (Figure 5.4.1 D), and sometimes the inner layer of the zona was sub-divided into 2 layers with a hollow appearing space in between (Figure 5.4.1 F, arrows) as if the patterning or the secretion of protein was temporarily interrupted during the formation of this part of the extracellular coat during oocyte growth, or the zona was ruptured by mechanical stress at retrieval or separation from cumulus.

Figure 5.4.2 Retardance-curve of oocytes from CC and NCC group. One scan belongs to the cohort of oocytes in the CC group (solid line), the other is characteristic for the NCC group (dotted line).

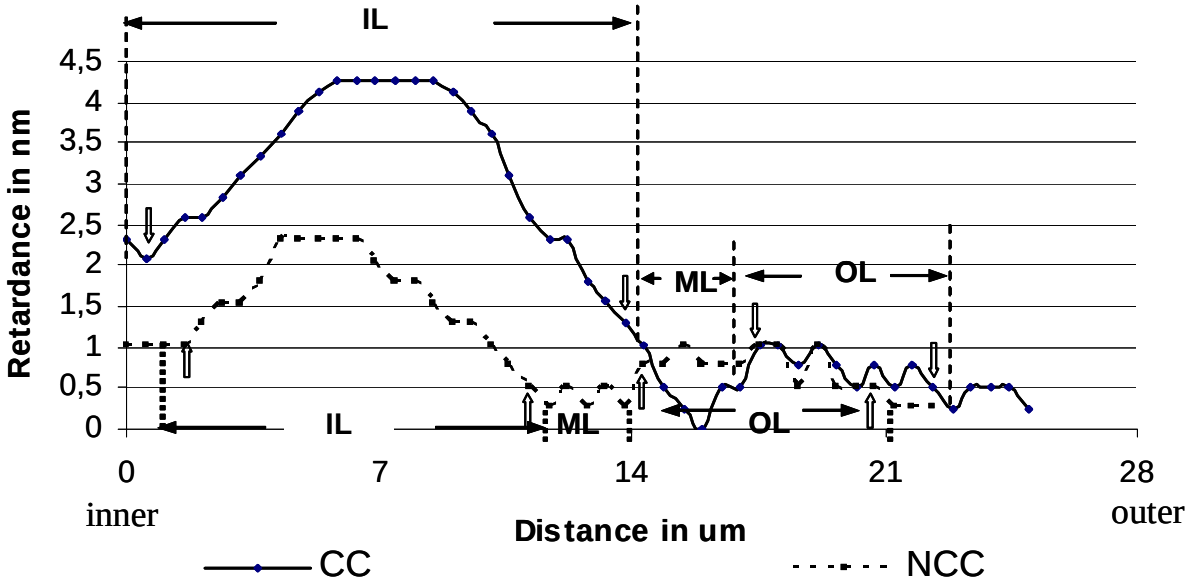

Two characteristic examples of cross sections along a line scan at 0.5 µm spaced measurement points to determine light retardance across the entire zona pellucida are shown by Figure 5.4.2. One characteristic scan is from the cohort of oocytes in the CC group (upper solid line), the other is characteristic for an oocyte of the NCC group (lower dotted line). The inner layer (IL) exhibits the highest retardance magnitude and cross-section thickness for both examples. The retardance magnitude of the outer layer (OL) tends to be overall lower than the inner layer as demonstrated in both line scans, while the middle layer (ML) consistently appears dark and least changing the light path. As can be seen in all images of oocytes in Figure 5.4.1 B-F, which were later used in transfers after ICSI, the majority of oocytes used for transfer in both groups contained a bi-polar, barrel-shaped meiotic spindle, which was localised close to the first polar body in most cases (Figure 5.4.1, double arrows).

Table 5.5 Mean retardance magnitude and thickness of the individual zona layers as assessed by PolScope microscopy in oocytes contributing to CC and NCC group.

	CC (transferred)	NCC (transferred)
Patients	23	40
Oocytes	65	101
Zona inner layer (x ± SD) Retardance (nm)	2.81 ± 0.60[1]	2.15 ± 0.41
Thickness (μm)	11.25 ± 1.44[1]	9.36 ± 1.74
Zona middle layer (x ± SD) Retardance (nm)	0.35 ± 0.08	0.35 ± 0.07
Thickness (μm)	3.92 ± 0.76	3.66 ± 0.65
Zona outer layer (x ± SD) Retardance (nm)	0.55 ± 0.18	0.55 ± 0.14
Thickness (μm)	4.80 ± 1.40	5.55 ± 1.03
Zona total thickness (x ± SD) (μm)	19.87 ± 1.92[2]	18.58 ± 1.82

[1] t-test, $P < 0.001$, significantly different from the NCC group.
[2] t-test, $P < 0.01$, significantly different from the NCC group.

5.4.2 Quantitative Analysis of Retardance Magnitude and Thickness of the Zona Layers in CC and NCC Groups

Mean retardance magnitude along the line scan across the zona pellucida has been quantitatively analysed. The quantitative analysis by PolScope revealed that the average retardance magnitude of the zona pellucida differed considerably between cohorts of oocytes in CC and NCC cycles. While differences in mean retardance were insignificant in the middle and outer layer, the mean magnitude of retardance of the inner layer of the zona pellucida was significantly higher in the oocytes of cycles leading to a conception

compared to those in the NCC group (2.81 ± 0.60 nm vs. 2.15 ± 0.41 nm, P < 0.001; Table 5.5). The mean retardance magnitude which reveals the density and organisation of zona pellucida appeared therefore correlated positively to a conception cycle.

Similar to the magnitude of retardance, thickness of the middle and outer layers did not differ significantly between groups, but the thickness of the inner layer was significantly increased in the pregnant group (11.25 ± 1.44 μm) compared to the non-conception group (9.36 ± 1.74 μm, P < 0.001, Table 5.5). The thickness of the zona pellucida was statistically different between the two groups although the magnitude of the absolute difference in thickness was low, on average only about 1.3 μm (Table 5.5). It appears that the relative thickness of the zona inner layer leads to an overall increase in thickness of the entire zona pellucida: It was significantly higher in a conception compared to a non conception cycle.

5.4.3 Mean Retardance as Predictive Parameter for Conception

After ICSI of all oocytes, only 2-3 embryos per patient are usually transferred. The 166 oocytes from 23 CC and 40 NCC were selected for embryo transfer at 18 hours post-insemination according to PN score and the general morphological criteria described above (s. Chapter 4.6). From the 166 oocytes transferred to patients after ICSI, over 60% in both groups comprised embryos with high PN score (A – C, high quality), while around one third of the oocytes used for transfer in both groups had developed to a pre-embryo with a PN score of D (lower quality; Figure 5.4.3 A). Only 3 oocytes with lower score (score = E) were selected also for transfers, notably, these were later shown to belong to the non-conception group. Therefore, the average number of embryos with good PN score used for transfer in CC and NCC groups did not differ much (numbers of embryos with PN score A-C were 1.8 ± 0.75 and 1.6 ± 0.85 in CC and NCC group, respectively). In contrast to the small differences in PN score between the two groups, retrospective comparison of embryo development on day 2 after fertilization between those embryos comprising the CC and the NCC group revealed striking differences in mitotic cycles at early embryogenesis (Figure 5.4.3 B). In total, 53.8% of the embryos in the CC group had developed to the 4-5-cell stage on day 2, whereas only 34.7% of embryos giving rise to the NCC group had reached this advanced stage (chi^2-Test, P <

0.05). In contrast, about 60% of the embryos in the NCC group had only ≤ 3 cells on day 2 of development after oocyte retrieval (Figure 5.4.3 B). In conclusion, the observations imply that high quality embryos, which can facilitate implantation and induce an increase in hCG-level in blood, developed faster than embryos, which failed to induce a pregnancy, in agreement with other reports in the literature (e.g. Lundin *et al.*, 2001; Neuber *et al.*, 2003; Nagy *et al.*, 2003). Although the embryos in the CC and NCC groups had a quite different developmental rate, the PN-stage oocytes selected by the Scott's score criteria at day 1 after ICSI were similar between the two groups at the one-cell stage. In fact, embryos with a Scott's score of A – C had the same chance (about 50%) to contribute to a conception after implantation, as the embryos with a score of D.

To obtain more information on oocyte quality, the 166 oocytes were divided into three groups based on their mean retardance magnitude of the inner layer of the zona pellucida. Group 1 had a retardance of over 3.0 nm; group 2 a retardance between 2.0 nm and 3.0 nm, and group 3 a retardance below 2.0 nm. Nearly 90% of the oocytes in the group 1 (25 oocytes) comprising oocytes with a retardance over 3.0 in the zona inner layer from a total of 28 oocytes were associated with a clinical pregnancy (Figure 5.4.4). In contrast, a retardance magnitude of over 3nm was observed in only 3 oocytes of the NCC group.

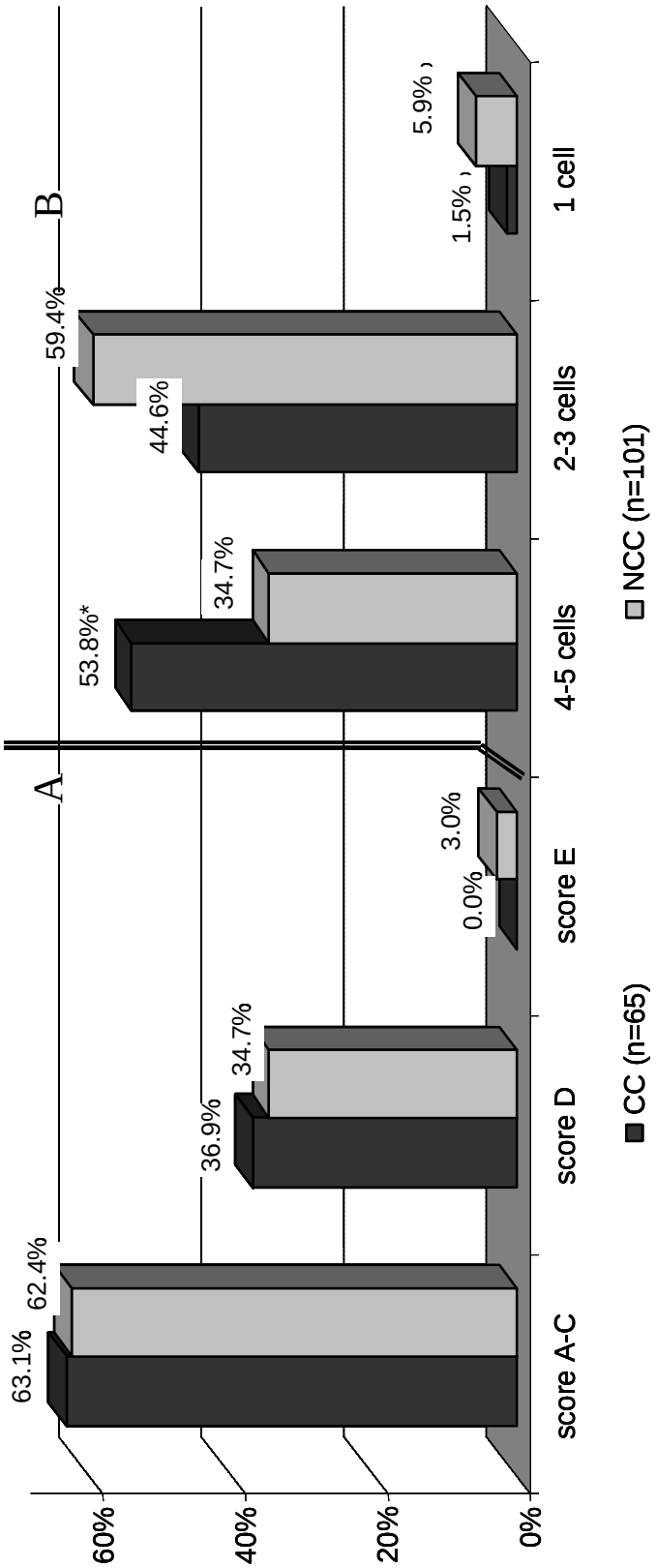

Figure 5.4.3 PN scores at 18 h post-insemination (A) and embryo development at day 2 (B): At day 1, 2-3 one-cell embryos with the best PN scores were selected for embryo transfer to each patient. Therefore, the embryo quality at day 1 appears similar in the CC and NCC groups. However, the embryo development at day 2 showed a significant difference between CC and NCC groups. *Embryos of CC group developed faster than the embryos of NCC group (χ^2-test: significant difference between CC and NCC groups; P < 0.05).

With the decrease of the magnitude of retardance in the zona inner layer, the percentage of oocytes resulting in a pregnancy cycle became dramatically reduced. Only 11.4% of the oocytes in the lowest retardance group belonged to a CC after ICSI and embryo transfer while the majority did not contribute to a conception (Figure 5.4.4; χ^2-test, $P < 0.001$).

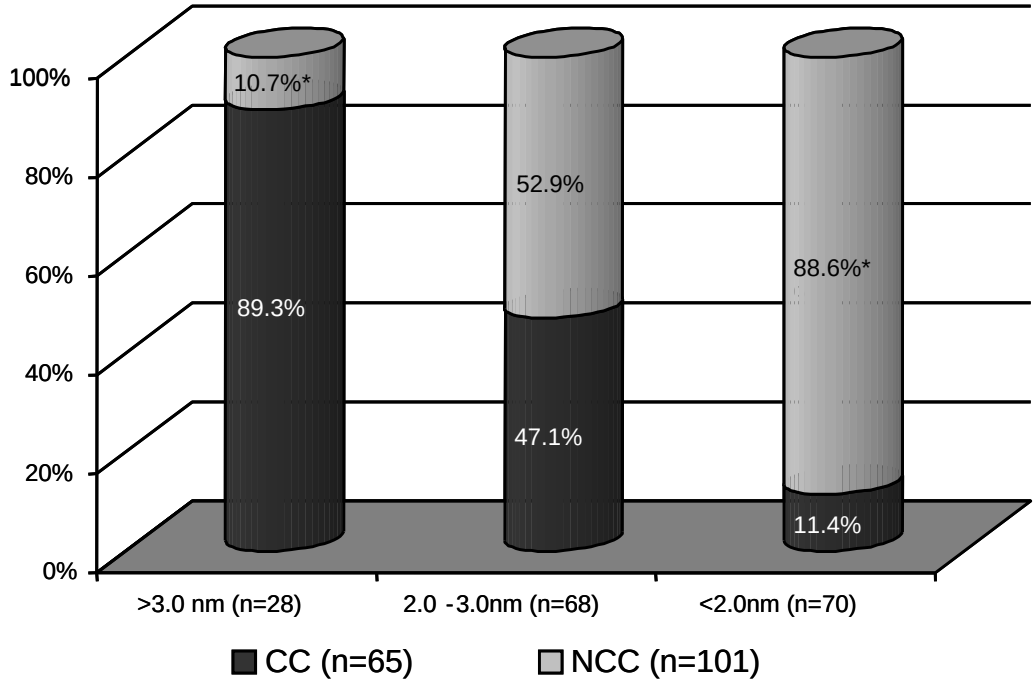

Figure 5.4.4 Quantitative analysis of the inner layer of the zona pellucida. With the decrease of the retardance magnitude in the inner layer of zona pellucida, the number of oocytes inducing a pregnancy reduced significantly (*χ^2-test, $P < 0.001$).

5.4.4 Relationship Between Thickness and Retardance

In a previous study, it has been suggested that the retardance of the zona pellucida, especially the inner layer of the zona pellucida, is positively correlated with zona thickness in a small cohort (Pelletier *et al.*, 2004). However, the relationship of two parameters correlated to a conception cycle was not analysed by Pelletier *et al.* (2004). In the current study, the correlation of retardance magnitude and thickness of the inner layer of the human zona pellucida was analysed in CC and NCC groups. The data are represented in Figure 5.4.5. Obviously, data for individual oocytes do not distribute randomly confirming the suggestion of Pelletier *et al.* (2004). The correlation coefficients of the retardance-thickness curves are slightly different with 0.43 and 0.56

for the CC and NCC groups, respectively. The data reveal that the retardance-thickness correlation is more clearly depicted by the regression analysis in the oocytes of the CC group, since the correlation coefficient of CC is higher than that of the NCC group (0.56 vs. 0.43).

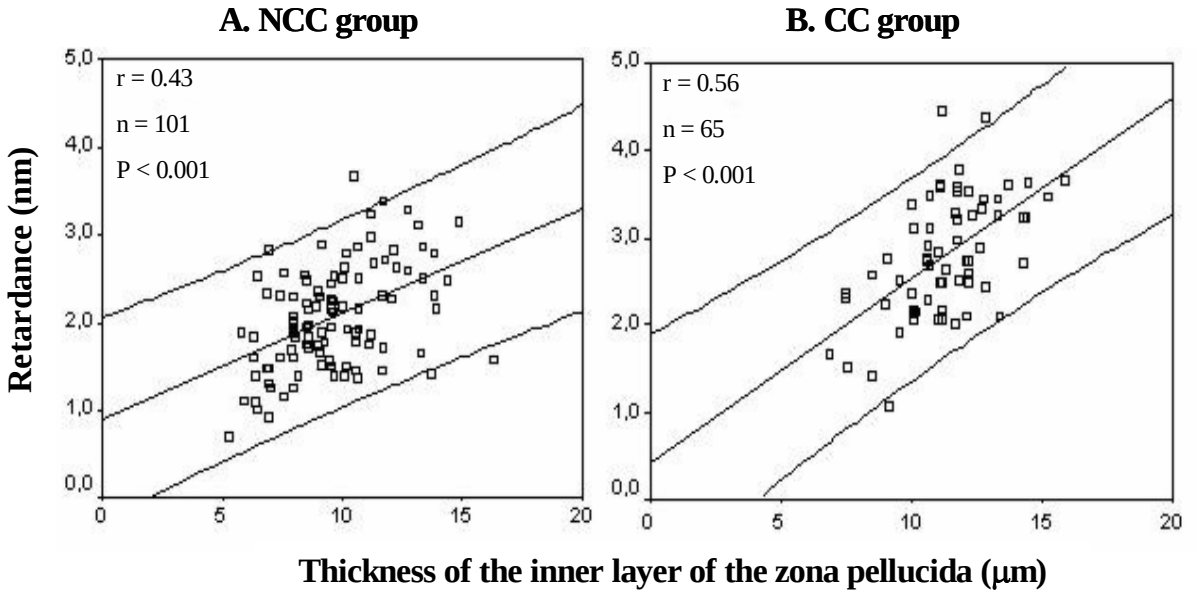

Figure 5.3.5 The linear relationship between retardance and thickness of the inner layer of the zona pellucida in oocytes of CC and NCC groups.

5.4.5 Influence of Maternal Age and Differences in Zona Thickness and Retardance between Transfer and Non-transfer Oocytes

The mean retardance and thickness of the zona inner layer and total zona were also compared between oocytes in CC and NCC from younger and more reproductively aged women (Table 5.6). In total, the numbers of patients in the young, middle and aged groups were 77, 54, and 35, respectively.

Table 5.6 Comparison of the mean retardance and the thickness of the zona inner layer and the total zona thickness in oocytes from young and aged women contributing to CC and NCC groups.

	Group	≤ 32 years (n = 77)		32 – 37 years (n=54)		≥ 37 years (n = 35)	
CC	Retardance (nm)*	38	2.79 ± 0.63	16	3.02 ± 0.70		2.51 ± 0.24
	Thickness (µm)*		11.15 ± 1.75		11.66 ± 1.02		10.93 ± 0.84
	Total thickness (µm)*		20.16 ± 2.34		19.00 ± 1.30		20.24 ± 0.65
NCC	Retardance (nm)	39	2.22 ± 0.35	38	2.14 ± 0.45		2.06 ± 0.46
	Thickness (µm)		8.79 ± 1.71		10.18 ± 1.84		8.97 ± 1.23
	Total thickness (µm)		18.07 ± 1.55		18.90 ± 1.69		18.86 ± 2.34

* No significant difference between conception and age (two-way ANOVA).

Among the total of 23 CC patients and 40 NCC patients, no significance was found in the mean retardance and thickness between the zona of oocytes from different age belonging to the group ≤ 32 years (group 1), 32 – 37 years (group 2) and ≥ 37 years (group 3), while values for mean retardance and thickness were lower in all oocytes from the NCC compared to the CC group at each age (Table 5.6).

6. Discussion

6.1 Analysis of Spindle Formation by PolScope in Improvement of *in vitro* Maturation and Selection of Human Oocytes

Hormone stimulation in IVF programmes usually promotes the maturation of most meiotic competent oocytes *in vivo*, but there are still some oocytes remaining at the germinal vesicle stage at the time of puncture, possibly due to a sub-optimal microenvironment in the follicle (Hardy *et al.*, 2000). It may be expected that such meiotically incompetent oocytes have a comparatively low maturational and developmental potential after culture without cumulus.

However, in the present study it was shown that a large proportion of the GV oocytes obtained from ICSI cycles were able to resume nuclear maturation, develop to metaphase II and emit a polar body. In comparison to previous studies, the yield of PB oocytes was high under the chosen culture conditions. For instance, 60.6% of failed *in vivo* matured GV oocytes cultured to metaphase II in the study by Cekleniak *et al.* (2001) and 67% of immature GV oocytes from stimulated cycles that were transiently arrested by phosphodiesterase 3 (PDE3) inhibitor reached metaphase II after recovery from the block (Nogueira *et al.*, 2005), similar to present data with oocytes that were maturation incompetent *in vivo* (66.1% with polar body at 36 h). However, only a limited number of oocytes emitting a PB *in vitro* had a well-organized spindle visible as a birefringent cell structure, similar to observations in previous studies (Wang *et al.*, 2002; Combelles *et al.*, 2002). This suggests that quality of the immature oocytes is comparatively low. It would require prospective studies with groups of patients donating oocytes from un-stimulated or stimulated cycles, or, possibly, such at risk for hyperstimulation syndromes, polycystic ovary syndrome etc. to evaluate maturation success, rate of spindle formation and developmental potential to further improve culture conditions and success in assisted reproduction.

In addition to previous work the present study shows that the proportion of *in vitro* maturing oocytes expressing a birefringent spindle was significantly lower compared to the *in vivo* maturing oocytes from the same patients ($P < 0.001$). Furthermore, the percentage of PB oocytes with birefringent spindles decreased substantially within only 12-18 h of metaphase II arrest (Figure 5.1.2). The dramatic reduction in the expression of a birefringent spindle may be due to accelerated ageing of *in vitro* maturing human

oocytes, similar to the observation in a previous study characterized by defaulted progression into interphase within 24 h of polar body emission of *in vitro* maturing human oocytes (Combelles *et al.*, 2002). According to experiences with unfertilized *in vivo* maturing human oocytes from other groups, e.g. in Italy where only those oocytes selected for embryo for transfer are inseminated, spindles are retained for over 24h provided oocytes are kept under suitable conditions (Laura Rienzi, personal communication). Thus, the present observations on rapid degeneration of the spindle of immature, *in vitro* cultured oocytes support the notion that this cohort should usually not be considered for fertilization and transfer, as long as other mature oocytes are available, because they appear to be mostly of low quality.

IVF utilizes the principle of gonadotrophin administration for oocyte maturation *in vivo* prior to ovulation. Some patients with polycystic ovarian syndrome (PCOS) have lower sensitivity to gonadotrophin stimulation and most oocytes after retrieval remain at germinal vesicle stage. *In vitro* maturation (IVM) of immature oocytes is becoming an attractive new alternative to obtain oocytes for IVF and ICSI, especially in patients with PCOS or predisposed to developing ovarian hyperstimulation syndrome (OHSS). Although maturation of oocytes *in vitro* from mildly stimulated or unstimulated cycles are continuously improved (e.g. Chian, 2004; Mikkelsen, 2005; Papanikolaou *et al.*, 2005, Rao and Tan, 2005), the success rate of IVM is still very low, due to the sub-optimal culture conditions. The data from *in vitro* maturing oocytes confirm that many GV-stage oocytes from stimulated ICSI cycles matured *in vitro* do not reach full cytoplasmic maturity to maintain spindle integrity and meiosis II arrest and that a large percentage fail to form a normal spindle, which can be responsible for the high risk for errors in chromosome segregation (Nogueira *et al.*, 2000). Besides the intrinsic defects in some of the oocytes (Combelles *et al.*, 2003) sub-optimal culture conditions in absence of cumulus may additionally contribute to the low quality of the oocytes that might be overcome by co-culture systems (Combelles *et al.*, 2005). Further studies with PolScope on kinetics of spindle formation and degeneration, including quantitative assessment of birefringence, could help to improve conditions for *in vitro* maturation. As compared to oocytes matured *in vivo*, the majority of oocytes matured *in vitro* did not express a birefringent spindle (19.6% vs. 83.9%). Due to the dramatically reduced rate on the expression of a birefringent spindle, the introduction of PolScope to evaluate quality of oocytes provides

new, essential information on oocyte quality in IVM. It may thus help to select oocytes with the best quality for fertilization, and by this greatly improve the clinical outcome from this source. For patients suffering from PCOS and OHSS the introduction of natural cycle *in vitro* maturation and ICF may be promising (Chian *et al.*, 2004) and should be assessed with respect to spindle integrity in oocytes.

6.2 PolScope Analysis of Birefringent Spindles in *in vivo* Maturing Oocytes

6.2.1 Non-invasive Nature of PolScope Analysis in ICSI cycles

The data in chapter 5.2.1 shows that the pregnancy rate of patients, whose oocytes were evaluated by PolScope is not significantly lower than the rate of patients whose oocytes were not viewed with the PolScope (Figure 5.2.1). Exposure to PolScope illumination did not affect the oocytes' health and their viability after fertilization. The design of PolScope is based on the same principle of light, as used for differential interference contrast optics (DIC), which has been used for clinical purposes for over 20 years. PolScope utilizes nearly circular polarized light with a wavelength of 546 nm as light source, which contains no detrimental component in either infrared or ultraviolet fields and therefore should not damage oocytes that are briefly examined. Moreover, the light intensity in the sample is approximately 60µW, which is also in the safe range that should not cause damage to oocytes (Liu *et al.*, 2000a). Studies with mouse oocytes viewed by PolScope showed that PolScope microscopy is non-invasive since imaged oocytes had a similar developmental capacity in cleavage rate and pregnancy rate, in comparison with controls (Liu *et al.*, 2000a). A further study with 770 human oocytes from 87 ICSI cycles confirmed that the light illumination with PolScope did not affect oocyte and embryo health in the human (Wang *et al.*, 2001c). PolScope has been used by several laboratories for non-invasive observation of the meiotic oocyte spindle and also the high order structure of the thick extracellular coat of human oocytes, the zona pellucida, in routine assisted reproduction (Wang *et al.*, 2001a,b,c; Eichenlaub-Ritter *et al.*, 2002; Rienzi *et al.*, 2003; Moon *et al.*, 2003; Pelletier *et al.*, 2004; Shen *et al.*, 2005). The rate of blastocyst formation of oocytes illuminated by PolScope (Wang *et al.*, 2001c) is equal to the rate of oocytes without illumination (Ebner *et al.*, 2005). Observations in human oocytes that were subjected to ICSI for assisted conception in the present study support the notion of the non-invasive nature of the technique and its safety with human oocytes.

6.2.2 Predictive Value of Qualitative Assessment of Spindle Birefringence in *in vivo* Maturing Human Oocytes

6.2.2.1 Predictive Value of Imaging the Meiotic Spindle by PolScope for Determination of Oocyte Maturity

Currently, the absence of germinal vesicle and extrusion of first polar body are used for determination of oocyte maturity. In the two-year study, 324 oocytes, which contained germinal vesicle and/or did not form a first polar body, were recognized as immature oocytes under a stereomicroscope after retrieval (Figure 5.2.2 A & B). However, still some immature oocytes arrested at the telophase I stage (n = 128) could not be determined (Figure 5.2.2 C), because they also possessed the first polar body and appeared morphologically similar to mature oocytes under an optical microscope. Thus, the current criteria for assessing mature oocytes appear to be inadequate. Imaging meiotic spindle by PolScope microscopy seems to be a more accurate parameter for determination of oocyte maturity. It can be used as an additional parameter for assessing meiotic maturation of oocytes. In fact, a recent study by Montag *et al.* (2006) revealed that it is possible to determine the ideal time for ICSI in such delayed oocytes by PolScope such that they have developed to metaphase II before being injected with sperm (Montag *et al.*, 2006).

6.2.2.2 Predictive Value of Qualitative Analysis of Spindle Presence

Most of the *in vivo* maturing oocytes expressed a birefringent spindle (83.9% of 1369 oocytes) comparable to observations by other groups (e.g. Wang *et al.*, 2001 a;b;c; Rienzi *et al.*, 2003; Moon *et al.*, 2003). In agreement with previous studies (Wang *et al.*, 2001a;b;c; Rienzi *et al.*, 2003; Moon *et al.*, 2003), oocytes without spindle had an overall lower capacity to develop into a normal embryo, and absence of a birefringent spindle was associated with a significantly higher risk for fertilization failure compared to oocytes with spindle (Figure 5.2.4, $P < 0.001$). Moreover, fertilization rate and percentage of oocytes forming a pre-embryo with a "good" PN score (score A-C) was higher in the oocytes with spindle compared to those without spindles. The data were also differently analysed, such that the “good” PN score was defined only by embryos with score A and B. The statistical significant difference on forming presumably high quality pre-embryos (score A and B) still existed between oocytes with and without birefringent spindle.

The poor quality of oocytes without spindles may be caused by an aberrant spindle with unordered spindle fibres and scattered chromosomes. Conventional microscopy showed the presence of unordered spindles and chromosomes in oocytes without birefringent spindle in the cohort that could be fixed from the immature *in vitro* cultured oocytes (Figure 5.1.1). From the seemingly mature oocytes of ICSI cycles which were fertilized 128 oocytes were still in telophase I according to the PolScope observation (Chapter 5.2.2; Figure 5.2.2 C). These data supported the idea that some of the oocytes which did not contain a birefringent spindle might not have reached metaphase II stage yet, at 38 hours after hCG administration. Such oocytes may be expected to have a lower potential to form high quality embryos compared to those in metaphase II. A dynamic observation of the meiotic cell cycle in human oocytes demonstrated that the meiotic spindle disappeared for around 40-60 minutes during the transition from metaphase I (MI) to metaphase II (MII) (Montag *et al.*, 2006). Thus, a spindle could not be detected in oocytes arrested in the MI/MII transition. The presence of a birefringent spindle is, therefore, an indicator for either oocyte quality or oocyte maturity. In the future it might be possible to wait for ICSI of such oocytes without spindle to assess presence of a spindle at a later time and thereby improve outcomes, in particular when none or only few oocytes with spindle are available in a patient. It is feasible that they suffer from prolonged oocyte maturation and that this could affect the potential to become pregnant after ICSI. Further studies have to show whether "postmaturation" for one to two hours might be helpful in such cases.

Generally, the mere analysis of presence/absence of a birefringent spindle in human metaphase II oocytes from ICSI cycles is of limited value for oocyte selection in IVF since the vast majority of oocytes (83.9%) had a birefringent spindle apparatus. From the oocytes without spindle some still developed to pre-embryos with good PN score. The latter may present oocytes that had only reached late telophase I or pre-metaphase II although they possessed a PB. The yield of high quality pre-embryos may therefore be improved by repeat assessment of the potentially "immature" meiosis II oocytes and fertilization at a later time. Especially in cases, where all or most oocytes from a patient are without spindle, it may become possible to improve outcomes by either prolonging the culture before ICSI (in cases with delayed development) or adjusting stimulation protocol and oocyte retrieval (e.g. in cases of accelerated maturation and degeneration of oocytes).

Visualization of meiotic spindle by PolScope may also help to determine the spindle position according to the first polar body, in order to avoid any damages of spindle apparatus during oocyte manipulation, for instance, during laser-assisted polar body biopsy (Montag *et al.*, 2004). In the present study it did not appear possible to assess alignment of the chromosomes at the equatorial plane, as has been for instance reported for mouse oocytes of controls and mice with mitochondrial dysfunction and accelerated ageing (Thouas *et al.*, 2006). It may be that the oocytes examined in the course of this study had most robust and dense spindles so that the area occupied by chromosomes did not show up against the surrounding spindle fibres. Since other groups showed images of birefringent meiosis II spindles with a clear middle area, it remains to be determined if this is related to the timing of PolScope analysis (directly after retrieval or 1-2h later/ directly after removal of cumulus or later) or culture/handling conditions and/or quality of oocytes. In this study, oocytes were imaged within 2 hours after retrieval, i.e. in 38 hours after hCG administration. It is the optimal timing to visualise meiotic spindle in oocytes from stimulated cycles (Cohen *et al.*, 2004). Since there was no adverse effect of PolScope imaging compared to outcomes in the controls, currently there is no evidence for suboptimal handling which might lead to changes obscuring chromosome positioning. One possible explanation is that the sensitivity of the PolScope imaging system in IVF Giessen is not high enough to obtain a high quality birefringent picture of the spindle. The sensitivity of the PolScope system (SpindleView 3.9) is 0.1 nm. However, the sensitivity of the PolScope system used in other laboratory may reach 0.02 nm (Silva *et al.*, 1997; 1999). Furthermore, using a more stable temperature controlling system, e.g. delta system (Wang *et al.*, 2001c), and a heated objective might help to improve observation of chromosomal positioning. For this in the future the determination of the direction of orientation of spindle fibres may have to be optimised by viewing retardance at any point of the image. Further work is required to see whether it will be possible to modify the protocols without adverse influence on oocytes to assess also chromosomal alignment, since it might contribute to assess spindle function, chromosomal constitution and oocyte quality.

6.2.2.3 Predictive Value of Spindle Positioning

Another approach to identify high and/or low quality oocytes is based on analysis of spindle position relative to the first polar body. There is an ongoing debate on the significance and origin of spindle displacement from the first polar body with respect to developmental potential (Rienzi *et al.*, 2003; Hardarson *et al.*, 2000; Cooke *et al.*, 2003; Ebner *et al*., 2003). In the present study a lower number of oocytes had spindles displaced for > 40° away from the PB compared to other reports (16.9% vs. 62.6% from Cooke group, Cooke *et al.*, 2003), fair proportion of the fertilized oocytes with displaced spindles still developed into pre-embryos with high or mediocre PN score in the present study. A larger deviation angle of > 40^{o} of the metaphase II spindle correlated positively to the rate of fertilization failure but not to the rate of multi-pronuclear formation that might be caused by damage of the spindle apparatus during sperm microinjection (Figure 5.2.5). In contrast to *in vivo* maturing oocytes, the spindle was essentially always located close to the PB in denuded *in vitro* maturing oocytes (Rienzi *et al.*, 2003). Deviation of the spindle from the first polar body may therefore be mainly caused by the mechanical stress by manipulation at or after oocyte retrieval, and this may be related to reduced oocyte quality (Rienzi *et al.*, 2003). In conclusion, the present observations support notions by other studies suggesting that the assessment of spindle positioning is not very predictive of oocyte quality and may be only useful in cases where the creation of supernumerary embryos is to be avoided (Rienzi *et al.*, 2003).

6.2.3 Reliability of Quantitative Assessment of Spindle Birefringence in Living Human Oocytes

By analysis of birefringence of kinetochore microtubules in images through optical planes through spindles of the fairly flat crane fly spermatocytes using PolScope, LaFountain and Oldenbourg (2004) recently succeeded in calculating the numbers of microtubules attached to each individual homologous chromosome in bivalents with respect to chromosome alignment. Such optical sectioning of spindles was not possible in the large, spherical human oocytes with the standard microscope equipment and 40 x or 20 x objective lenses used in this study. Although calculation of mean retardance of the spindle does not provide an absolute quantitative assessment of numbers of microtubule fibres in spindles and density of fibres at each point of measurement, the analysis of mean

birefringence provides information on the quality of the spindle with respect to density/high order of spindle fibres and length and width of the spindle apparatus. Still, one has to keep in mind that the oocyte spindle is not a homogenous organelle and is highly dynamic. Previous quantitative measurements assessed major retardance, e.g. upon thawing after freezing of human oocytes (Bianchi *et al.*, 2005). The line scan was in the middle of the spindle body, along the long axis of the spindle, irrespective of whether longer or shorter segments of chromosome arms might be located in this region and might have contributed to background or to a lower value in the assessment of average retardance. As there are differences in optics and culture conditions it is difficult to standardize measurements and compare absolute values between different laboratories. Liu *et al.* (2000b) encountered a similar difficulty when they calculated mean retardance in mouse oocyte spindles after parthenogenetic activation or fertilization either in the whole spindle area or in line scans through the spindle equator. They found for both methods of calculation different absolute values of mean retardance but concordantly and reproducibly observed significant increases in mean retardance values upon activation (Liu *et al.*, 2000b; Navarro *et al.*, 2005). It appears that calculation of mean retardance of the spindle along a line scan under standard conditions in a unit helps to minimize experimental variables and provides a good semi-quantitative estimate of the overall order and density of tubules within the spindle apparatus in assessment of oocyte quality.

6.2.4 Predictive Value of Quantitative Analysis of the Birefringent Properties of the Meiotic Spindle in Oocytes

Data in the current and previous studies showed that the majority of *in vivo* maturing oocytes contained a birefringent spindle (Wang *et al.*, 2000c, Moon *et al.*, 2003; Rienzi *et al.*, 2003). In addition, the study revealed that there are quantitative individual differences in birefringence properties of the oocyte spindle and these appear related to the oocytes' quality and developmental potential. Clearly, qualitative and quantitative PolSope imaging alone may not be suitable alone to select top oocytes and embryos with high viability for implantation. However, the present study shows for the first time that the mean retardance magnitude revealing the density and organization of spindle apparatus correlates positively with the quality of pre-embryos after insemination.

Several recent studies suggest that pre-embryos with low PN score are more likely to develop into chromosomally aberrant embryos compared to those with high PN score (Chen *et al.*, 2003; Gianaroli *et al.*, 2003; Balaban *et al.*, 2004; Kahraman *et al.*, 2002; Edirisinghe *et al.*, 2005). In accordance, oocytes with spindles with low birefringence that develop to pre-embryos with lower PN scores may be more frequently abnormal compared to healthy oocytes with robust spindles that presumably have highly organized microtubular fibres and normal chromosomal constitution. Observations on conception involving transfers with high and low PN score embryos confirmed that PN scoring was positively correlated with conception cycles and that transfer with embryos of lower scores were associated with failures to conceive much more frequently than those involving better PN score embryos, irrespective of the scoring systems. Concomitantly, mean magnitude of retardance of light by the spindle was positively correlated to conception cycles. The observations were confirmed by data from a study with a small cohort of oocytes obtained in the IVF Unit in Hospital Raffaele, Milan Italy. In total, a small cohort of 59 oocytes from 28 ICSI cycles (mean maternal age 33.7± 4.3 years) was evaluated by PolScope, due to the prescription in Italy that a maximum of three embryos is allowed to generate during each cycle. Oocytes were grouped according to pronuclear score described by Tesarik and Greco (1999), including morphological features of pronuclear and cytoplasm. As in the present study there was a tendency that more oocytes producing pre-embryos of higher quality (score 0) had high spindle retardance and those developing into embryos with mediocre quality (score 1 & 2) or poor quality had lower mean retardance (score 3-5) (Tab. 6.1). The pronuclear scoring system described by Tesarik und Greco (1999) is similar to the Scott scoring system (Scott and Smith, 1998). Both systems used presently account for pronuclear size and position, number and alignment of NPB (nucleolar precursor bodies), and the morphological feature of cytoplasm. The limited size of the samples in both centres and the relative heterogeneity of patients precluded to compare effectiveness between PN scoring according to the Scott and Smith (1998) or the Tesarik and Greco (1999) criteria. Pregnancy and implantation rates were high during the course of the study in the Giessen IVF unit and future prospective studies have to reveal whether quantitative PolScope imaging as an additional parameter for selection of best embryos for transfer may help to increase rates of conceptions further.

Due to the strict legal regulations in Germany, embryo quality was only assessed by PN scoring in selection of pre-embryos for transfer since legal restrictions do not allow studying non-transfer embryo fate and development further. From the present data it appears that effectiveness of scoring according to mean retardance rather than PN scoring may overcome limitations of the PN scoring systems and thus contribute to identification of high quality oocytes already before ICSI. Low retardance due to spindle abnormality and chromosomal imbalance may be just the tip of the iceberg indicating deficiencies in the oocytes causing development of low quality embryos. Other problems, for instance, changes in expression pattern (Hamatani *et al.*, 2004) or failure to mediate activation of zygotic gene expression may all contribute to failure in conception from such oocytes.

Table 6.1: Quantitative assessment of spindle retardance in oocytes developing into pre-embryos with different PN score in the IVF Unit in Hospital Raffaele, Milan Italy, mean maternal age, mean retardance of spindle in oocytes developing into pre-embryos that contribute to a conception cycle (CC; gestational sac) or non-conception cycle (NCC); PN score of pre-embryos from selected oocytes from patients of different age according to criteria by Tesarik and Greco (1999).

PN score (Tesarik & Greco)	Numbers of Pre-embryos	Mean Maternal Age (y)	Mean Retardance of all (nm)	Implantation (Sacs) (%)	Mean Retardance in CC (nm)
Group 1: Score 0	15	32.5 ± 5.2	2.15 ± 0.86	4 (26.7)	3.02 ± 1.05
Group 2: Score 1	16	34.9 ± 3.6	1.96 ± 0.39	3 (18.8)	2.46 ± 0.48
Group 3: Score 2	20	34.8 ± 3.2	1.86 ± 0.67	2 (10.0)	2.68 ± 0.14
Group 4: Score 3-5	8	33.4 ± 4.8	1.59 ± 0.35[a, b]	0 (0)	
Total	59	33.7 ± 4.3	1.93 ± 0.64	9 (15.3)	2.76 ± 0.73
Total in NCC (From Group 1-5)	50	33.9 ± 4.1	1.78 ±0.50		
Total in CC (From Group 1-3)	9	32.6 ± 5.2	2.76 ±0.73[c]		

Chi-Square: Significant difference to group 1: [a]$P < 0.05$; Significant difference to group 2: [b]$P < 0.05$.
T-Test: Significant difference to NCC, [c] $p = 0.002$.

Thus, mean retardance by spindles in oocytes was not correlated to conception cycles comprising 2-3 oocytes that were chosen for transfer after ICSI. From the observation it appears that these oocytes were, in fact, the best ones from the individual patients, since mean retardance of spindles of transfer oocytes was significantly higher compared to those of the non-transfer oocytes. According to present observations, the oocytes with the most robust spindles were therefore selected for transfer by employing PN scoring. The retrospective studies suggest that both methods for selection appear equivalent, and that selection by spindle analysis may be as powerful as PN scoring to identify healthy oocytes.

6.2.5 Correlation Between Morphology of the Meiotic Spindles and Maternal Age

A large cohort of patients who had between 4 and 20 oocytes at retrieval was included in this study. The data suggest that oocytes with low mean retardance magnitude of spindle mainly develop to pre-embryos with presumably poor quality according to PN score. Due to legal restrictions further development of embryo could only be analysed in embryos which were selected for transfer. There was no evidence for a significant correlation between length or mean retardance by the spindle and maternal age when comparing age groups of patients $\leq$ 30 years, 31-35 years and over 36 years (Table 5.3), although there was a minor age-related reduction in mean retardance value. Mean retardance of spindles was also calculated in all oocytes of individual patients with respect to high and low numbers of retrieved oocytes or cycles that had or had no immature GV stage at retrieval and did not detect a correlation. This suggests that overall oocyte quality in terms of spindle retardance is not directly influenced by stimulation response resulting in maturation of few or large numbers of oocytes.

The present study may have failed to detect age-associated correlations since cycles with very low or high numbers of oocytes were excluded from the analysis. For instance, it is feasible that predominantly poor responders with three or even fewer oocytes may have short spindles with low mean retardance, or that stimulation of maturation of more than 20 oocytes has adverse effects on the overall quality of the retrieved oocytes. The short protocol used in stimulation of aged patients may also optimise follicular and oocyte maturation *in vivo* such that some age-related effects are reduced. Data from the small

cohort in Milan including more patients of advanced age and cycles with few oocytes showed a significant correlation between mean retardance magnitude and maternal age. It supports the notion that overall spindle quality may decline with advancing age, in accordance with immunofluorescent studies and previous reports (Battaglia *et al.*, 1996; De Santis *et al.*, 2005).

6.3 Highly Ordered Structure of the Zona Pellucida May Reflect Health and Quality of Living Human Oocytes

The zona pellucida is an extracellular matrix that comprises a three dimensional structure composed of heterodimeric filaments of ZP2 and ZP3 proteins and linked by ZP1 protein (Green, 1997). Studies in animal models with defined genetic constitution and mutations have shown the relevance of a functionally intact zona (Liu *et al.*, 1996; Rankin *et al.*, 1999 and 2001a,b). It has been suggested that the oocyte's zona morphology may be influenced by hormonal homeostasis and reproductive age of the woman (Bertrand *et al.*, 1996), and that the thickness of the zona pellucida in individual embryos from a patient might be correlated to developmental capacity and implantation rate (Gabrielsen *et al.*, 2001).

Due to the paracrystalline network structure of the zona (Wassarman *et al.*, 2004), orientation-independent polarization microscopy can now be used for qualitative and quantitative analyses in living oocytes, similar to studies on spindle expression (Oldenbourg, 1996; Keefe *et al.*, 1997; Silva *et al.*, 1997; Pelletier *et al.*, 2004; Eichenlaub-Ritter *et al.*, 2002 and 2004; Wang *et al.*, 2001a,b;c; Keefe *et al.*, 2003, Moon *et al.*, 2003; and Rienzi *et al.*, 2003 and 2005). Using PolScope microscopy to image and quantitatively analyze birefringence of the spindle and zona pellucida in mammalian oocytes may, therefore, obtain more essential information for the assessment of oocyte quality and risk assessment in aneuploidy research, especially from oocytes subjected directly to a treatment in infertile patients. The procedure is fast, provides immediate information and has no adverse effects on the oocytes. Oocytes from 63 cycles, which were assessed for spindle birefringence, were also assessed for morphology and integrity of the zona pellucida in the current study. Electron microscopic analysis by other groups showed two layers with zona filaments: a tight or looser meshed network on the outside and repetitive structures characterized by numerous short and straight filaments

anastomosing with each other in the inner layer, separated by a translucent space (Familiari *et al.*, 1992; Nikas *et al.*, 1994). PolScope analysis confirms the bilaminar, tripartite nature of the zona (Keefe *et al.*, 1997; Pelletier *et al.*, 2004) as identified in several species (Baranska *et al.*, 1975; Andrews *et al.*, 1992; Gilchrist *et al.*, 1997; Green, 1997; Keefe *et al.*, 1997; Ebenspaecher *et al.*, 2001; Dunbar *et al.*, 2001; El Mestrah *et al.*, 2002; Sinowatz *et al.*, 2001; Jimenez-Movilla *et al.*, 2004). Filaments of the inner zona are oriented radically, whereas filaments of the outer zona are oriented tangentially. The middle layer represents minimal birefringence due to the random orientation of filaments in the layer (Keefe *et al.*, 1997; Silva *et al.*, 1997). Such order can be analysed by examining vector orientation in PolScope microscopy (Figure 2.1.7 B). The inner and outer layers are, therefore, highly birefringent, as expected from the paracrystalline arrangement of zona fibrils, while the middle layer appears dark.

When human oocytes mature from the GV-stage to meiosis II the thickness of the zona increases progressively but becomes thinner after fertilization prior to hatching (Dirnfeld *et al.*, 2003; Pelletier *et al.*, 2004). Accordingly, there was evidence that the retardance magnitude of the zona pellucida changes stage-specifically and correlates with the overall zona thickness at the immature and mature stages of oogenesis and the pre-implantation period (Pelletier *et al.*, 2004). Stage-specific alterations in zona thickness were interpreted to reflect the maturation status: the extent of cross-linking and the degree of deposition of zona fibres, as well as fertilization-induced changes in structural and functional properties of the zona associated with normal development. It has been suggested that the overall variability in zona thickness at day 2 of human embryogenesis is an indicator for implantation potential (Gabrielsen *et al.*, 2001). The data from the present study showed that the retardance magnitude and thickness of zona inner layer varied between different oocytes. Oocytes with a high retardance of the inner layer of the zona pellucida contributed significantly more often to a conception cycle compared to those with low retardance of the zona inner layer. These data demonstrated a positive correlation between the texture of the zona, as quantitatively assessed by the magnitude of retardance of light in PolScope microscopy in freshly retrieved human oocytes, and pregnancy rate after ICSI. A brief report using semi-quantitative Polarization methods recently confirmed the present observations suggesting that high zona retardance is associated with high quality embryos (Montag *et al.*, 2006)

6.3.1 Mean retardance magnitude of the inner layer is a novel indicator of oocyte developmental capacity after fertilization

Although significant in comparison, the differences in thickness between CC and NCC groups were not extensive in the present study (on average 1.3 μm). Accordingly, it does not appear to be useful to measure zona thickness for oocyte selection. In contrast, the magnitude of retardance in the inner layer of the zona is over 30% higher in oocytes of the CC compared to NCC group before actual *in vitro* fertilization by ICSI, and before zona hardening and thinning had been initiated. This correlated with fast embryonal development, as may be characteristic for embryos with high developmental potential and a normal chromosomal constitution (e.g. Lundin *et al.*, 2001; Neuber *et al.*, 2003; Gianaroli *et al.*, 2003; Nagy *et al.*, 2003; Ziebe *et al.*, 2003).

A robust zona with high-order structured fibres probably reflects the health of an oocyte and its full maturation to metaphase II (Pelletier *et al.*, 2004). It indicates that the oocyte, and possibly the granulosa cells within the follicle, (Sinowatz *et al.*, 2001; Gook *et al.*, 2004) were capable of secreting co-ordinately large amounts of glycosylated zona proteins, which were assembled into a high-order network during folliculogenesis and oocyte growth (Nikas *et al.*, 1994). Expression of zona proteins from the oocyte and other sites may contribute in unknown ways to establish polarity gradients, improve oocyte/somatic cell signalling e.g. by transzonal projections (Albertini and Barrett, 2003), and thus support oocyte maturation and acquisition of high developmental potential, irrespective of functions at and after fertilization (Thompson, 2006).

A thick and solid zona could also be of advantage in ICSI, because it protects the oocyte particularly well from mechanical stress during the microinjection procedure and stress-related changes during the preimplantation development affecting, for instance, amino acid uptake (Leese, 2004). However, ICSI has been successful in cases of zona-free human oocytes (Ding *et al.*, 1999; Takahashi *et al.*, 1999; Hsieh *et al.*, 2001; Stanger *et al.*, 2001), while implantation appeared more jeopardized by absence of a zona in some patients (Hsieh *et al.*, 2001). Zona pellucida thickness also appears positively correlated to embryo quality after IVF (Dirnfeld *et al.*, 2003).

The efficient association of embryonal and uterine factors with the zona of the embryo could be of importance, in that an accumulation of autocrine and paracrine factors at the zona could enhance oocyte or embryo development (Celik-Ozenci *et al.*, 2003) and help

to create a specific micro-milieu around the embryo prior to hatching, which supports and enhances development during the preimplantaion period (Seshagiri *et al.*, 1994; for discussion see Herrler and Beier, 2000; Herrler *et al.*, 2003). The embryo secretes gonadotrophines, growth factors and components mediating signalling in the extracellular space with potentially autocrine and paracrine stimulatory effects (Herrler *et al.*, 2003; Liu and Armant, 2004). Recent scanning electron-microscopic studies demonstrated that growth hormone can alter the structure and pore size of the zona pellucida of blastocysts in the bovine (Kolle *et al.*, 2004) and may act in concert with IGF-I to optimise blastocyst development (Markham and Kaye, 2003). Assisted zona hatching was not performed in the protocol suggesting that a robust zona with a highly structured inner layer in oocytes prior to ICSI does not compromise implantation after ICSI. However, there were no oocytes with extremely thick zona observed in the presently analysed cohort. It may be that extremes can compromise fertilization and development (Nawroth *et al.*, 2001). Further studies need to be exploring this possibility, which could not be performed in the present study due to the limited number of cycles. Since not all oocytes from a patient's cohort were screened for zona thickness, it is also currently not possible to discriminate between predictive value of zona retardance for most oocytes of a patient or usefulness of quantitative analysis to select oocytes from a cohort.

6.3.2 Maternal age and organisation of zona pellucida

From polar body analysis and pre-implantation genetic diagnosis it appears that chromosomal imbalance is a major cause of developmental arrest and implantation failure in ART, especially in aged patients (e.g. Munne, 2003; Pellestor *et al.*, 2003; Clyde *et al.*, 2001; Kuliev *et al.*, 2003; Ziebe *et al.*, 2003). Nearly 50% of the embryos transferred in the youngest age group involved conception cycles but only about 30% of the embryos transferred in the age groups over 32 years involved in the zona study. Certainly, zona thickness and texture are not expected to relate to chromosomal constitution of the oocyte, and it is doubtful whether analysis of the zona pellucida will improve pregnancy rate in aged patients, in which aneuploidy of the embryo may be the primary source of implantation failure (Pellestor *et al.*, 2003; Munne *et al.*, 2004). A clear correlation between zona thickness and retardance and reproductive age within the CC and NCC groups was not found in the limited sample. However, when calculating overall zona

retardance of the inner layer including oocytes of the CC and the NCC group, there was a minor reduction in retardance of the inner layer from about 2.5 nm in the youngest to 2.4 nm in the intermediate and 2.2 nm in the oldest age group. Patients subjected to ICSI are in general comparatively young, and presumably less susceptible to meiotic errors at oogenesis compared to more aged cohorts. In a large cytogenetic study with nearly 1400 human oocytes only 9% of the unfertilized human oocytes of patients aged about 32 years were chromosomally unbalanced (Pellestor *et al.*, 2003), in contrast to about fifty percent or more aberrant oocytes examined directly by cytogenetics or by polar body analysis with fluorescent *in situ* hybridisation in women of an average age of about 38 years (Pellestor *et al.*, 2003; Kuliev *et al.*, 2003). In fact, nearly all oocytes used for transfer, which were included in this study, contained birefringent spindles as assessed by PolScope. Probably, most were euploid since they developed into an embryo with a good PN score (Magli *et al.*, 2001; Gianaroli *et al.*, 2003; Gamiz *et al.*, 2003; Balaban *et al.*, 2004). Selection for morphological criteria may reduce the risk to transfer a chromosomally unbalanced embryo (Ziebe *et al.*, 2003), and may contribute to select good quality oocytes in younger patients with male factor indication. From the study it appears that fast developmental rate correlated not only with pregnancy cycles but that it also correlated with magnitude of zona retardance in the inner layer of the zona of the unfertilised oocyte. So, zona retardance may be a valuable early and non-invasive marker of oocyte quality. The positive correlation between zona birefringence and oocyte developmental potential after insemination has been confirmed by a prospective study (Montag *et al.*, 2006). Zona birefringence was analysed in oocytes from 30 ICSI cycles. Two embryos with possibly high retardance magnitude of zona inner layer were selected for embryo transfer per cycle. Due to the small number of cycles, a significant difference on pregnancy rate was only found in cycles in which 2 embryos with high zona birefringence were transferred and the cycles in which both embryos presenting low zona birefringence (Montag *et al.*, 2006). This study supported the idea that the birefringence of the zona inner layer may be a novel indicator for oocyte quality diagnosis. Predictive analysis of zona birefringence using PolScope may become a powerful tool to improve the success rate of ICSI and the treatment of infertile couples. Still, controlled prospective studies of a large number of patients are now required to validate whether quantitative

zona imaging can improve pregnancy rate, or can help to identify embryos with high developmental capacity in order to reduce numbers of transferred embryos.

6.4 Application of PolScope Microscopy in Assessment of Oocyte Quality in Human Assisted Reproduction

Although more than one embryo is usually transferred, rates of implantation and pregnancies in assisted reproduction are still fairly low (Fauser *et al.*, 2002). Especially, when ethical and legal considerations limit selection after fertilization, it appears important to identify non-invasive markers of oocyte quality to obtain reasonable implantation and pregnancy rates (e.g. Zollner *et al.*, 2002; Ebner *et al.*, 2003). Although oocytes that failed to be fertilized or those with fertilization abnormalities from IVF programmes provided a large source for information on the ultrastructure of the spindle and zona pellucida (Hodges *et al.*, 2002; Magerkurth *et al.*, 1999; Familiari *et al.*, 2001), it has not been possible to relate this to oocyte developmental potential. Electron microscopy, immunochemical and molecular methods require invasive techniques (e.g. Philips and Shalgi, 1980; Takagi *et al.*, 1989; Eichenlaub-Ritter and Betzendahl 1995; Vanroose *et al.*, 2000; Bogner *et al.*, 2004). Metabolic and morphological markers obtained during culture (e.g. Houghton and Leese, 2004) cannot be used in such cases. Suitable assays and parameters of predictive factors in the cumulus or in the follicular fluid of the oocyte, which are associated with quality and developmental competence of an individual oocyte from a cohort, are currently not available, and biopsy and chromosomal analysis of the first and second polar body (Kuliev *et al.*, 2003; Gitlin *et al.*, 2003) are costly, time consuming and also not considered acceptable by some patients. Therefore, the search for cheap and fast, non-invasive methods to identify factors associated with structural and functional integrity of the oocyte has been intensified (Wang *et al.*, 2001a;b;c; Keefe *et al.*, 2003; Eichenlaub-Ritter *et al.*, 2002; Rienzi *et al.*, 2003).

PolScope microscopy has more advantages in comparison with other invasive procedures mentioned above. It is safe, non-toxic, easy to manipulate and suitable for clinical use. PolScope microscopy may provide more data on morphology and organisation of ultra structures in living status, which reflect the health and developmental potential of living

oocytes. Therefore, the introduction of the newly developed non-invasive procedure may greatly improve the success rate in assisted reproduction.

6.4.1 Novel Ways to Assess Oocyte Quality Non-invasively

To improve the success rate, embryos with presumably high implantation potential have been selected for transfer in IVF/ICSI programmes. The prolonged culture of embryos to blastocysts stage enables a high implantation rate following the transfer of selected blastocysts (Gardner *et al.*, 1998). The approach of accounting for pronuclear size and position, and number and alignment of NPB (nucleolar precursor bodies) at the pronuclear stage is an alternative to predictively assess human embryo quality in countries where the selection of embryos at blastocysts stage is restricted by ethical and legal considerations. The pronuclear scoring system was originally introduced by Scott and Smith (1998) and supported by Tesarik and Greco (1999). This scoring system includes morphological features such as clear cytoplasmic halo, and has been commonly and successfully employed in IVF and ICSI programmes to assess embryo quality (Scott, 2003; Payne *et al.*, 2005). However, in some countries, such as Italy, the quality assessment and selection have to be performed even before the fertilization of oocytes. Due to the Italian IVF law, the generation of more than three embryos per cycle is prohibited. Thus, the approach to predictively and non-invasively identify oocytes and embryos with highest developmental potential is extremely interesting for countries with a strict embryo protection law, such as Germany and Italy. The present study showed that mean retardance magnitude of the spindle in living oocytes was positively correlated to PN score and conception cycles. The findings suggest that selection by spindle analysis may be as powerful as or even better than PN scoring to identify healthy oocytes in a patient's cohort. From the present data it appears that effectiveness of scoring according to mean retardance rather than PN scoring may overcome limitations of the PN scoring system and thus contribute to identification of high quality oocytes already before ICSI. This notion was supported by the analysis of conception in patients with transfers with more than one high PN score embryo and such with low PN score embryos (Table 5.4).

Furthermore, the quantitative analysis of mean retardance magnitude of zona pellucida suggests a more clear view of oocyte health and quality. In the 23 CC and 40 NCC cycles included in zona study, PN score did not differ greatly between embryos of both groups

nor were there striking differences in the expression of a spindle. In contrast, embryos in the CC and NCC groups had a quite different developmental rate and fate (Figure 5.4.3). Compared to the currently used PN scoring system, retardance magnitude of zona retardance may reflect the real fate of embryos in the early developmental stage more accurately, and appears, therefore, to present a novel unique marker for oocytes and embryos with high developmental potential, which possess an otherwise similarly good morphology.

To improve the sensitivity of the PN selection criteria, a complete multi-factor selection system based on the optical property of spindle apparatus and zona pellucida will be developed in the future for quick and efficient quantitative assessment of mean retardance by the spindle and the zona inner layer. Measurements should provide a straightforward approach to score oocytes in ICSI cycles non-invasively before fertilization. Such screening might present an option to improve selection, especially in conditions where ethical and legal regulations restrain suitability of post-insemination screening. The novel PolScope selection criteria may provide a unique aspect of embryo quality and the developmental capacity. The predictive quality assessment by PolScope may help to greatly improve the efficiency of the embryo selection, especially to accurate determine pre-embryos quality, which contain a similar score, and therefore, help to reduce the number of embryo for transfer as well as the risk of multiple pregnancies in the countries, where the ethical and legal considerations prohibit the selection of embryos at an early embryo stage, such as Germany. The expected improvement of ART outcomes may benefit more infertile couples by resolving their psychological and social suffering.

To determine the efficiency of the novel non-invasive criteria, the fertilization rate and pregnancy rate of the oocytes selected by the newly developed criteria will be compared with the oocytes (control) selected by the morphological assessment criterion. The information by PolScope can be used together with other parameters for oocyte selection before or after ICSI. Especially in cases where legal and ethical considerations prohibit selection at a more advanced stage of embryogenesis, including screening at the pronuclear stage, zona imaging may offer new options in oocyte selection since the procedure is fast, provides immediate information and has no adverse effects on the oocytes. In fact, it can be employed together with routine screening for expression and localisation of the spindle in living oocytes by enhanced polarising technology.

Due to the low birefringence property, chromosome behaviour cannot be analysed by the currently used PolScope imaging system. Polar body biopsy should be employed in combination with PolScope microscopy in future studies, to directly evaluate whether a highly ordered spindle revealed by a high mean retardance magnitude correlates with a lower risk of abnormal chromosome constitution compared to a spindle with low retardance. The novel non-invasive quantitative parameter of PolScope may also reveal a normal oocyte growth in follicles. An optimal stimulations protocol may thus be generated for individual patients by the way of analysing the mean retardance magnitudes of spindle and zona pellucida. In addition, analysis of the displacement of the meiotic spindle may also help to resolve the handling problem during oocyte manipulation.

The advantage of PolScope microscopy, to directly and non-invasively evaluate oocyte's ultrastructures *in vivo*, also enables the application of PolScope in epidemiological research, such as the identification of negative-positive factors in environment, nutrition and lifestyles. It has been reported that exposure to aneugen affecting polymerization of spindle microtubules may induce chromosomal congression failures in the spindle and chromosomal non-disjunction to produce aneuploid oocytes in mouse (Shen *et al.*, 2005).

The current study confirmed that the PolScope illumination does not produce any adverse effects on oocyte health. However, a prolonged exposure of oocytes during observations used for quantitative assessments of spindle and zona birefringence may cause a drop in temperature or alterations in the pH of the culture media. Currently, the calculation of birefringence using the first generation of PolScope software is still fairly complicated and time-consuming. Thus, future studies should aim at the analysis program to be improved continually to ensure a brief imaging period and a fast and exact calculation of birefringence of the subject. Recently, an advanced user platform with ultra-sensitive digital camera and powerful measurement tools, named "Oosight" system, has been developed for a more convenient observation using PolScope methodology (Figure 6.4.1 A). Oosight provides a fast and effortless solution for the real-time detection and assessment of birefringent structures in the oocytes, opening possibilities to study and

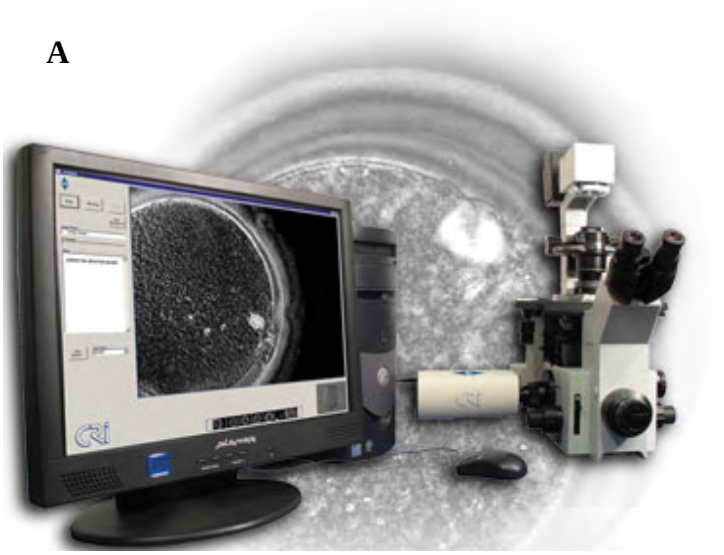

Figure 6.4.1 The newly developed PolScope imaging system – Oosight Imaging System

A: The Oosight™ Imaging System is a next-generation, improved version of PolScope system.

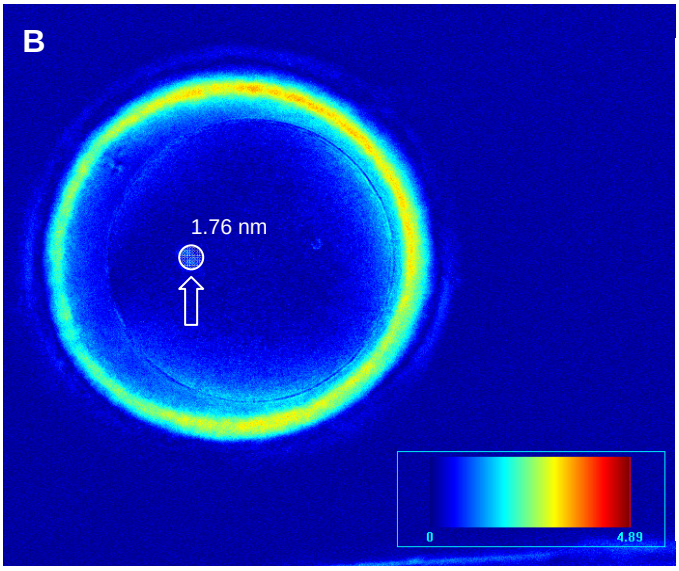

B: A birefringent image of human oocyte with pseudocolour overlay of retardance taken by Oosight system. The colour indicates the retardance magnitude of individual pixel on the image (Blue = 0 nm; Red = 4.89 nm).

Open arrow: Mean retardance magnitude of an interest region, i.e. spindle region, can be defined by selecting an area on the image.

record also spindle dynamics. Besides the measurement of birefringence through a line scan, Oosight provides also an “area measurement” function to measure the birefringence of a defined region of interest (Figure 6.4.1 B). The birefringent data can be displayed directly on the screen (Figure 6.4.1 B). This might produce even better and more accurate information of spindle and birefringent properties of organelles in oocytes.

The current work clearly demonstrates that PolScope microscopy is a novel procedure of predictive and non-invasive control of oocyte quality and maturity. It may provide useful

information on improvement of the experimental protocol and condition in IVF laboratory, i.e. prolongation of the culture period of oocytes after punctures waiting for the delayed maturation to metaphase II stage and optimal timing of fertilization for all oocytes, etc. introduction of the PolScope system in ART has thus the potential to increase the success in the IVF laboratory in an easy and feasible way, and might help to greatly improve the treatment of infertile couples.

7. References

Albertini DF and Rider V (1994) Patterns of intercellular connectivity in the mammalian cumulus-oocyte complex. *Microsc Res Tech* **27**, 125-133.

Albertini, DF and Barrett SL (2003) Oocyte-somatic cell communication. *Reprod Suppl* **61**, 49-54.

Alberts B, Johnson A, Lewis J, Raff M, Roberts K, Walter P (2002) Molecular Biology of the Cell 4th ed. *New York and London*: Garland Science.

Akiyama T, Nagata M, Aoki F. (2006) Inadequate histone deacetylation during oocyte meiosis causes aneuploidy and embryo death in mice. *Proc Natl Acad Sci* U S A. [Epub ahead of print]

Amos WB, White JG (2003) How the Confocal Laser Scanning Microscope entered Biological Research. *Biology of the Cell* **95**, 335–342.

Andrews JC, Howard JG, Bavister BD and Wildt DE (1992) Sperm capacitation in the domestic cat (*Felis catus*) and leopard cat (*Felis bengalensis*) as studied with a salt-stored zona pellucida penetration assay. *Mol Reprod Dev* **31**, 200-207.

Balaban B, Urman B. (2003) Embryo culture as a diagnostic tool. Reprod Biomed Online. **7(6)**, 671-682.

Balaban B, Yakin K, Urman B, Isiklar A and Tesarik J (2004) Pronuclear morphology predicts embryo development and chromosome constitution. *Reprod Biomed Online* **8**, 695-700.

Banks JD, Heald R. (2001) Chromosome movement: dynein-out at the kinetochore. *Curr Biol*. **11(4)**, R128-131.

Baranska W, Konwinski M and Kujawa M (1975) Fine structure of the zona pellucida of unfertilized egg cells and embryos. *J Exp Zool* **192**, 193-202.

Battaglia DE, Klein NA, Soules MR (1996) Changes in centrosomal domains during meiotic maturation in the human oocyte. *Mol Hum Reprod* **2**, 2217-2222.

Bendel-Stenzel M, Anderson R, Heasman J, Wylie C (1998) The origin and migration of primordial germ cells in the mouse. *Semin Cell Dev Biol.* **9(4)**, 379-391.

Bertrand E, Van den Bergh M, Englert Y (1996) Clinical parameters influencing human zona pellucida thickness. *Fertil Steril* **66**, 408-411.

Bianchi V, Coticchio G, Fava L, Flamigni C, Borini A. (2005) Meiotic spindle imaging in human oocytes frozen with a slow freezing procedure involving high sucrose concentration. *Hum Reprod* **20**, 1078-1083.

Bogner K, Hinsch KD, Nayudu P, Konrad L, Cassara C and Hinsch E (2004) Localization and synthesis of zona pellucida proteins in the marmoset monkey (*Callithrix jacchus*) ovary. *Mol Hum Reprod* **10**, 481-488.

Bolton VN, Hawes SM, Taylor CT, Parsons JH. (1989) Development of spare human preimplantation embryos in vitro: an analysis of the correlations among gross morphology, cleavage rates, and development to the lastocyst. *J In Vitro Fert Embryo Transf.* **6(1)**, 30-35.

Bornens M and Karsenti E (1984) The centrosome. *In Membranes, Structure and Function*. Vol.6. E.E. Bittar editor. John Veley & Sons, Inc.

Briggs D, Miller D, Gosden R. Molecular biology of female gametogenesis. In: Fauser B, Rutherford A, Strauss J, Van Steirteghem A. (Eds) *Molecular Biology in Reproductive Medicine*. New York: Parthenon, 1999; 251–269.

Brunet S, Maro B. (2005) Cytoskeleton and cell cycle control during meiotic maturation of the mouse oocyte: integrating time and space. *Reproduction* **130(6),** 801-811.

Can A, Semiz O. (2000) Diethylstilbestrol (DES)-induced cell cycle delay and meiotic spindle disruption in mouse oocytes during in-vitro maturation. *Mol Hum Reprod* **6(2)**, 154-162.

Can A., Semiz O., Cinar O. (2005) Bisphenol-A induces cell cycle delay and alters centrosome and spindle microtubular organization in oocytes during meiosis. *Mol Hum Reprod* **11(6)**, 389-396.

Carlsson IB, Scott JE, Visser JA, Ritvos O, Themmen AP, Hovatta O (2006) Anti-Mullerian hormone inhibits initiation of growth of human primordial ovarian follicles in vitro. *Hum Reprod*. [Epub ahead of print].

Celik-Ozenci C, Akkoyunlu G, Kayisli UA, Arici A and Demir R (2003) Localization of vascular endothelial growth factor in the zona pellucida of developing ovarian follicles in the rat: a possible role in destiny of follicles. *Histochem Cell Biol* **120**, 383-390.

Cekleniak NA, Combelles CM, Ganz DA, Fung J, Albertini DF, Racowsky C. (2001) A novel system for in vitro maturation of human oocytes. *Fertil Steril*. **75(6)**, 1185-1193.

Chen CK, Shen GY, Horng SG, Wang CW, Huang HY, Wang HS, Soong YK. (2003) The relationship of pronuclear stage morphology and chromosome status at cleavage stage. *J Assist Reprod Genet* **20**, 413-420.

Chian RC. (2004) In-vitro maturation of immature oocytes for infertile women with PCOS. *Reprod Biomed Online*. **8(5),** 547-552.

Clyde J.M., Gosden R.G., Rutherford A.J., Picton H.M. (2001) Demonstration of a mechanism of aneuploidy in human oocytes using Multifluor fluorescence in situ hybridization. *Fertil Steril* **76(4)**, 837-840.

Cohen Y, Malcov M, Schwartz T, Mey-Raz N, Carmon A, Cohen T, Lessing JB, Amit A, Azem F. (2004) Spindle imaging: a new marker for optimal timing of ICSI? *Hum Reprod*. **19(3)**, 649-654.

Cohen J, Trounson A, Dawson K, Jones H, Hazekamp J, Nygren KG, Hamberger L. (2005) The early days of IVF outside the UK. *Hum Reprod Update*. **11(5)**, 439-459.

Cohen PE, Pollack SE, Pollard JW (2006) Genetic analysis of chromosome pairing, recombination, and cell cycle control during first meiotic prophase in mammals. *Endocr Rev*. **27(4)**, 398-426.

Combelles CM, Cekleniak NA, Racowsky C, Albertini DF. (2002) Assessment of nuclear and cytoplasmic maturation in in-vitro matured human oocytes. *Hum Reprod*. **17(4)**, 1006-1016.

Combelles CM, Albertini DF, Racowsky C. (2003) Distinct microtubule and chromatin characteristics of human oocytes after failed in-vivo and in-vitro meiotic maturation. *Hum Reprod*. **18(10)**, 2124-2130.

Combelles CM, Fissore RA, Albertini DF, Racowsky C. (2005) In vitro maturation of human oocytes and cumulus cells using a co-culture three-dimensional collagen gel system. *Hum Reprod*. **20(5)**, 1349-1358.

Conti M, Hsieh M, Park JY, Su YQ (2006) Role of the epidermal growth factor network in ovarian follicles. *Mol Endocrinol*. **20(4)**, 715-723.

Cooke S, Tyler JP, Driscoll GL (2003) Meiotic spindle location and identification and its effect on embryonic cleavage plane and early development. *Hum Reprod* **18**, 2397-2405.

Cukurcam S., Sun F., Betzendahl I., Adler I.D., Eichenlaub-Ritter U. (2004) Trichlorfon predisposes to aneuploidy and interferes with spindle formation in *in vitro* maturing mouse oocytes. *Mutat Res* **564(2)**, 165-178.

Dawson KJ, Conaghan J, Ostera GR, Winston RM, Hardy K. (1995) Delaying transfer to the third day post-insemination, to select non-arrested embryos, increases development to the fetal heart stage. *Hum Reprod*. **10(1)**, 177-182.

De Brabander, M J. (1982) A model for the microtubule organizing activity of the centrosomes and kinetochores in mammalian cells. *Cell Biol. Int. Rep*. **6**, 901-915.

De Felici M, Klinger FG, Farini D, Scaldaferri ML, Iona S, Lobascio M (2005) Establishment of oocyte population in the fetal ovary: primordial germ cell proliferation and oocyte programmed cell death. *Reprod Biomed Online.* **10(2)**, 182-191.

De La Fuente R., Viveiros M.M., Wigglesworth K., Eppig J.J. (2004) ATRX, a member of the SNF2 family of helicase/ATPases, is required for chromosome alignment and meiotic spindle organization in metaphase II stage mouse oocytes. *Dev Biol* **272(1)**, 1-14.

De Pennart H., Verlhac M.H., Cibert C., Santa Maria A., Maro B. (1993) Okadaic acid induces spindle lengthening and disrupts the interaction of microtubules with the kinetochores in metaphase II-arrested mouse oocytes. *Dev Biol* **157(1),** 170-181.

De Rycke M, Liebaers I, Van Steirteghem A (2002) Epigenetic risks related to assisted reproductive technologies: risk analysis and epigenetic inheritance. *Hum Reprod.* **17(10)**, 2487-2494.

De Santis L, Cino I, Rabellotti E (2005) Polar body morphology and spindle imaging as predictors of oocyte quality. *Reprod Biomed Online* **11**, 36-42.

Diaz H, Esponda P (2004) Postovulatory ageing induces structural changes in the mouse zona pellucida. *J Submicrosc Cytol Pathol.* **36(2)**, 211-217.

Ding J, Rana N and Dmowski WP (1999) Intracytoplasmic sperm injection into zona-free human oocytes results in normal fertilization and blastocyst development. *Hum Reprod* **14**, 476-478.

DIR Jahrbuch (2004) pp 17.

Dirnfeld M, Shiloh H, Bider D, Harari E, Koifman M, Lahav-Baratz S and Abramovici H (2003) A prospective randomized controlled study of the effect of short coincubation of gametes during insemination on zona pellucida thickness. *Gynecol Endocrinol* **17**, 397-403.

Dunbar BS, Timmons TM, Skinner SM and Prasad SV (2001) Molecular analysis of a carbohydrate antigen involved in the structure and function of zona pellucida glycoproteins. *Biol Reprod* **65**, 951-960.

Eberspaecher U, Becker A, Bringmann P, van der Merwe L and Donner P (2001) Immunohistochemical localization of zona pellucida proteins ZPA, ZPB and ZPC in human, cynomolgus monkey and´mouse ovaries. *Cell Tissue Res* **303**, 277-287.

Ebner T, Moser M, Sommergruber M and Tews G (2003) Selection based on morphological assessment of oocytes and embryos at different stages of preimplantation development: a review. *Hum Reprod Update* **9**, 251-262.

Ebner T., Moser M., Sommergruber M., Gaiswinkler U., Shebl O., Jesacher K., Tews G. (2005) Occurrence and developmental consequences of vacuoles throughout preimplantation development. *Fertil Steril* **83(6)**, 1635-1640.

Edirisinghe WR, Jemmott R, Smith C, Allan J. (2005) Association of pronuclear Z score with rates of aneuploidy in *in vitro*-fertilised embryos. *Reprod Fertil* **17**, 529-534.

Edwards RG, Craft I. (1990) Development of assisted conception. *Br Med Bull*. **46(3)**, 565-579.

Edwards RG, Hansis C. (2005) Initial differentiation of blastomeres in 4-cell human embryos and its significance for early embryogenesis and implantation. *Reprod Biomed Online*. **11(2)**, 206-218.

Eggan K, Jurga S, Gosden R, Min IM, Wagers AJ. (2006) Ovulated oocytes in adult mice derive from non-circulating germ cells. *Nature 441(7097)*, 1109-1114.

Eichenlaub-Ritter U, Boll I. (1989) Age-related non-disjunction, spindle formation and progression through maturation of mammalian oocytes. *Prog Clin Biol Res.* **318**, 259-269.

Eichenlaub-Ritter U., Betzendahl I. (1995) Chloral hydrate induced spindle aberrations, metaphase I arrest and aneuploidy in mouse oocytes. *Mutagenesis* **10**, 477-486.

Eichenlaub-Ritter U (1996) Parental age-related aneuploidy in human germ cells and offspring: a story of past and present. *Environ Mol Mutagen.* **28(3)**, 211-236.

Eichenlaub-Ritter U (1998) Genetics of oocyte ageing. *Maturitas* **30**, 143-169.

Eichenlaub-Ritter U, Shen Y, Tinneberg HR (2002) Manipulation of the oocyte, possible damage to the spindle apparatus. *Reprod Biomed Online* **5**, 117-124.

Eichenlaub-Ritter U., Vogt E., Yin H. Gosden R. (2004) Spindles, mitochondria and redox potential in ageing oocytes. *Reprod Biomed Online* **8**, 45-58.

Eichenlaub-Ritter U., Vogt E., Betzendahl I. (2005) Model for aging: knockdown of Mad2 expression predisposes to non-disjunction in mammalian oocytes possessing aberrant spindles. *Hum Reprod* **20**, Supl 1, i70.

El-Mestrah M, Castle PE, Borossa G and Kan FW (2002) Subcellular distribution of ZP1, ZP2, and ZP3 glycoproteins during folliculogenesis and demonstration of their topographical disposition within the zona matrix of mouse ovarian oocytes. *Biol Reprod* **66**, 866-876.

Epifano O, Liang LF, Familari M, Moos MC, Jr and Dean J (1995) Coordinate expression of the three zona pellucida genes during mouse oogenesis. *Development* **121**, 1947-1956.

Eppig JJ (1991) Intercommunication between mammalian oocytes and companion somatic cells. *BioEssays* **13**, 569-574.

Eppig JJ. Regulation of mammalian oocyte maturation. In: Adashi EY, Leung PCK. (Eds) *The Ovary*. New York: Raven, 1993; 185–207.

Eppig JJ, Pendola FL, Wigglesworth K, Pendola JK (2005) Mouse oocytes regulate metabolic cooperativity between granulosa cells and oocytes: amino acid transport. *Biol Reprod*. **73(2),** 351-357.

Familiari G, Relucenti M, Ermini M, Verlengia C, Nottola SA and Motta PM (2001) The human zona pellucida and scanning electron microscopy. Reality or artifacts? *Ital J Anat Embryol* **106(2 Suppl 2),** 33-41.

Familiari G, Nottola SA, Macchiarelli G, Micara G, Aragona C and Motta PM (1992) Human zona pellucida during *in vitro* fertilization: an ultrastructural study using saponin, ruthenium red, and osmium-thiocarbohydrazide. *Mol Reprod Dev* **32**, 51-61.

Fauser B, Bouchard P, Bennink H, Collins J, Devroey P, Evers J and van Steirteghem A (2002) Alternative approaches in IVF. *Hum Reprod Update* **8**, 1-9.

Feinberg EC, Larsen FW, Catherino WH, Zhang J, Armstrong AY. (2006) Comparison of assisted reproductive technology utilization and outcomes between Caucasian and African American patients in an equal-access-to-care setting. *Fertil Steril*. **85(4)**, 888-894.

Feyereisen E, Mendez Lozano DH, Taieb J, Hesters L, Frydman R, Fanchin R (2006) Anti-Mullerian hormone: clinical insights into a promising biomarker of ovarian follicular status. *Reprod Biomed Online*. **12(6)**, 695-703.

Fortune JE, Cushman RA, Wahl CM, Kito S. (2000) The primordial to primary follicle transition. *Mol Cell Endocrinol*. **163(1-2)**, 53-60.

Gabrielsen A, Lindenberg S and Petersen K (2001) The impact of the zona pellucida thickness variation of human embryos on pregnancy outcome in relation to suboptimal embryo development. A prospective randomized controlled study. *Hum Reprod* **16**, 2166-2170.

Gamiz P, Rubio C, de los Santos MJ, Mercader A, Simon C, Remohi J and Pellicer A (2003) The effect of pronuclear morphology on early development and chromosomal abnormalities in cleavage-stage embryos. *Hum Reprod* **18**, 2413-2419.

Gardner DK, Vella P, Lane M, Wagley L, Schlenker T, Schoolcraft WB. (1998) Culture and transfer of human blastocysts increases implantation rates and reduces the need for multiple embryo transfers. *Fertil Steril*. **69(1)**, 84-88.

Gianaroli L, Magli MC, Ferraretti AP, Fortini D and Grieco N (2003) Pronuclear morphology and chromosomal abnormalities as scoring criteria for embryo selection. *Fertil Steril* **80**, 341-349.

Gilbert AB, Davidson MF, Wells JW. (1983) Detection of gonadotrophic hormones on isolated granulosa cells of the domestic hen, Gallus domesticus, by an immunohistochemical method. Histochem J. **15(8)**, 753-761.

Gilchrist RB, Nayudu PL and Hodges JK (1997) Maturation, fertilization, and development of marmoset monkey oocytes *in vitro*. *Biol Reprod* **56**, 238-246.

Gitlin SA, Gibbons WE and Gosden RG (2003) Oocyte biology and genetics revelations from polar bodies. *Reprod Biomed Online* **6**, 403-409.

Gook D, Martic M, Borg J and Edgar DH (2004) Identification of zona pellucida proteins during human folliculogenesis. *Hum Reprod* **19**, Suppl 1 pp140.

Gosden R, Bownes M. Molecular and cellular aspects of oocyte development. In: Grudzinskas J, Yovich J. (Eds) *Gametes – The Oocyte*. Cambridge: Cambridge University Press, 1995; 23–53
Gosden R (1999) Early psychosis. *Br J Psychiatry*. **174**, 461-462.

Green DP (1997) Three-dimensional structure of the zona pellucida. *Rev Reprod* **2**, 147-156.

Greve JM, and Wassarman PM (1985) Mouse egg extracellular coat is a matrix of interconnected filaments possessing a structural repeat. *J Mol Biol* **181**, 253-264.

Gueth-Hallonet C, Antony C, Aghion J, Santa-Maria A, Lajoie-Mazenc I, Wright M, Maro B. (1993) gamma-Tubulin is present in acentriolar MTOCs during early mouse development. *J Cell Sci.* **105 (Pt 1),** 157-166.

Hamatani T, Falco G, Carter MG (2004) Age-associated alteration of gene expression patterns in mouse oocytes. *Hum Mol Genet* **13**, 2263-2278.

Hamilton DK, Wilson T. (1982) Three-dimensional surface measurement using the confocal scanning microscope. *Applied Physics B: Lasers and Optics*, **27**, 211-213.

Hampton T. (2004) Panel reviews health effects data for assisted reproductive technologies. *JAMA*. **292(24)**, 2961-2962.

Hansen DV, Tung JJ, Jackson PK (2006) CaMKII and polo-like kinase 1 sequentially phosphorylate the cytostatic factor Emi2/XErp1 to trigger its destruction and meiotic exit. *Proc Natl Acad Sci.* **103(3)**, 608-613.

Harada M, Miyano T, Matsumura K, Osaki S, Miyake M, Kato S (1997) Bovine oocytes from early antral follicles grow to meiotic competence in vitro: Effect of FSH and hypoxanthine. *Theriogenology*. **48(5)**, 743-755.

Hardarson T, Lundin K, Hamberger L. (2000) The position of the metaphase II spindle cannot be predicted by the location of the first polar body in the human oocyte. *Hum Reprod*. **15(6),** 1372-1376.

Hardy K, Wright CS, Franks S, Winston RM. (2000) In vitro maturation of oocytes. *Br Med Bull*. **56(3)**, 588-602.

Henkel RR, Schill WB. (2003) Sperm preparation for ART. *Reprod Biol Endocrinol.* **1**, 108.

Herrler A and Beier HM (2000) Early embryonic coats: morphology, function, practical applications. An overview. *Cells Tissues Organs* **166(2)**, 233-246.

Herrler A, von Rango U and Beier HM (2003) Embryo-maternal signalling: how the embryo starts talking to its mother to accomplish implantation. *Reprod Biomed Online* **6**, 244-256.

Hodges C.A., Ilagan A., Jennings D., Keri R., Nilson J., Hunt P.A. (2002) Experimental evidence that changes in oocyte growth influence meiotic chromosome segregation. *Hum Reprod* **17(5)**, 1171-1180.

Homer H.A., McDougall A., Levasseur M., Yallop K., Murdoch A.P., Herbert M. (2005) Mad2 prevents aneuploidy and premature proteolysis of cyclin B and securin during meiosis I in mouse oocytes. *Genes Dev* **19(2),** 202-207.

Homer HA. (2006) Mad2 and spindle assembly checkpoint function during meiosis I in mammalian oocytes. *Histol Histopathol*. **21(8)**, 873-886.

Hoodbhoy T and Dean J (2004) Insights into the molecular basis of sperm-egg recognition in mammals. *Reproduction* **127**, 417-422.

Houghton FD, Leese HJ. (2004) Metabolism and developmental competence of the preimplantation embryo. *Eur J Obstet Gynecol Reprod Biol*. **115 Suppl 1**, S92-96.

Hoyt MA, Totis L, Roberts BT (1991) Cerevisiae genes required for cell cycle arrest in response to loss of microtubule function. *Cell* **66(3)**, 507-517.

Hsieh YY, Chang CC and Tsai HD (2001) Zona-free oocyte fertilized with intracytoplasmic sperm injection and underwent further division: case report and literature review. *Chang Gung Med J* **24**, 599-602.

Hunt P, LeMaire R, Embury P, Sheean L, Mroz K (1995) Analysis of chromosome behavior in intact mammalian oocytes: monitoring the segregation of a univalent chromosome during female meiosis. *Hum Mol Genet*. **4(11)**, 2007-2012.

Hussein TS, Thompson JG, Gilchrist RB. (2006) Oocyte-secreted factors enhance oocyte developmental competence. *Dev Biol.* [Epub ahead of print]

Hyman, A., Drechsel, D., Kellogg, D., Salser, S., Sawin, K., Steffen, P., Wordemann, L. and Mitchison, T. (1991) preparation of modiÆed tubulins. *Meth. Enzymol*. **196**, 478-485.

Illmensee K, Levanduski M, Zavos PM (2006) Evaluation of the embryonic preimplantation potential of human adult somatic cells via an embryo interspecies bioassay using bovine oocytes. *Fertil Steril*. **85 Suppl 1**, 1248-1260.

Inoué S. (1953) Polarization optical studies of the mitotic spindle. 1. The demonstration of spindle fibers in living cells. *Chromosoma* **5**, 487-500.

Jensen JT, Schwinof KM, Zelinski-Wooten MB, Conti M, DePaolo LV, Stouffer RL. (2002) Phosphodiesterase 3 inhibitors selectively block the spontaneous resumption of meiosis by macaque oocytes in vitro. *Hum Reprod*. **17(8),** 2079-2084.

Jimenez-Movilla M, Aviles M, Gomez-Torres MJ, Fernandez-Colom PJ, Castells MT, De Juan J, Romeu A and Ballesta J (2004) Carbohydrate analysis of the zona pellucida and cortical granules of human oocytes by means of ultrastructural cytochemistry. *Hum Reprod* **19**, 1842-1855.

Jin L, Qian X, Kulig E, Sanno N, Scheithauer BW, Kovacs K, Jr Young WF and Lloyd RV (1997) Transforming growth factor-beta, transforming growth factor-beta receptor II, and p27Kip1 expression in nontumorous and neoplastic human pituitaries. *American Journal of Pathology*, **151**, 509-519.

Kahraman S, Kumtepe Y, Sertyel S, Donmez E, Benkhalifa M, Findikli N, Vanderzwalmen P. (2002) Pronuclear morphology scoring and chromosomal status of embryos in severe male infertility. *Hum Reprod* **17**, 3193-3200.

Kallio M, Eriksson JE, Gorbsky GJ (2000) Differences in spindle association of the mitotic checkpoint protein Mad2 in mammalian spermatogenesis and oogenesis. *Dev Biol*. **225(1)**, 112-123.

Keefe D, Tran P, Pellegrini C and Oldenbourg R (1997) Polarized light microscopy and digital image processing identify a multilaminar structure of the hamster zona pellucida. *Hum Reprod* **12**, 1250-1252.

Keefe D, Liu L, Wang W and Silva C (2003) Imaging meiotic spindles by polarization light microscopy: principles and applications to IVF. *Reprod Biomed Online* **7**, 24-29.

Kolle S, Stojkovic M, Reese S, Reichenbach HD, Wolf E and Sinowatz F (2004) Effects of growth hormone on the ultrastructure of bovine preimplantation embryos. *Cell Tissue Res* **317**, 101-108.

Kolman A (2005) Activity of epothilones. *Curr Opin Investig Drugs*. **6(6)**, 616-622.

Koyama K, Hasegawa A, Mochida N, Calongos G (2005) Follicular dysfunction induced by autoimmunity to zona pellucida. *Reprod Biol*. **5(3)**, 269-278.

Kudo NR, Wassmann K, Anger M, Schuh M, Wirth KG, Xu H, Helmhart W, Kudo H, McKay M, Maro B, Ellenberg J, de Boer P, Nasmyth K. (2006) Resolution of chiasmata in oocytes requires separase-mediated proteolysis. *Cell* **126(1)**, 135-146.

Kuliev A, Cieslak J, Ilkevitch Y and Verlinsky Y (2003) Chromosomal abnormalities in a series of 6,733 human oocytes in preimplantation diagnosis for age-related aneuploidies. *Reprod Biomed Online* **6**, 54-59.

LaFountain JR Jr, Oldenbourg R (2004) Maloriented bivalents have metaphase positions at the spindle equator with more kinetochore microtubules to one pole than to the other. *Mol Biol Cell* **15**, 5346-5355.

Leese HJ (2004) What is a good embryo? Metabolic assessment. *Hum Reprod* **19** Suppl 1 pp68.

Lefievre L, Conner SJ, Salpekar A, Olufowobi O, Ashton P, Pavlovic B, Lenton W, Afnan M, Brewis IA, Monk M et al. (2004) Four zona pellucida glycoproteins are expressed in the human. *Hum Reprod* **19**, 1580-1586.

LeMaire-Adkins, R., Radke K., and Hunt P.A. (1997) Lack of checkpoint control at the metaphase/Anaphase Transition: A mechanism of meiotic nondisjunction in mammalian females. *J. Cell. Biol*. **139**, 1611-1619.

Li R, Murray AW (1991) Feedback control of mitosis in budding yeast. *Cell* **66(3)**, 519-531.

Liu C, Litscher ES, Mortillo S, Sakai Y, Kinloch RA, Stewart CL and Wassarman PM (1996) Targeted disruption of the *mZP3* gene results in production of eggs lacking a zona pellucida and infertility in female mice. *Proc Natl Acad Sci* **93**, 5431-5436.

Liu L, Oldenbourg R, Trimarchi JR, Keefe DL (2000a) A reliable, noninvasive technique for spindle imaging and enucleation of mammalian oocytes. *Nat Biotechnol.* **18**, 223-225.

Liu L, Trimarchi JR, Oldenbourg R, Keefe DL (2000b) Increased birefringence in the meiotic spindle provides a new marker for the onset of activation in living oocytes. *Biol Reprod*. **63(1)**, 251-258.

Liu Z and Armant DR (2004) Lysophosphatidic acid regulates murine blastocyst development by transactivation of receptors for heparin-binding EGF-like growth factor. Exp Cell Res **296**, 317-326.

Lundin K, Bergh C and Hardarson T (2001) Early embryo cleavage is a strong indicator of embryo quality in human IVF. *Hum Reprod* **16**, 2652-2657.

Ludwig M, Diedrich K. (2002) Follow-up of children born after assisted reproductive technologies. *Reprod Biomed Online*. **5(3)**, 317-322.

Magerkurth C, Topfer-Petersen E, Schwarty P and Michelmann HW (1999) Scanning electron microscopy analysis of the human zona pellucida: influence of maturity and fertilization on morphology and sperm binding pattern. *Hum Reprod* **14**, 1057-1066.

Magli MC, Gianaroli L and Ferraretti AP (2001) Chromosomal abnormalities in embryos. *Mol Cell Endocrinol* **183 Suppl 1**, S29-34.

Mailhes JB, Marchetti F, Young D, London SN. (1996) Numerical and structural chromosome aberrations induced by etoposide (VP16) during oocyte maturation of mice: transmission to one-cell zygotes and damage to dictyate oocytes. *Mutagenesis* **11(4)**, 357-361.

Mailhes J.B., Mastromatteo C., Fuseler J.W. (2004) Transient exposure to the Eg5 kinesin inhibitor monastrol leads to syntelic orientation of chromosomes and aneuploidy in mouse oocytes. *Mutat Res* **559(1-2)**, 153-167.

Markham KE and Kaye PL (2003) Growth hormone, insulin-like growth factor I and cell proliferation in the mouse blastocyst. *Reproduction* **125**, 327-336.

Maro B, Howlett SK, Webb M (1985) Non-spindle microtubule organizing centers in metaphase II-arrested mouse oocytes. *J. Cell Biol*.**101**, 1665-1672.

McKee BD (2004) Homologous pairing and chromosome dynamics in meiosis and mitosis. *Biochim Biophys Acta*. **1677(1-3)**, 165-180.

Mehlmann LM (2005) Stops and starts in mammalian oocytes: recent advances in understanding the regulation of meiotic arrest and oocyte maturation. *Reproduction.* **130(6)**, 791-799.

Miller DJ, Shi X and Burkin H (2002) Molecular basis of mammalian gamete binding. *Recent Prog Horm Res* **57**, 37-73.

Minsky M (1961). Microscopy apparatus patent 3,013,467.

Minsky M (1988). Memoir on inventing the confocal scanning microscope. *Scanning* **10**, 128-138.

Mikkelsen AL (2005) Strategies in human in-vitro maturation and their clinical outcome. *Reprod Biomed Online*. **10(5)**, 593-599.

Miyano T (2003) Bringing up small oocytes to eggs in pigs and cows. *Theriogenology.* **59(1)**, 61-72.

Montag M, van der Ven K, Dorn C, van der Ven H. (2004) Outcome of laser-assisted polar body biopsy and aneuploidy testing. *Reprod Biomed Online*. **9(4),** 425-429.

Montag M, Schimming T, Gassner P, van der Ven H (2006) Oocyte zona birefringence intensity is associated with embryonic implantation potential. *Hum Reprod* **21 suppl.** pi67.

Moon J.H., Hyun C.S., Lee S.W., Son W.Y., Yoon S.H., Lim J.H. (2003) Visualization of the metaphase II meiotic spindle in living human oocytes using the Polscope enables the prediction of embryonic developmental competence after ICSI. *Hum Reprod* **18**, 817-820.

Moor RM, Dai Y, Lee C, Fulka Jr J. (1998) Oocyte maturation and embryonic failure. *Hum Reprod Update* **4**, 223–236.

Moos J, Faundes D, Kopf GS and Schultz RM (1995) Composition of the human zona pellucida and modifications following fertilization. **Hum. Reprod 10**, 2467-2471.

Motta PM, Makabe S, Naguro T and Correr S (1994) Oocyte follicle cells association during development of human ovarian follicle. A study by high resolution scanning and transmission electron microscopy. *Arch Histol Cytol* **57**, 369-394.

Munne S. (2003) Preimplantation genetic diagnosis and human implantation--a review. *Placenta.* **24 Suppl B**, S70-76.

Munne S, Bahce M, Sandalinas M, Escudero T, Marquez C, Velilla E, Colls P, Oter M, Alikani M and Cohen J (2004) Differences in chromosome susceptibility to aneuploidy and survival to first trimester. *Reprod Biomed Online* **8**, 81-90.

Munne S. (2005) Analysis of chromosome segregation during preimplantation genetic diagnosis in both male and female translocation heterozygotes. *Cytogenet Genome Res.* **111(3-4)**, 305-309.

Nagy ZP, Dozortsev D, Diamond M, Rienzi L, Ubaldi F, Abdelmassih R and Greco E (2003) Pronuclear morphology evaluation with subsequent evaluation of embryo morphology significantly increases implantation rates. *Fertil Steril* **80**, 67-74.

Nawroth F, Muller P, Wolf C, Sudik R. (2001) Is the Zona pellucida thickness of metaphase-II oocytes in an IVF/ICSI program influenced by the patient's age? *Gynecol Obstet Invest*. **52(1),** 55-59.

Navarro PA, Liu L, Trimarchi JR *et al.* (2005) Noninvasive imaging of spindle dynamics during mammalian oocyte activation. *Fertil Steril* **83 Suppl 1**, 1197-1205.

Neuber E, Rinaudo P, Trimarchi JR and Sakkas D (2003) Sequential assessment of individually cultured human embryos as an indicator of subsequent good quality blastocyst development. *Hum Reprod* **18**, 1307-1312.

Nikas G, Paraschos T, Psychoyos A and Handyside AH (1994) The zona reaction in human oocytes as seen with scanning electron microscopy. *Hum Reprod* **9**, 2135-2138.

Nilsson EE, Kezele P, Skinner MK (2002) Leukemia inhibitory factor (LIF) promotes the primordial to primary follicle transition in rat ovaries. *Mol Cell Endocrinol*. **188(1-2)**, 65-73.

Nogueira D, Staessen C, Van de Velde H, Van Steirteghem A. (2000) Nuclear status and cytogenetics of embryos derived from *in vitro*-matured oocytes. *Fertil Steril* **74**, 295-298.

Nogueira D, Cortvrindt R, Everaerdt B, Smitz J (2005) Effects of long-term in vitro exposure to phosphodiesterase type-3 inhibitors on follicle and oocyte development. *Reproduction* **130(2)**, 177-186.

Oehninger S (2003) Biochemical and functional characterization of the human zona pellucida. *Reprod Biomed Online* **7**, 641-648.

Oldenbourg, R. (1991) Analysis of edge birefringence. *Biophys. J.* **60**, 629–641.

Oldenbourg R., Terada H., Tiberio R., Inoue S. (1993) Image sharpness and contrast transfer in coherent confocal microscopy. *J Microsc* **172 (Pt 1)**, 31-39.

Oldenbourg R., Mei G. (1995) New polarized light microscope with precision universal compensator. *J Microscopy* **180**, 140-147.

Oldenbourg R (1996) A new view on polarization microscopy. *Nature* **381**, 811-812.

Oldenbourg R, Salmon ED, Tran PT (1998) Birefringence of Single and Bundled Microtubules. *Biophys J*. **74**, 645-654.

Oldenbourg R (1999) Polarized light microscopy of spindles. *Methods Cell Biol.* **61**, 175-208.

Papanikolaou EG, Platteau P, Albano C, Nogueira D, Cortvrindt R, Devroey P, Smitz J. (2005) Immature oocyte in-vitro maturation: clinical aspects. *Reprod Biomed Online*. **10(5),** 587-592.

Pawlowski WP, Cande WZ (2005) Coordinating the events of the meiotic prophase. *Trends Cell Biol*. **15(12)**, 674-681.

Payne JF, Raburn DJ, Couchman GM, Price TM, Jamison MG, Walmer DK. (2005) Relationship between pre-embryo pronuclear morphology (zygote score) and standard day 2 or 3 embryo morphology with regard to assisted reproductive technique outcomes. *Fertil Steril* **84**, 900-909.

Pellestor F, Andreo B, Arnal F, Humeau C and Demaille J (2003) Maternal aging and chromosomal abnormalities : new data drawn from *in vitro* unfertilized human oocytes. *Hum Genet* **112**, 195-203.

Pelletier C, Keefe DL and Trimarchi JR (2004) Noninvasive polarized light microscopy quantitatively distinguishes the multilaminar structure of the zona pellucida of living human eggs and embryos. *Fertil Steril* **81**, 850-856.

Phillips DM and Shalgi RM (1980) Surface properties of the zona pellucida. *J Exp Zool* **213**, 1-8.

Picton H, Briggs D, Gosden R (1998) The molecular basis of oocyte growth and development. *Mol Cell Endocrinol.* **145(1-2)**, 27-37.

Picton HM, Danfour MA, Harris SE, Chambers EL, Huntriss J (2003) Growth and maturation of oocytes in vitro. *Reprod Suppl*. **61**, 445-462.

Plachot M (1992) Cytogenetic analysis of oocytes and embryos. *Ann Acad Med Singapore*. **21(4)**, 538-544.

Qi H, Williams Z and Wassarman PM (2002) Secretion and assembly of zona pellucida glycoproteins by growing mouse oocytes microinjected with epitope-tagged cDNAs for mZP2 and mZP3. *Mol Biol Cell* **13**, 530-541.

Rankin T, Talbot P, Lee E and Dean J (1999) Abnormal zonae pellucida in mice lacking ZP1 result in early embryonic loss. *Development* **126**, 3847-3855.

Rankin TL, O'Brien M, Lee E, Wigglesworth K, Eppig J and Dean J (2001a) Defective zonae pellucidae in Zp2-null mice disrupt folliculogenesis, fertility and development. *Development* **128**, 1119-1126.

Rankin T, Soyal S and Dean J (2001b) The mouse zona pellucida: folliculogenesis, fertility and pre-implantation development. *Mol Cell Endocrinol* **163**, 21-25.

Rao GD, Tan SL (2005) In vitro maturation of oocytes. *Semin Reprod Med*. **23(3)**, 242-247.

Rieder CL, Salmon ED (1998) The vertebrate cell kinetochore and its roles during mitosis. *Trends Cell Biol* . **8**, 310-318.

Rienzi L, Ubaldi F, Martinez F, Iacobelli M, Minasi MG, Ferrero S, Tesarik J and Greco E (2003) Relationship between meiotic spindle location with regard to the polar body position and oocyte developmental potential after ICSI. *Hum Reprod* **18**, 1289-1293.

Rienzi L, Ubaldi F, Iacobelli M, Minasi MG, Romano S, Greco E (2005) Meiotic spindle visualization in living human oocytes. *Reprod Biomed Online* **10**, 192-198.

Roberts BT, Farr KA, Hoyt MA (1994) The Saccharomyces cerevisiae checkpoint gene BUB1 encodes a novel protein kinase. *Mol Cell Biol* **14(12)**, 8282-8291.

Roberts R, Iatropoulou A, Ciantar D, Stark J, Becker DL, Franks S, Hardy K (2005) Follicle-stimulating hormone affects metaphase I chromosome alignment and increases aneuploidy in mouse oocytes matured in vitro. *Biol Reprod*. **72(1),** 107-118.

Rodriguez-Mari A, Yan YL, Bremiller RA, Wilson C, Canestro C, Postlethwait JH (2005) Characterization and expression pattern of zebrafish Anti-Mullerian hormone (Amh) relative to sox9a, sox9b, and cyp19a1a, during gonad development. *Gene Expr Patterns*. **5(5)**, 655-667.

Rudner AD, Murray AW (1996) The spindle assembly checkpoint. *Curr. Opin. Cell Biol*. **8**, 773-780.

Saito T, Otani S, Fujimoto T, Suzuki T, Nakatsuji T, Arai K, Yamaha E (2004) The germ line lineage in ukigori, Gymnogobius species (Teleostei: Gobiidae) during embryonic development. *Int J Dev Biol*. **48(10)**, 1079-1085.

Sathananthan AH, Selvaraj K, Girijashankar ML, Ganesh V, Selvaraj P, Trounson AO. (2006) From oogonia to mature oocytes: inactivation of the maternal centrosome in humans. *Microsc Res Tech.* **69(6)**, 396-407.

Sato H, Ellis GW and Inoué S (1975) Microtubular origin of mitotic spindle form birefringence: demonstration of the applicability of Wiener's equation. *J Cell Biol* **67**, 501-517.

Schmidt A, Rauh NR, Nigg EA, Mayer TU. (2006) Cytostatic factor: an activity that puts the cell cycle on hold. *J Cell Sci*. **119(Pt 7)**, 1213-1218.

Scott LA and Smith S (1998) The successful use of pronuclear embryo transfers the day following oocyte retrieval. *Hum Reprod* **13**, 1003-1013.

Scott L (2003) Pronuclear scoring as a predictor of embryo development. *Reprod Biomed Online* **6**, 201-214.

Seshagiri PB, Terasawa E and Hearn JP (1994) The secretion of gonadotrophin-releasing hormone by peri-implantation embryos of the rhesus monkey: comparison with the secretion of chorionic gonadotrophin. *Hum Reprod* **9**, 1300-1307.

Shen Y, Betzendahl I, Sun F, Tinneberg HR and Eichenlaub-Ritter U (2005) Non-invasive method to assess genotoxicity of nocodazole interfering with spindle formation in mammalian oocytes. *Reprod Toxicol* **19**, 459-471.

Shimada M, Hernandez-Gonzalez I, Gonzalez-Robayna I, Richards JS. (2006) Paracrine and autocrine regulation of epidermal growth factor-like factors in cumulus oocyte complexes and granulosa cells: key roles for prostaglandin synthase 2 and progesterone receptor. *Mol Endocrinol*. **20(6),** 1352-1365.

Shivers CA, Dunbar BS (1977) Autoantibodies to zona pellucida: a possible cause for infertility in women. *Science* **197**, 1082-1084.

Shoji S, Yoshida N, Amanai M, Ohgishi M, Fukui T, Fujimoto S, Nakano Y, Kajikawa E, Perry AC. (2006) Mammalian Emi2 mediates cytostatic arrest and transduces the signal for meiotic exit via Cdc20. *EMBO J*. **25(4)**, 834-845.

Silva CP, Silva V, Kommineni K, Keefe D. (1997) Effect of in vitro culture of mammalian embryos on the architecture of the zona pellucida. *Biol Bull*. **193(2)**, 235-236.

Silva C.P., Kommineni K., Oldenbourg R., Keefe D.L. (1999) The first polar body does not predict accurately the location of the metaphase II meiotic spindle in mammalian oocytes. *Fertil Steril*. **71(4),** 719-721.

Simini B (1999) Italy moves on with in-vitro fertilisation legislation. *Lancet*. **353(9168),** 1950.

Sinowatz F, Topfer-Petersen E, Kolle S and Palma G (2001) Functional morphology of the zona pellucida. *Anat Histol Embryol* **30**, 257-263.

Soini S, Ibarreta D, Anastasiadou V, Ayme S, Braga S, Cornel M, Coviello DA, Evers-Kiebooms G, Geraedts J, Gianaroli L, Harper J, Kosztolanyi G, Lundin K, Rodrigues-Cerezo E, Sermon K, Sequeiros J, Tranebjaerg L, Kaariainen H; ESHG;ESHRE. (2006) The interface between assisted reproductive technologies and genetics: technical, social, ethical and legal issues. *Eur J Hum Genet.* **14(5)**, 588-645.

Soyal SM, Amleh A and Dean J (2000) FIGalpha, a germ cell-specific transcription factor required for ovarian follicle formation. *Development* **127**, 4645-4654.

Stalf T, Herrero J, Mehnert C, Manolopoulos K, Lenhard A and Gips H (2002) Influence of polarization effects in ooplasma and pronuclei on embryo quality and implantation in an IVF program. *J Assist Reprod Genet* **19**, 355-362.

Stanger JD, Stevenson K, Lakmaker A and Woolcott R (2001) Pregnancy following fertilization of zona-free, coronal cell intact human ova: Case Report. *Hum Reprod* **16**, 164-167.

Steuerwald N.M., Steuerwald M.D., Mailhes J.B. (2005) Post-ovulatory aging of mouse oocytes leads to decreased MAD2 transcripts and increased frequencies of premature centromere separation and anaphase. *Mol Hum Reprod* **11(9)**, 623-630.

Sugiura K, Pendola FL, Eppig JJ. (2005) Oocyte control of metabolic cooperativity between oocytes and companion granulosa cells: energy metabolism. *Dev Biol*. **279(1)**, 20-30.

Sun QY, Nagai T (2003) Molecular mechanisms underlying pig oocyte maturation and fertilization. *J Reprod Dev*. **49(5)**, 347-359.

Szollosi, D. (1972) Changes of some cell organelles during oogenesis in mmmals. *In oogenesis*, J.D. Biggers and A.W. Schuetz, editors, University park Press, Baltimore, MD. 47-64.

Tan AL, Rida PC, Surana U (2005) Essential tension and constructive destruction: the spindle checkpoint and its regulatory links with mitotic exit. *Biochem J.* 386(Pt 1),1-13.

Takagi J, Dobashi M, Araki Y, Imai Y, Hiroi M, Tonosaki A and Sendo F (1989) The development of porcine zona pellucida using monoclonal antibodies: II. Electron microscopy. *Biol Reprod* **40,** 1103-1108.

Takahashi K, Araki Y and Motoyama M (1999) Normal development of a zona-free oocyte to the blastocyst stage following ICSI. *Hum Reprod* **14**, 2677.

Tarkovski AK. (1966) An air-drying methods for chromosome preparation from mouse eggs. *Cytogenetics* **5**, 394-400.

Tarin JJ, Vendrell FJ, Ten J, Blanes R, van Blerkom J, Cano A. (1996) The oxidizing agent tertiary butyl hydroperoxide induces disturbances in spindle organization, c-meiosis, and aneuploidy in mouse oocytes. *Mol Hum Reprod*. **2(12)**, 895-901.

Tateno H., Kamiguchi Y. (2001) Meiotic stage-dependent induction of chromosome aberrations in Chinese hamster primary oocytes exposed to topoisomerase II inhibitor etoposide. *Mutat Res* **476(1-2)**, 139-148.

Tesarik J, Greco E (1999) The probability of abnormal preimplantation development can be predicted by a single static observation on pronuclear stage morphology. *Hum Reprod* **14**, 1318-1323.

Thompson (2006) The impact of nutrition of the cumulus oocyte complex and embryo on subsequent development in ruminants. *J Reprod Dev.* **52(1)**, 169-175.

Thomas FH, Vanderhyden BC. (2006) Oocyte-granulosa cell interactions during mouse follicular development: regulation of kit ligand expression and its role in oocyte growth. *Reprod Biol Endocrinol.* **4,** 19.

Thouas GA, Trounson AO, Jones GM. (2006) Developmental effects of sublethal mitochondrial injury in mouse oocytes. *Biol Reprod*. **74(5)**, 969-977.

Tran PT, Inoue S, Salmon ED, Oldenbourg R. (1994) Muscle fine structure and microtubule birefringence measured with a new pol-scope. *Biol Bull*. **187(2)**, 244-245.

Tran P, Salmon ED, Oldenbourg R. (1995) Quantifying single and bundled microtubules with the polarized light microscope. *Biol Bull*. **189(2)**, 206.

Tsafriri A, Cao X, Ashkenazi H, Motola S, Popliker M, Pomerantz SH. (2005) Resumption of oocyte meiosis in mammals: on models, meiosis activating sterols, steroids and EGF-like factors. *Mol Cell Endocrinol*. **234(1-2)**, 37-45.

Tsubamoto H, Hasegawa A, Nakata Y, Naito S, Yamasaki N and Koyama K (1999) Expression of recombinant human zona pellucida protein 2 and its binding capacity to spermatozoa. *Biol Reprod* **61**, 1649-1654.

Twisk M, Mastenbroek S, van Wely M, Heineman MJ, Van der Veen F, Repping S. (2006) Preimplantation genetic screening for abnormal number of chromosomes (aneuploidies) in in vitro fertilisation or intracytoplasmic sperm injection. *Cochrane Database Syst Rev*. **(1)**, CD005291.

Vanroose G, Nauwynck H, Soom AV, Ysebaert MT, Charlier G, Van Oostveldt P and de Kruif A (2000) Structural Aspects of the Zona pellucida of *in vitro*-produced bovine embryos: A scanning electron and confocal laser scanning microscopic study. *Biol Reprod* **62**, 463-469.

Verlinsky Y, Cohen J, Munne S, Gianaroli L, Simpson JL, Ferraretti AP, Kuliev A. (2004) Over a decade of experience with preimplantation genetic diagnosis: a multicenter report. *Fertil Steril*. **82(2)**, 292-294.

Visser JA, de Jong FH, Laven JS, Themmen AP. (2006) Anti-Mullerian hormone: a new marker for ovarian function. *Reproduction.* **131(1)**, 1-9.

Vodermaier HC (2001) Cell cycle: Waiters serving the Destruction machinery. *Curr Biol*. **11(20)**, R834-837.

Volarcik K., Sheean L., Goldfarb J., Woods L., Abdul-Karim F.W., Hunt P. (1998) The meiotic competence of in-vitro matured human oocytes is influenced by donor age, evidence that folliculogenesis is compromised in the reproductively aged ovary. *Hum Reprod* **13**, 154-160.

Walters KA, Binnie JP, Campbell BK, Armstrong DG, Telfer EE. (2006) The effects of IGF-I on bovine follicle development and IGFBP-2 expression are dose and stage dependent. *Reproduction*. **131(3)**, 515-523.

Wang W.H., Meng L., Hackett R.J., Odenbourg R., Keefe D.L. (2001a) Limited recovery of meiotic spindles in living human oocytes after cooling-rewarming observed using polarized light microscopy. *Hum Reprod*. **16**, 2374-2378.

Wang W.H., Meng L., Hackett R.J., Odenbourg R., Keefe D.L. (2001b) The spindle observation and its relationship with fertilization after intracytoplasmic sperm injection in living human oocytes. *Fertil Steril*. **75**, 348-353.

Wang WH, Meng L, Hackett RJ and Keefe DL (2001c) Developmental ability of human oocytes with or without birefringent spindles imaged by Polscope before insemination. *Hum Reprod* **16**,1464-1468.

Wang WH, Keefe DL (2002) Prediction of chromosome misalignment among *in vitro* matured human oocytes by spindle imaging with the PolScope. *Fertil Steril* **78**, 1077-1081.

Wassarman PM (1988) Zona pellucida glycoproteins. *Annual Review Biochem* **57**, 415-442.

Wassarman PM (2002) Sperm receptors and fertilization in mammals. *Mt Sinai J Med* **69(3)**, 148-155.

Wassarman P, Chen J, Cohen N, Litscher E, Liu C, Qi H and Williams Z (1999) Structure and function of the mammalian egg zona pellucida. *J Exp Zool* **285**, 251-258.

Wassarman PM, Jovine L and Litscher ES (2004) Mouse zona pellucida genes and glycoproteins. *Cytogenet Genome Res* **105**, 228-234.

Wassmann K, Liberal V, Benezra R. (2003) Mad2 phosphorylation regulates its association with Mad1 and the APC/C. *EMBO J*. **22(4)**, 797-806.

Weaver BA, Cleveland DW (2005) Decoding the links between mitosis, cancer, and chemotherapy: The mitotic checkpoint, adaptation, and cell death. *Cancer Cell*. **8(1)**, 7-12.

Webb RJ, Bains C, Cruttwell C and Carroll J (2002) Gap-junctional communication in mouse cumulus-oocyte complexes: implications for the mechanism of meiotic maturation. *Reproduction* **123**, 41-52.

Wordeman L, Mitchison TJ (1995) Identification and partial characterization of mitotic centromere-associated kinesin, a kinesin-related protein that associates with centromeres during mitosis. *J Cell Biol*. **128(1-2)**, 95-104.

Yamaguchi S, Kimura H, Tada M, Nakatsuji N, Tada T (2005) Nanog expression in mouse germ cell development. *Gene Expr Patterns*. **5(5)**, 639-646.

Yanagimachi R. (1994) Mammalian Fertilization. In Knobil E and Neill JD (eds.) The Physiology of Reproduction. Raven Press, New York, pp 189-317.

Yin H., Baart E., Betzendahl I., Eichenlaub-Ritter U. (1998a) Diazepam induces meiotic delay, aneuploidy and predivision of homologues and chromatids in mammalian oocytes. *Mutagenesis* **13(6),** 567-580.

Yin H, Cukurcam S, Betzendahl I, Adler ID, Eichenlaub-Ritter U. (1998b) Trichlorfon exposure, spindle aberrations and nondisjunction in mammalian oocytes. *Chromosoma.* **107(6-7)**, 514-522.

Ziebe S, Lundin K, Loft A, Bergh C, Nyboe Andersen A, Selleskog U, Nielsen D, Grondahl C, Kim H and Arce JC (2003) FISH analysis for chromosomes 13, 16, 18, 21, 22, X and Y in all blastomeres of IVF pre-embryos from 144 randomly selected donated human oocytes and impact on pre-embryo morphology. *Hum Reprod* **18**, 2575-2581.

Zollner U, Zollner KP, Hartl G, Dietl J and Steck T (2002) The use of a detailed zygote score after IVF/ICSI to obtain good quality blastocysts: the German experience. *Hum Reprod* **17**, 1327-1333.

Zuelke K.A., Perreault S.D. (1995) Carbendazim (MBC) disrupts oocyte spindle function and induces aneuploidy in hamsters exposed during fertilization (meiosis II). *Mol Reprod Dev* **42(2)**, 200-209.

Erklärung

Ich erkläre: Ich habe die vorgelegte Dissertation selbständig, ohne unerlaubte fremde Hilfe und nur mit den Hilfen angefertigt, die ich in der Dissertation angegeben habe. Alle Textstellen, die wörtlich oder sinngemäß aus veröffentlichten oder nicht veröffentlichten Schriften entnommen sind, und alle Angaben, die auf mündlichen Auskünften beruhen, sind als solche kenntlich gemacht. Bei den von mir durchgeführten und in der Dissertation erwähnten Untersuchungen habe ich die Grundsätze guter wissenschaftlicher Praxis, wie sie in der „Satzung der Justus-Liebig-Universität Gießen zur Sicherung guter wissenschaftlicher Praxis“ miedergelegt sind, eingehalten.“

Danksagung

Ich bedanke mich bei allen, die mich bei der Erstellung und Anfertigung der vorliegenden Arbeit unterstützt haben.
Meinen wissenschaftlichen Betreuern, Herrn Prof. Dr. Dr. h.c. H.-R. Tinneberg und Frau Prof. Dr. U. Eichenlaub-Ritter, möchte ich für die Überlassung des interessanten Themas und für ihren vielseitigen fachlichen Rat danken. Ich verdanke ihnen viele anregende Gespräche, hilfreiche Unterstützung und ständige rückhaltlose Förderung. Sie haben mich in die Zell- und Reproduktionsbiologie eingeführt und damit meine weitere Arbeit grundlegend beeinflusst. Bei Herrn Prof. Dr. Dr. h.c. H.-R. Tinneberg bedanke ich mich für die Bereitstellung des Arbeitsplatzes in dem Zentrum für Frauenheilkunde und Geburtshilfe des Universitätsklinikums Gießen und Marburg GmbH, Standort Gießen. Bei Frau Prof. Dr. U. Eichenlaub-Ritter von der Universität Bielefeld bedanke ich mich für die umfassende konstruktive und intensive Betreuung und viele wertvolle Diskussionen während aller Phasen der Arbeit. Für das freundliche Überlassen der humanen Eizellen bedanke ich mich bei dem gesamten IVF Team des Zentrums für IVF Gießen (CIF) unter der Leitung von Herrn Prof. Dr. Dr. h.c. H.-R. Tinneberg. Ohne ihre stetige Unterstützung wäre diese Arbeit nicht möglich gewesen.
Weiterhin bedanke ich mich bei Herrn W. Pabst und Frau M. Mann für die Unterstützung bei der statistischen Auswertung. Ebenfalls möchte ich mich bei Frau Dr. U. Gamerdinger vom Institut für Pathologie für die Mitbenutzung des konfokalen Mikroskopes bedanken. Ich bin Herrn T. McKinnon und Herrn W. Pfeiffer für die Korrektur meines Manuskripts sehr dankbar.
Ein ganz besonderer Dank gilt meiner Familie und meinen Eltern, die mich während meiner gesamten Promotion vorbehaltlos unterstützt haben.

Lebenslauf

Persönlichen Daten

Anschrift	Grünbergerstr. 107 35394 Gießen Tel. : 0176/23198700 e-mail: yingshen1@hotmail.com
Geburtsdatum	03.11.1972 in Beijing, China

Ausbildung

09.1979 – 07.1991	Grund-, Mittel- und Oberschule in Beijing, China
09.1991 – 07.1996	Studium der Human Medizin an der „Capital University of Medical Science“in Beijing, China
04.1999 – 10.2002	Studium der Biologie an der Universität Bielefeld
04.2003 – 05.2007	Promotion bei Prof. Dr. Dr. h.c. Tinneberg im Fachbereich Medizin der Justus-Liebig-Universität Giessen

Famulaturen

03.1994 – 07.1996	Beijinger Xuanwu Hospital, Beijing, China

Berufstätigkeiten

08.1996 – 10.1997	Beijinger sechsten Hospital, Beijing, China Ärztin für Innere Medizin
03.2001 – 12.2002	Fakultät für Biologie, Universität Bielefeld Wissenschaftliche Mitarbeiterin in der Arbeitsgruppe von Prof. Dr. Eichenlaub-Ritter Wissenschaftliche Mitarbeiterin
01.2003 – 06.2005	Medizinisch Zentrum für Frauenheilkunde und Geburtshilfe des Fachbereichs Medizin der Justus-Liebig-Universität Giessen Wissenschaftliche Mitarbeiterin

Publikationen

I. Artikeln:

1. **Shen Y**., Stalf T., Mehnert C., Tinneberg H.-R., Eichenlaub-Ritter U. (2006) Retardance of human oocyte spindle correlates positively with pronuclear score after ICSI. Reprod Biomed Online 12(6), 737-751.

2. **Shen Y**, Betzendahl I, Sun F, Tinneberg HR and Eichenlaub-Ritter U (2005) Non-invasive method to assess genotoxicity of nocodazole interfering with spindle formation in mammalian oocytes. Reprod Toxicol 19, 459-471.

3. **Shen Y**., Stalf T., Mehnert C., Eichenlaub-Ritter U., Tinneberg H.-R. (2005) High magnitude of light retardation by the zona pellucida is associated with conception cycles. Hum Reprod 20, 1596-1606.

4. Eichenlaub-Ritter U., Winterscheidt U., Vogt E., **Shen Y**., Tinneberg H.-R., Sorensen R. (2007) 2-methoxyestradiol induces spindle aberrations, failure in chromosome congression and nondisjunction in mouse oocytes. Biol Reprod. [Epub ahead of print]

5. Stalf T, Mehnert C, Hajimohammad A, Manolopoulos K, **Shen Y**, Schuppe HC, Diemer T, Schill WB, Weidner W, Tinneberg HR. (2005) Influence of motility and vitality in intracytoplasmic sperm injection with ejaculated and testicular sperm. Andrologia. 37(4), 125-130.

6. Sun F, Betzendahl I, **Shen Y**, Cortvrindt R, Smitz J, Eichenlaub-Ritter U (2004) Preantral follicle culture as a novel in vitro assay in reproductive toxicology testing in mammalian oocytes. Mutagenesis 19(1), 13-25.

7. Eichenlaub-Ritter U, **Shen Y**, Tinneberg HR (2002) Manipulation of the oocyte: possible damage to the spindle apparatus. Reprod Biomed Online. 5(2), 117-124.

8. **Shen Y**., Betzendahl I., Tinneberg H.-R., Eichenlaub-Ritter U. Enhanced polarizing microscopy as new tool in aneuploidy research in oocytes. Mutagenesis. (Review, in revision).

II. Vorträge

1. **Shen Y**, Stalf T, Mehnert C, Eichenlaub-Ritter U. and Tinneberg H-R (2005) Quantitative comparison of the optical properties of the zona pellucida of oocytes contribution to conception or non-conception cycles after ICSI. (21st Annual meeting of the European society of human reproduction and embryology, 19-22 Jun. 2005, Copenhagen, Denmark)

2. **Shen Y.**, Stalf T, Mehnert C, Tinneberg H-R and Eichenlaub-Ritter U (2005) Zona pellucida und Spindelapparat als Indikatoren der Oozytenqualität. (38. Jahrestagung Physiologie und Pathologie der Fortpflanzung; 30. Verterinär-Humanmedizinische Gemeinschaftstagung, Feb. 2005, Zürich, Schweiz)

3. **Shen Y**, Manolopoulos K, Stalf T, Mehnert C, Tinneberg H-R and Eichenlaub-Ritter U (2004) Korrelationen zwischen der Spindelintegrität der Eizelle und dem PN-Score des Embryonen. (55. Kongress der Deutschen Gesellschaft für Gynakologie und Geburtshilfe, 14-17.Sept. 2004, Hamburg Germany)

4. Tinneberg H.-R. and **Shen Y**. (2004) Application of new light Microscopy method for the improvement of IVF/ICSI treatment (The 4th Jordanian International Conference for Fertility and Genetics)

5. **Shen Y**, Stalf T, Mehnert C, Tinneberg H-R and Eichenlaub-Ritter U. (2004) Optical property of the meiotic spindle correlated with oocyte's quality. (5. Kolloquium der jungen forschenden Reproduktionsmediziner, 23-25 Apr. 2004, Kiel Germany)

6. Eichenlaub-Ritter U., Sun F., Winterscheid U., **Shen Y**., Betzendahl I. (2003) In vitro approaches to the study of aneuploidy in oocytes. Mutagenesis Suppl. (Annual conference of EEMS, Aberdeen 2003).

7. **Shen Y**, Stalf T, Mehnert C, Tinneberg H-R and Eichenlaub-Ritter U (2003) Non-invasive method to detect oocyte quality after IVM and Select human oocytes with high quality prior to ICSI. (3. Tagung des Arbeitskreises Molekularbiologie, 07-08. Nov. 2003, Giessen Germany)

8. **Shen Y**., Tinneberg H.-R., Eichenlaub-Ritter U. (2002) Prädiktiver Wert von Spindelaberrationen für Aneuploidie und Qualität von Oozyten. (3. Kolloquium „Junge forschende reproduktionsmediziner“, Mai 2002, Düsseldorf Germany)

9. Eichenlaub-Ritter U., Sun F., Cukurcan S., **Shen Y**. (2002) The genetic consequences of environmental toxicity. (Annual Conference of SSF. Reproduction Leeds, 2002.)

III. Posters und Abstracts

1. **Shen Y**, Tinneberg H-R, Stalf T, Vogt E and Eichenlaub-Ritter U (2003) Polscope to improve in-vitro maturation and select human oocytes with high developmental potential prior to ICSI.

2. **Shen Y,** Tinneberg H.-R., Eichenlaub-Ritter U. (2002) Polscope to detect spindle aberrations in oocytes. Hum Reprod. 17 Suppl. (18th Annual meeting of the European society of human reproduction and embryology, Vienna, Austria)

3. **Shen Y**, Michel G, Tinneberg H.-R. and Eichenlaub-Ritter U (2001) Nicht-invasive Untersuchung der Ultrastruktur von Oozyten mittels Polscope-Mikroskopie. Zentralblatt für Gynäkologie 7, P49, pA43.

4. Vogt E., Betzendahl I., **Shen Y.**, Eichenlaub-Ritter U. (2004) Spindle Checkpoint and Mad 2 expression in mammalian oocytes. Eur J Cell Biol 83 Suppl. 54, 80 (Annual conference of German society of cell biology, Magdeburg 2004).

Preise

Die beste Poster- Präsentation der 200. Tagung der Nordreihen-Westfallen Gesellschaft für Gynäkologie und Geburtshilfe, Essen, Deutschland, 2001

Preis für das beste Poster der gemeinsamen Jahrestagung der Deutschen Gesellschaft für Andrologie und Deutschen Gesellschaft für Reproduktionsmedizin, München, Deutschland 2003

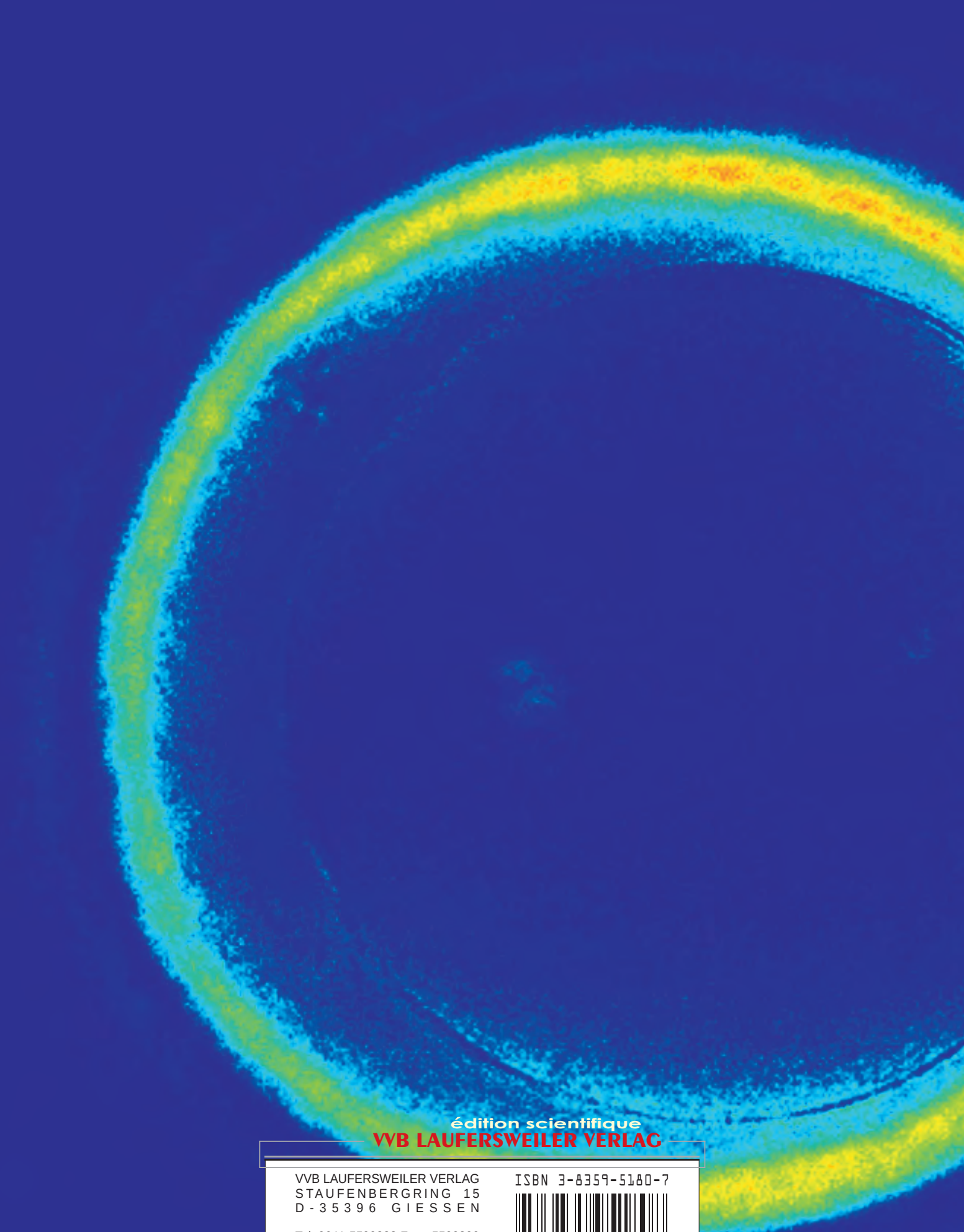

édition scientifique
VVB LAUFERSWEILER VERLAG

VVB LAUFERSWEILER VERLAG
STAUFENBERGRING 15
D-35396 GIESSEN

Tel: 0641-5599888 Fax: -5599890
redaktion@doktorverlag.de
www.doktorverlag.de

ISBN 3-8359-5180-7

9 783835 951808